

Journal of Hydrology

Seasonal rainfall trends of a key Mediterranean area in relation to large-scale atmospheric circulation: how does current global change affect the rainfall regime? --Manuscript Draft--

Manuscript Number:	HYDROL44505R1
Article Type:	Research paper
Keywords:	climatic patterns; Current Global Warming; East Atlantic; North Atlantic Oscillation; Western Mediterranean Oscillation; rainfall trend
Corresponding Author:	Marco Luppichini ITALY
First Author:	Marco Luppichini
Order of Authors:	Marco Luppichini Monica Bini Michele Barsanti Roberto Giannecchini Giovanni Zanchetta
Abstract:	<p>Current global warming causes a change in atmospheric dynamics, with consequent variations in the rainfall regimes. Understanding the relationship between global climate patterns, global warming, and rainfall regimes is crucial for the creation of future scenarios and for the relative modification of water management. The aim of this study is to improve knowledge of the relationship between North Atlantic Oscillation (NAO), East Atlantic (EA), and Western Mediterranean Oscillation (WeMO) with the seasonal rainfalls in Tuscany, Italy. The study area occupies a strategic position since it lies in a transition zone between the wet area of northern Europe and the dry area of the northern coast of Africa. This research, based on a statistical correlation method and on linear models, is designed to understand the relationship between seasonal rainfalls and climate patterns. The results of this study demonstrate that the use of linear models can yield more information than traditional statistical correlations. The results show a decrease in rainfall in the warm period of the year, namely in the summer, when its expression is most visible. This phenomenon is ascribable to current global warming, which causes an increase in sea-surface temperatures. An increase in the Northern Atlantic Sea Surface Temperature and in the Mediterranean Sea Surface Temperature causes a reduction of the Iceland Low, with an extension of the Azores High. Moreover, an increase in the Genoa Gulf SST induces a weakening of the Genoa Gulf Low, one of the main cyclogenetic systems of the Mediterranean.</p>
Suggested Reviewers:	Florian Börgel florian.boergel@io-warnemuende.de MATTHEW DEITCH mdeitch@ufl.edu Joan Albert LÓPEZ-BUSTINS jlopezbustins@ub.edu Raquel Lorente-Plazas raquel.lorente1@um.es Rebeca Izquierdo rebeca@creaf.uab.es
Response to Reviewers:	

Influence of large-scale atmospheric circulation on the rainfall of a key Mediterranean area: how does current global change affect the rainfall regime?

Marco Luppichini^{1,2,*}, Monica Bini^{2,3,4}, Michele Barsanti⁵, Roberto Giannecchini^{2,4,6}, Giovanni Zanchetta^{2,4,7}

¹ Department of Earth Sciences, University of Study of Florence, Via La Pira 4, Florence, Italy

² Department of Earth Sciences, University of Pisa, Via S. Maria, 52, 56126 Pisa, Italy

³ Istituto Nazionale di Geofisica e Vulcanologia (INGV), Via Vigna Murata 605, 00143 Roma, Italy

⁴ CIRSEC Centro Interdipartimentale di Ricerca per lo Studio degli Effetti del Cambiamento Climatico dell'Università di Pisa, Via del Borghetto 80, 56124 Pisa, Italy

⁵ Department of Civil and Industrial Engineering, University of Pisa, Largo L. Lazzarino, 56122 Pisa, Italy

⁶ Institute of Geosciences and Earth Resources, IGG-CNR, via Moruzzi 1, 56124 Pisa, Italy

⁷ Istituto di Geologia Ambientale e Geoingegneria, IGAG-CNR, Rome, Italy

Abstract

Current global warming causes a change in atmospheric dynamics, with consequent variations in the rainfall regimes. Understanding the relationship between global climate patterns, global warming, and rainfall regimes is crucial for the creation of future scenarios and for the relative modification of water management. The aim of this study is to improve the knowledge of the relationship of North Atlantic Oscillation (NAO), East Atlantic (EA), and Western Mediterranean Oscillation (WeMO) with the seasonal rainfall in Tuscany, Italy. The study area occupies a strategic position since it lies in a transition zone between the wet area of northern Europe and the dry area of the northern coast of Africa. This research, based on a statistical correlation method and on linear models, is designed to understand the relationship between seasonal rainfalls and climate patterns. The method of linear models innovative in this thematic area, can yield more information than statistical correlations. The results show a possible decrease in rainfall in the warm period of the year, namely in the summer, when its expression is most visible. This phenomenon is ascribable to current global warming, which causes an increase in sea-surface temperatures. An increase in the Northern Atlantic Sea Surface Temperature (SST) and in the Mediterranean Sea Surface Temperature (SST) causes a reduction of the Iceland Low, with an extension of the Azores High. Moreover, an increase in the Genoa Gulf SST induces a weakening of the Genoa Gulf Low, one of the main cyclogenetic systems of the Mediterranean.

28 **Keywords:** Climatic Patterns, Current Global Warming, East Atlantic, North Atlantic Oscillation, Western
29 Mediterranean Oscillation, rainfall trend, Tuscany.

30 **Introduction and goals**

31 Current global warming causes effects at different scale levels, including changes in the hydrological cycle (Allan,
32 2011; Bates et al., 2008). The effects are visible in air temperature trends and, more complexively, in rainfall, in the
33 form of frequency and intensity of extreme events and changes in soil moisture (Blöschl et al., 2019; Stagl et al., 2014;
34 Xu et al., 2011), with wide implications in terms of social-economic conditions and financial policy (European
35 Environment Agency, 2019). The Mediterranean region is an ideal research testbed for current climatic changes both
36 for its location and historico-cultural importance, and for having been considered a hot spot for future climatic changes
37 (Giorgi, 2006). The Mediterranean, located between the European humid domain and the North African arid belt,
38 provides alternating circulation regimes with large spatial and temporal variability (Dünkeloh and Jacobeit, 2003).
39 Furthermore, the highly populated and industrialized Mediterranean region shows an increase in the demand of water
40 supply. In this context, a correct characterization of rainfall regimes can improve the management of water resources
41 (Tramblay et al., 2020) and extreme events (Cardoso Pereira et al., 2020; Myhre et al., 2019). Several studies have
42 identified a general decrease (although with some exceptions) in the annual rainfall amount in the area of the
43 Mediterranean basin (Bertola et al., 2019; Blöschl et al., 2019; Caloiero et al., 2018, 2011; Colantoni et al., 2015;
44 Deitch et al., 2017; Dünkeloh and Jacobeit, 2003; Halifa-Marín et al., 2021; Longobardi and Villani, 2010; Martin-Vide
45 and Lopez-Bustins, 2006; Philandras et al., 2011; Ríos-Cornejo et al., 2015); and atmospheric patterns related to
46 mesoscale circulation (Brandimarte et al., 2011; Caloiero et al., 2011; Halifa-Marín et al., 2021; Lopez-Bustins et al.,
47 2008; Luppichini et al., 2021; Martinez-Artigas et al., 2021; Ríos-Cornejo et al., 2015; Trigo et al., 2004). During the
48 winter months, one of the main drivers of rainfall variability in southern Europe and in the Mediterranean is the
49 presence of different pressure fields over the Northern Atlantic Ocean and their variability indicated as the North
50 Atlantic Oscillation (NAO) (Hurrell, 1995). NAO is defined by an index measured as a north-southern dipole of
51 pressure anomalies, with one pole located at higher latitude (Iceland Low 80°N) and the other at the central latitudes of
52 the North Atlantic between 35°N and 40°N (Azores High).

53 The East Atlantic (EA) index is similar to that of NAO but is displaced south-eastward to the approximate nodal
54 lines of the NAO pattern. The EA index is often interpreted as a downward-shifted NAO model, but its strong
55 subtropical link entails a different peculiarity. The EA value is positive when a significant drop in pressure occurs in the
56 Atlantic Ocean; at the same time, the subtropical oceanic anticyclone belt considerably rises in latitude and reinforces
57 itself. In response, the African anticyclone gains energy and invasiveness over the Mediterranean, subjecting this area to

58 frequent pulses of hot and dry Saharan air in all seasons (Climate Prediction Center, 2021; Mellado-Cano et al., 2019).
59 The NAO and EA indexes present interannual and annual variabilities with positive and negative phases. The rainfall in
60 the Mediterranean can be associated with a negative phase of NAO and/or EA, when we observe an expansion of the
61 Iceland Low. Instead, during a positive phase of NAO and/or EA, Northern Europe is the rainiest area (Rousi et al.,
62 2020).

63 The Western Mediterranean oscillation (WeMO) is an index often used to study variability in rainfall in alternative
64 to NAO in the Mediterranean region. The WeMO index is the difference of atmospheric pressure in a dipole, with the
65 first pole located in Padua (45.40°N, 11.48°E) in northern Italy and the second one located in San Fernando, Cádiz
66 (36.28°N, 6.12°W) in southwestern Spain (Climatic Research Unit, 2021). Specifically, the former is located in the Po
67 plain (an area with relatively high barometric variability due to the different influence of the central European
68 anticyclone and the Genoa Gulf Low), while the latter pole is located in the Gulf of Cádiz in the southwest of the
69 Iberian Peninsula, often subject to the influence of the Azores anticyclone and, episodically, to the cut-off of
70 circumpolar lows or to its own cyclogenesis (Halifa-Marín et al., 2021; Lopez-Bustins et al., 2020; Martin-Vide and
71 Lopez-Bustins, 2006). A positive phase of WeMO is associated with a low-pressure area in the Ligurian Sea and with
72 an anticyclone in the Gulf of Cadiz. Instead, a negative phase of the index determines a low in the Gulf of Cadiz and an
73 anticyclone in Central Europe. During the positive phase, in the Iberian Peninsula the winds are typically west and
74 northwest coming from the North Atlantic area. These winds cross the continental areas of the peninsula, and become
75 dry, causing rainfall on the north-western coasts and the inland. Conversely, a negative WeMO phase is associated with
76 humid air masses travelling over the Mediterranean Sea. When these winds reach the eastern side of the Iberian
77 Peninsula, they are laden with moisture, resulting in an increase in rainfall, sometimes torrential, in this area (Halifa-
78 Marín et al., 2021; Martin-Vide and Lopez-Bustins, 2006).

79 Both NAO and EA are influenced by the Sea Surface Temperature (SST) of the Northern Atlantic Ocean (NASST)
80 and of the Mediterranean (MSST). An increase in NASST and in MSST is correlated to an expansion of the Azores
81 High and to a consecutive reduction of the Iceland Low, which cause a formation of the NAO and EA positive phases
82 (Frankignoul et al., 2003; Robertson et al., 2000; Visbeck et al., 2001). More recently, NAO has been correlated to the
83 Atlantic Multidecadal Oscillation (AMO), a representative index of the NASST trend (Knight et al., 2005). AMO
84 changes the zonal position of the NAO center of action, moving the cyclonic area closer to Europe or North America.
85 During a positive phase of AMO, the Icelandic Low moves further towards North America, while the Azores High
86 moves further towards Europe (and viceversa) for the negative phase of AMO (Börgel et al., 2020). WeMO is also
87 influenced by the NASST and MSST, but also by the Genoa Gulf Sea Surface Temperature (GGSST), with positive
88 values correlating to low values of SST (Martín et al., 2012; Martin-Vide and Lopez-Bustins, 2006). Current global

89 warming causes a progressive increase in NASST, MSST and GGSST (Pastor et al., 2020; Wang and Dong, 2010) so
90 that NAO and EA are likely to be characterized by more positive phases, and WeMO by more negative phases.

91 The purpose of this study is to understand the rainfall seasonal trends of the last 70 years in Tuscany (central Italy),
92 in relation to mesoscale circulation and to the indices defined above. The region has a strategic location: it is located in
93 the northern sector of the Mediterranean, in the proximity of the Genoa Gulf, by far the most active cyclogenetic centre
94 of the Mediterranean (Trigo et al., 2002). The rainfall dataset used came from several raingauges with high spatial
95 density and temporal activity from 1950 to 2020. The large number of raingauges allowed us to investigate the rainfall
96 trend in great detail and with direct measurements. The same dataset was used by Luppichini et al. (2020), who
97 employed different types of elaboration to understand the variable influence of NAO on the Tuscany rainfall. The
98 rainfall trends are compared with the NAO, EA and WeMO indices by means of mathematical and statistical methods to
99 understand the climatic trends influencing the rainfall regime in the area. We investigated the link between the different
100 indices by using traditional statistical methods (Spearman, 1904), but also by introducing in this field an innovative
101 approach, which employs a linear model to understand the influence of each index on the rainfall prediction. The
102 combination of these different methods helped us to comprehend the accuracy and the advantages of the new method
103 proposed.

104 In our study, we compared these SSTs with the atmospheric indices to improve knowledge on the rainfall trend and
105 to understand possible future scenarios.

106 **Study area**

107 As expected, the mean annual precipitation (MAP) in Tuscany is influenced by morphology (Figure 1a). The rainiest
108 areas are located at the highest altitudes (Apuan Alps and Northern Apennines; Figure 1b). In particular, the Apuan
109 Alps in north-western Tuscany show some of the highest rainfall amounts in Italy (Giannecchini and D'Amato Avanzi,
110 2012; Rapetti and Vittorini, 1994), often characterized by high intensity (D'Amato Avanzi et al., 2004; Giannecchini,
111 2006). In Tuscany, MAP is in a range of 400-3000 mm/year with a clear gradient from the northern to the southern and
112 it is linked to the morphology (Figure 1a). The main rainy season is autumn, with a progressive decrease that generally
113 starts in December. The mean rainfall in the DJF season is ca 300 mm, ca 250 mm in MAM, ca 130 mm in JJA, and ca
114 350 mm in SON.

115 **FIGURE 1**

116 **Materials and Methods**

117 **Dataset**

118 *Rainfall dataset and processing*

119 The raingauge dataset was provided by the Tuscany Region Hydrologic Service (SIR) network and includes 1103
120 raingauges (Figure 1c). The data were obtained by an automated download procedure through an HTTP request. The
121 activity period of each raingauge is variable. The older stations have been monitoring since the beginning of the last
122 century, even if a temporal continuity of the data is not always guaranteed for some stations. SIR provides the daily
123 rainfall data for each raingauge in the operation period. To obtain longer and more complete time series from this
124 dataset, we grouped the stations according to a stringent protocol. This procedure is necessary to reconstruct the time
125 series of the stations that have experienced minor changes in position or that have undergone an administrative variation
126 (e.g., a slight change in name or identification code). In many cases, stations have consecutive intermittent activity
127 times due to the decommissioning of one and the subsequent installation of a new one. In these cases, we merged the
128 stations by assigning the same, or part of the same name, with a difference in quote (less than 20%) of the measurement,
129 and a maximum distance (less than 2 km). The geographic coordinates of the merged stations derived from a cartesian
130 mean of the original coordinates of the origin stations.

131 By using the data available and following the procedure described above, a total of 117 time series were obtained from
132 1950 to 2020. The rainfall data can also be useful for comparison with the results of the models (see section Linear
133 Models), which predict rainfall anomalies; instead, the absolute values are expressed as percentage anomalies of rainfall
134 (PAR), and are calculated as follows:

$$PAR = \frac{x_i - \bar{x}_i}{\bar{x}_i} \cdot 100 \quad (1)$$

135 where, x_i is the rainfall amount, \bar{x}_i is the rainfall amount mean of the period 1961-1990. The PAR is averaged with a
136 ten-year mobile window.

137 *Climatic Dataset*

138 The NAO dataset is provided by the Climate Analysis Section of the US National Center for Atmospheric Research
139 (NCAR). This dataset is based on the principal (PC)-based index component of the NAO, which are the time series of
140 the leading Empirical Orthogonal Function (EOF) of SLP anomalies over the Atlantic sector, 20°-80°N, 90°W-40°E.
141 This index is used to measure the yearly NAO, by tracking the seasonal movements of the Icelandic Low and Azores

142 High. The dataset has a monthly frequency from January 1889 to December 2020. PC-based indices are more optimal
143 representations of the full spatial patterns of the NAO (National Center for Atmospheric Research Staff (Eds), 2021).

144 The EA dataset used in this study is provided by the National Weather Service of NOAA. The frequency of the
145 dataset is on a monthly basis, from 1950 to 2020. The index is standardized by the 1981-2010 climatology (Climate
146 Prediction Center, 2021).

147 The WeMO index is provided by the Climatic Research Unit (CRU) of the University of East Anglia (Climatic
148 Research Unit, 2021). The time series starts in 1821 and has a monthly frequency.

149 The trends of NASS, MSST, and GGSST are calculated from the Extended Reconstructed Sea Surface Temperature
150 (ERSST) dataset version 5 (NOAA, 2021), and they are expressed using a 10-year mobile window of anomalies. The
151 anomalies are referred to the mean of the period 1961-1990. NASS is calculated in the area 0N-65N 80W-0E, MSST
152 in the area 38N-49N 0E-28E, and GGSST in the area 42.8N-44.8N 7.6E-10.76E.

153 Statistical Correlation

154 We calculated the correlation coefficient in order to identify a possible relationship between atmospheric
155 teleconnection and rainfall amount. Some authors (Caloiero et al., 2011; Izquierdo et al., 2014; Luppichini et al., 2021;
156 Nalley et al., 2019; Vergni et al., 2016) use the Spearman's correlation coefficient (SCC) (Spearman, 1904) to
157 understand the relationship between atmospheric index and rainfall amount. This relationship is suitable for
158 monotonically-related variables, even when their relationship is not linear. The range of Spearman's coefficients is
159 between -1 and 1; positive values indicate a tendency of one variable to increase or decrease together with another
160 variable, whereas negative values indicate a trend in which the increase in the values of one variable is associated with
161 the decrease in the values of the other variable, and viceversa. We calculated the SCC between the three atmospheric
162 teleconnections and the rainfall for the four seasons: winter from December to February (DJF), spring from March to
163 May (MAM), summer from June to August (JJA) and autumn from September to November (SON). SCC was
164 calculated using a 10-year moving time-window from 1950 to 2020. The result of the correlation was assigned to the
165 year halfway through each ten-year period.

166 Linear Models

167 The simplest mathematical model is the linear one. We can create linear models able to predict the rainfall amount
168 by using the NAO, WeMO and EA time series. The equation of a linear model predicting the rainfall (R_p), by using the
169 NAO, WeMO and EA time series, is the following:

$$R_p = \alpha NAO + \beta WeMO + \gamma EA + \delta \quad (2)$$

170 We can analyse the setting of the independent variable coefficients (α , β , γ) to understand the role of each input on the
171 prediction of rainfall. The simplicity of the linear models does not allow to have the best prediction models, but it
172 certainly allows to analyse the influence of the input clearly and to exclude synergy between the inputs. We created a
173 linear model for each raingauge time series and for the four seasons. The different dimensionality of the three
174 atmospheric teleconnections could influence the information expressed by the parameters of models α , β and δ . For this
175 reason, we scaled the time series of NAO, WeMO and EA in the range between 0 and 1 for the studied period (1950-
176 2020), applying the following equation:

$$Ts = \frac{Ts - Ts_m}{Ts_M - Ts_m} \quad (3)$$

177 where Ts is the index time series in the range 0 and 1, Ts_M is the maximum value of the index, and Ts_m is the
178 minimum value of the index. The fitting of the linear models is executed using the SciPy library in Python Language
179 and, in more detail, the “curve_fit” method (Virtanen et al., 2020).

180 **Results**

181 **Rainfall Trends**

182 Figure 2 reports the values of PAR calculated for each time series used in this work. The graphs indicate a small
183 variability of PAR between each time series, excluding the possibility of different influences on the linear model
184 outcomes by the input stations. The rainfall trends expressed in PAR are shown in FiguresFigure 3-6. These trends are
185 very different in the four seasons. From 1950 to 1985, the DJF season was characterized by a slow rainfall reduction
186 followed by a sudden decrease around the 90’s. The first years of the 1990’s presented a PAR reduction of about 30-
187 40%. Starting from 2000, we can observe a progressive increase in winter rainfall with a return of the amount recorded
188 before 1990 (Figure 3). Until the 1990s, the MAM rainfall trend was identified by an oscillation. From the 1990’s to the
189 2010’s, we observe PAR values between ca -10 and -20%. After 2008, there was an increase in precipitation (Figure 4).
190 The JJA season was characterized by a progressive reduction of rainfall starting from 1965 with the minimum values of
191 -30% around 2005. The last years were marked by a weakly increase in rainfall (Figure 5). Finally, rainfall in the SON
192 season presented a certain variability over an approximate 20-year period. The maximum rainfall amount was recorded
193 around 1965 and 1995, while the minimum values were referred to the period 1970-1990 (Figure 6).

194

FIGURE 2

195 Atmospheric Teleconnection Trends

196 From 1950 to 2020, NAO was characterized by an intensification of the positive phase in the DJF and MAM
197 seasons (Figure 3 and 4). In the JJA season, NAO was characterized by a positive phase until 2005, whereas the index
198 was characterized by a negative phase, except for some years. Finally, NAO was more variable in the SON season with
199 periods characterized by negative alternated with positive phases (Figure 6).

200 From 1950 to 2020, the EA time series was characterized by an intensification of the positive phase starting from
201 1985 for the DJF period (Figure 3), and from 1995 for the MAM and JJA periods (Figure 4 and 5). The SON period
202 presented a higher index fluctuation, with a negative phase until 1980, followed by a more positive ten-year phase and
203 then by a negative phase until 2000. From 2000 to 2020, we can observe an increase in the positive phase except for
204 some cases (Figure 6).

205 In DJF, WeMO was characterized by a positive phase with a decrease in the 1990-2010 period (Figure 3). Around
206 2005 we observed a drastic change in the WeMO index in the MAM, JJA and SON seasons with a negative persistence
207 phase (Figures 4-6). Before 2005, the index in these seasons was characterized by positive phases except for some years
208 in which the values of the index were negative (Figures 4-6).

209 Sea surface temperature trends

210 Figures 3-6 show the trends of NASST, MSST and GGSST display a clear increasing trend starting from the 1980's
211 in all seasons. Such increase only started around the 2010's for DJF and GGSST, while it increased starting from 1980s
212 in the other seasons. The increase in SST was higher in the summer than in the other seasons.

213

214

FIGURE 3

215

FIGURE 4

216

FIGURE 5

217

FIGURE 6

218 Statistical Correlation

219 Figure 7 reports the results obtained from the Spearman's correlation coefficient. In the DJF season, rainfall is
220 correlated with WeMO and anticorrelated with NAO and EA. Rainfall increases during a negative phase of NAO or EA
221 and a positive phase of WeMO. During this period, each atmospheric teleconnection has a similar effect on the rainfall

222 amount. In the MAM season, the strongest correlation is with WeMO, and even in this case a positive phase of the
223 index corresponds to a rainfall increase in the study area. NAO and EA are weakly anticorrelated with the rainfall
224 amount. The strongest correlation is with EA in the JJA season, and a negative phase of this index indicates an increase
225 in rainfall in the area. On other hand, a positive phase of EA corresponds to reduced precipitation in summer. NAO and
226 WeMO are weakly correlated with the rainfall, but do not have a clear behaviour. Even in the SON season, the strongest
227 correlation is with EA. The correlation in this season is positive, which indicates that a positive EA phase determines
228 increased precipitation in the area. The spatial correlation distribution is homogenous with no clear spatial pattern,
229 especially when the correlations are strong, providing a precise indication of the relationship (Figure 7).

230 **FIGURE 7**

231 Linear Models

232 In Figure 8a-d, we report four examples of the prediction of PAR by means of linear models referred to the DJF,
233 MAM, JJA and SON seasons. The cases shown represent the results of the lineal models because they have Root Mean
234 Square Error (RMSE) values similar to the error medians calculated on the whole dataset (Figure 8e). Figure 8e also
235 reports the RMSE of the entire dataset. SON, followed by DJF, is the season with the highest average errors.

236 Figure 9 shows the mean values of coefficients α , β and γ for the linear models in each season (blue circles). We
237 can observe a change in the values of the three coefficients from one season to another. The red circles in Figure 9 show
238 the relative weights of each coefficient. In the DJF season, the coefficient with the greatest weight is α with a mean
239 value of about 55%, followed by β and γ . The coefficients indicate that NAO has more influence on the rainfall trend
240 than WeMO and EA in DJF. In this season, increased precipitation is linked to a negative phase of NAO (α is negative)
241 and a positive phase of WeMO (β is positive). A positive γ is not to be understood as a positive link between rainfall
242 and index, but it works as a compensation with respect to the α coefficient in the model. In the MAM season, β
243 (WeMO) has the highest weight in the results of the models, followed by α and γ . In particular, the amount of
244 precipitation is correlated with a positive phase of WeMO and with a negative phase of NAO. Again, EA has less
245 influence on the model than the other two indices. In the JJA season EA is the most important index, with the greatest
246 coefficient (γ). In particular, the summer rainfall seems to be linked to a negative phase of EA. Less important, the
247 summer rainfall is linked to a negative phase of WeMO. In the SON season, NAO has the greatest weight and is
248 followed by WeMO and EA, which have less influence on the rainfall trend. In this case, the coefficients are all
249 negative, so that rainfall is correlated to a negative phase of these indices.

250 **FIGURE 8**

252 **Discussion**253 **Mathematical and statistical relationship between atmospheric teleconnections and rainfall**

254 The statistical correlation calculated with Spearman's method represents a first indication of the influence of climate
255 patterns on the local rainfall trend (Figure 7). In accordance with several studies (Caloiero et al., 2011; Deser et al.,
256 2017; Ferrari et al., 2013; George et al., 2004; López-Moreno et al., 2011; Luppichini et al., 2021; Riaz et al., 2017;
257 Vergni and Chiaudani, 2015; Vicente-Serrano and López-Moreno, 2008; West et al., 2019), NAO influence is
258 predominant in winter, with an anticorrelation between index and rainfall amount. In agreement with the obtained SCC,
259 an increase in the Azores High, and consequently a decrease in the Iceland Low, determine reduced winter rainfall in
260 the study area. The correlation between NAO and rainfall decreases during the successive seasons with a minimum
261 correlation in the summer. In winter and in spring, the correlation with WeMO is strong and it is characterized by a
262 positive sign. This implies the formation of the Genoa Gulf Low and its reinforcement increases the amount of rainfall
263 in the study area. This can be ascribed to the direction of the moist air masses coming from the Atlantic Ocean and
264 directed to the north-western coast of Spain and to the Mediterranean (Degeai et al., 2020; Martín et al., 2012; Martín-
265 Vide and Lopez-Bustins, 2006). In this dynamic state the moist air masses can reach Tuscany, enhancing local
266 cyclogenesis and rainfall. The SCC values indicate that the influence of the Genoa Gulf Low decreases in summer and
267 autumn (Figure 7). The correlation between rainfall and EA is strong in winter and summer; in summer, the main
268 correlation with rainfall is particularly with EA. In winter, the link between EA and rainfall is the same for NAO. In
269 summer, the greater representativeness of EA than of NAO on the Azores High allows a better understanding of the link
270 between rainfall and global climate in this season. In detail, the formation of the Azores High and of the African High
271 results in an increase in the EA index, and this means that there is reduced precipitation in the study area. In autumn, the
272 statistical correlations do not allow to make a link between large-scale circulation and rainfall. Indeed, we can observe a
273 weak anticorrelation with NAO, a weak correlation with EA, and no correlation with WeMO. This method seems
274 unsuitable to represent the autumn season with its atmospheric dynamics.

275 The results of the linear models are conformant to the statistical correlation results for the DJF, MAM and JJA
276 seasons, whereas we can observe some differences in SON. The strong correspondence between the two methods in
277 DJF, MAM and JJA makes it possible to validate our linear model. In autumn, the analysis of the linear models
278 identifies an important role of NAO, and therefore a link between the northern Atlantic atmospheric circulation and the
279 rainfall in the study area. In autumn, the coefficients of NAO (α) are set negative and this means that an increase in the

280 index is linked to a decrease in rainfall in the study area. This mathematical result is more plausible than that obtained
281 from the analysis of correlations based on the notions of atmospheric physics that we introduced previously. The linear
282 model-based method allowed us to refine our investigations and to improve our knowledge of the dynamics in the
283 Mediterranean over the seasons.

284 The use of our linear models offers the advantage of clarifying the role and influence of large-scale atmospheric
285 circulation on rainfall over the study region in different seasons, and this may appear controversial when using only the
286 statistical correlation. These linear methods can also be useful for rainfall prediction, although it is not the intention of
287 this paper to produce the best model for predictions. If we wanted to reduce the model errors, we should have chosen a
288 more complex model able to better adapt to the variability of the inputs; however, it would have been difficult to
289 understand the influence of each input parameter, which is the main scope of this paper.

290 Long-term rainfall trends and relationship with climate patterns

291 This study identified a confused trend for the DJF, MAM and SON rainfall, while JJA rainfall clearly tends to
292 decrease (Figures 3-6). These results agree with those of other studies based on different rainfall datasets (Caloiero et
293 al., 2018; Deitch et al., 2017; Philandras et al., 2011). More specifically, Deitch et al. (2017) studied the seasonal trend
294 of rainfall in the Mediterranean area, demonstrating a negative trend for summer rainfall and no trend for
295 winter/autumnal rainfall in Tuscany.

296 The DJF seasons are characterized by significantly decreased precipitation between 1984 and 2005 (Figure 3). This
297 period is marked by a positive phase of NAO and EA and a negative phase of WeMO. Starting around 1984, the
298 increase in NAO and EA is due to an increase in NASST (Figure 3). An increase in NASST is correlated to an
299 expansion of the Azores High and a consecutive reduction of the Iceland Low, resulting in the formation of the NAO
300 and EA positive phases (Börgel et al., 2020; Frankignoul et al., 2003; Robertson et al., 2000; Visbeck et al., 2001). The
301 successive increase in rainfall from 2005 to 2020 seems to have been caused by an increase in the WeMO, and therefore
302 by an increase in the Genoa Gulf Low persistence. This could indicate a change of the main climatic driver with respect
303 to the previous period (Figure 3).

304 The MAM season presents a decrease in the amount of rainfall in the period between 1985 and 2008 (Figure 4). The
305 WeMO constantly decreases with progressive intensification of the negative phase. This indicates a gradual reduced
306 intensity of the Genoa Gulf Low. As a matter of fact, the GGSST has progressively increased since 1985. Furthermore,
307 NAO and EA are in a persistent positive phase. Since 2008, there has been a weak increase in the precipitation trend.

308 The JJA rainfall trends have the highest correlation with EA, while NAO and WeMO have a lower influence (Figure
309 7 and 9). The increase in NASST, MSST and GGSST induces the NAO and EA indices to a positive phase, and WeMO
310 to a negative phase. This process induces a progressive reduction of rainfall trends in this season.

311 SON is characterized by rainfall trend variability with two wet periods and two dry periods (Figure 6). Each dry
312 period is marked by an increase in NAO, whereas the wet period results from an increase in WeMO linked to a weak
313 decrease in GGSST (Figure 6).

314 The increase in sea surface temperature is greater in the warm periods of the year and it is caused by current global
315 warming. From these observations, we can evince that the warm periods of the year are marked by a greater decrease in
316 precipitation resulting in less water availability in the environmental system.

317 **Conclusions**

318 This study helps to gain a better knowledge of the rainfall trends of the last 70 years in Tuscany, a key area of the
319 Mediterranean Basin, strongly influenced by the cyclogenetic activity related to the Genoa Gulf Low. These trends are
320 analyzed on the basis of the trend of the main atmospheric drivers of the northern hemisphere. The location of the study
321 area allows to understand the influences of Atlantic atmospheric circulation and of the Mediterranean atmospheric
322 circulation on rainfall. Along with the Spearman's traditional coefficient analysis, this study proposes a new
323 mathematical method to investigate the relationship between climate pattern and rainfall. The method based on the use
324 of linear models has resulted to be valid, with similar results derived from a statistical correlation. This new method has
325 allowed a more detailed comprehension of the link between climate patterns and precipitation in the study area. In
326 Tuscany, rainfall amount is influenced by Northern Atlantic atmospheric circulation and by the Genoa Gulf Low. The
327 influences of the two atmospheric systems vary during the year: in winter, rainfall is strongly correlated to the three
328 indices; in spring, the main influence is represented by WeMO, indicating an important role played by the Genoa Gulf
329 Low; in summer, the main driver is EA, which represents better than NAO the influence of the Azores High in this
330 season; in autumn, the strongest correlation is with NAO.

331 The amount of precipitation in the study area is influenced by the SSTs that induce a variation in the Northern
332 Atlantic and Mediterranean atmospheric circulation (Börgel et al., 2020; Frankignoul et al., 2003; Robertson et al.,
333 2000; Visbeck et al., 2001). Current global warming determines an increase in the SSTs and this increase is higher in
334 the warm seasons of the year. The results of this study show that in these seasons there is the greatest reduction of water
335 availability, on account of a direct decrease in precipitation.

336 In conclusion, current global warming can be responsible for less rainfall in this area, and this occurs mainly in the
337 warm seasons when temperature increase is highest.

338

339 **Conflicts of Interest:** The authors declare no conflict of interest. The funders had no role in the design of the study;
340 in the collection, analyses, or interpretation of data; in the writing of the manuscript, or in the decision to publish the
341 results.

342 **Acknowledgements:** The authors are grateful to the Tuscany Region Hydrologic Service for providing the data
343 used in this work.

344 **Funding:** This research was funded by project no. 249792 “Dalla Preistoria all'Antropocene: Nuove Tecnologie per
345 la valorizzazione dell'eredità culturale della Versilia (PANTAREI)” Tuscany Region (call POR FSE 2014-2020, Resp.
346 M. Bini); by the collaborative research agreement no. 579999-2019 “Autorità di Bacino Distrettuale Appennino
347 Settentrionale” (Resp. Monica Bini and Roberto Giannecchini); and by the project: “Cambiamenti globali e impatti
348 locali: conoscenza e consapevolezza per uno sviluppo sostenibile della pianura Apuo-versiliese” Fondazione Cassa
349 Risparmio di Lucca, (Resp. M. Bini).

350 Reference

- 351 Allan, R.P., 2011. Human influence on rainfall. *Nature* 470, 344–345. <https://doi.org/10.1038/470344a>
- 352 Bates, B., Kundzewicz, Z.W., Wu, S., Burkett, V., Doell, P., Gwary, D., Hanson, C., Heij, B., Jiménez, B., Kaser, G.,
353 Kitoh, A., Kovats, S., Kumar, P., Magadza, C.H.D., Martino, D., Mata, L., Medany, M., Miller, K., Arnell, N.,
354 2008. *Climate Change and Water*. Technical Paper of the Intergovernmental Panel on Climate Change.
- 355 Bertola, M., Viglione, A., Hall, J., Blöschl, G., 2019. Flood trends in Europe: are changes in small and big floods
356 different? *Hydrology and Earth System Sciences Discussions* 1–23. <https://doi.org/10.5194/hess-2019-523>
- 357 Blöschl, G., Hall, J., Viglione, A., Perdigão, R.A.P., Parajka, J., Merz, B., Lun, D., Arheimer, B., Aronica, G.T.,
358 Bilibashi, A., Boháč, M., Bonacci, O., Borga, M., Čanjevac, I., Castellarin, A., Chirico, G.B., Claps, P., Frolova,
359 N., Ganora, D., Gorbachova, L., Gül, A., Hannaford, J., Harrigan, S., Kireeva, M., Kiss, A., Kjeldsen, T.R.,
360 Kohnová, S., Koskela, J.J., Ledvinka, O., Macdonald, N., Mavrova-Guirguinova, M., Mediero, L., Merz, R.,
361 Molnar, P., Montanari, A., Murphy, C., Osuch, M., Ovcharuk, V., Radevski, I., Salinas, J.L., Sauquet, E., Šraj,
362 M., Szolgay, J., Volpi, E., Wilson, D., Zaimi, K., Živković, N., 2019. Changing climate both increases and
363 decreases European river floods. *Nature* 573, 108–111. <https://doi.org/10.1038/s41586-019-1495-6>
- 364 Börgel, F., Frauen, C., Neumann, T., Meier, H.E.M., 2020. The Atlantic Multidecadal Oscillation controls the impact of
365 the North Atlantic Oscillation on North European climate. *Environmental Research Letters* 15.
366 <https://doi.org/10.1088/1748-9326/aba925>

367 Brandimarte, L., di Baldassarre, G., Bruni, G., D'Odorico, P., Montanari, A., D'Odorico, P., Montanari, A., 2011.
368 Relation Between the North-Atlantic Oscillation and Hydroclimatic Conditions in Mediterranean Areas. *Water*
369 *Resources Management* 25, 1269–1279. <https://doi.org/10.1007/s11269-010-9742-5>

370 Caloiero, T., Caloiero, P., Frustaci, F., 2018. Long-term precipitation trend analysis in Europe and in the Mediterranean
371 basin. *Water and Environment Journal* 32, 433–445. <https://doi.org/https://doi.org/10.1111/wej.12346>

372 Caloiero, T., Coscarelli, R., Ferrari, E., Mancini, M., 2011. Precipitation change in Southern Italy linked to global scale
373 oscillation indexes. *Nat. Hazards Earth Syst. Sci.* 11, 1683–1694. <https://doi.org/10.5194/nhess-11-1683-2011>

374 Cardoso Pereira, S., Marta-Almeida, M., Carvalho, A.C., Rocha, A., 2020. Extreme precipitation events under climate
375 change in the Iberian Peninsula. *International Journal of Climatology* 40, 1255–1278.
376 <https://doi.org/https://doi.org/10.1002/joc.6269>

377 Climate Prediction Center, 2021. East Atlantic [WWW Document]. URL
378 <https://www.cpc.ncep.noaa.gov/data/teledoc/ea.shtml> (accessed 9.22.21).

379 Climatic Research Unit, 2021. Mediterranean Oscillation Indices (MOI) [WWW Document]. URL
380 <https://crudata.uea.ac.uk/cru/data/moi/> (accessed 9.22.21).

381 Colantoni, A., Delfanti, L., Cossio, F., Baciotti, B., Salvati, L., Perini, L., Lord, R., 2015. Soil Aridity under Climate
382 Change and Implications for Agriculture in Italy. *Applied Mathematical Sciences* 9, 2467–2475.
383 <https://doi.org/10.12988/ams.2015.52112>

384 D'Amato Avanzi, G., Giannecchini, R., Puccinelli, A., 2004. The influence of the geological and geomorphological
385 settings on shallow landslides. An example in a temperate climate environment: the June 19, 1996 event in
386 northwestern Tuscany (Italy). *Engineering Geology* 73, 215–228.
387 <https://doi.org/https://doi.org/10.1016/j.enggeo.2004.01.005>

388 Deitch, M.J., Sapundjieff, M.J., Feirer, S.T., 2017. Characterizing Precipitation Variability and Trends in the World's
389 Mediterranean-Climate Areas. *Water* 9. <https://doi.org/10.3390/w9040259>

390 Deser, C., Hurrell, J.W., Phillips, A.S., 2017. The role of the North Atlantic Oscillation in European climate projections.
391 *Climate Dynamics* 49, 3141–3157. <https://doi.org/10.1007/s00382-016-3502-z>

392 Dünkeloh, A., Jacobeit, J., 2003. Circulation dynamics of Mediterranean precipitation variability 1948–98. *International*
393 *Journal of Climatology* 23, 1843–1866. <https://doi.org/https://doi.org/10.1002/joc.973>

394 European Environment Agency, 2019. Economic losses from climate -related extremes in Europe. *Indicator*
395 *Assessment*.

396 Ferrari, E., Caloiero, T., Coscarelli, R., 2013. Influence of the North Atlantic Oscillation on winter rainfall in Calabria
397 (southern Italy). *Theoretical and Applied Climatology* 114, 479–494. <https://doi.org/10.1007/s00704-013-0856-6>

398 Frankignoul, C., Friederichs, P., Kestenare, E., 2003. Influence of Atlantic SST anomalies on the atmospheric
399 circulation in the Atlantic-European sector, *ANNALS OF GEOPHYSICS*.

400 George, D.G., Järvinen, M., Arvola, L., 2004. The influence of the North Atlantic Oscillation on the winter
401 characteristics of Windermere (UK) and Pääjärvi (Finland).

402 Giannecchini, R., 2006. Relationship between rainfall and shallow landslides in the southern Apuan Alps (Italy).
403 *Natural Hazards and Earth System Science* 6, 357–364. <https://doi.org/10.5194/nhess-6-357-2006>

404 Giannecchini, R., D'Amato Avanzi, G., 2012. Historical research as a tool in estimating hydrogeological hazard in a
405 typical small alpine-like area: The example of the Versilia River basin (Apuan Alps, Italy). *Physics and*
406 *Chemistry of the Earth, Parts A/B/C* 49, 32–43. <https://doi.org/10.1016/J.PCE.2011.12.005>

407 Giorgi, F., 2006. Climate change hot-spots. *Geophysical Research Letters* 33.
408 <https://doi.org/https://doi.org/10.1029/2006GL025734>

409 Halifa-Marín, A., Lorente-Plazas, R., Pravia-Sarabia, E., Montávez, J.P., Jiménez-Guerrero, P., 2021. Atlantic and
410 Mediterranean influence promoting an abrupt change in winter precipitation over the southern Iberian Peninsula.
411 *Atmospheric Research* 253. <https://doi.org/10.1016/j.atmosres.2021.105485>

412 Hurrell, J.W., 1995. Decadal Trends in the North Atlantic Oscillation: Regional Temperatures and Precipitation.
413 *Science* 269, 676 LP – 679. <https://doi.org/10.1126/science.269.5224.676>

414 Izquierdo, R., Alarcón, M., Aguiillaume, L., Àvila, A., 2014. Effects of teleconnection patterns on the atmospheric
415 routes, precipitation and deposition amounts in the north-eastern Iberian Peninsula. *Atmospheric Environment* 89,
416 482–490. <https://doi.org/https://doi.org/10.1016/j.atmosenv.2014.02.057>

417 Knight, J.R., Allan, R.J., Folland, C.K., Vellinga, M., Mann, M.E., 2005. A signature of persistent natural thermohaline
418 circulation cycles in observed climate. *Geophysical Research Letters* 32. <https://doi.org/10.1029/2005GL024233>

419 Longobardi, A., Villani, P., 2010. Trend analysis of annual and seasonal rainfall time series in the Mediterranean area.
420 *International Journal of Climatology* 30, 1538–1546. <https://doi.org/https://doi.org/10.1002/joc.2001>

421 Lopez-Bustins, J.A., Arbiol-Roca, L., Martin-Vide, J., Barrera-Escoda, A., Prohom, M., 2020. Intra-annual variability
422 of the Western Mediterranean Oscillation (WeMO) and occurrence of extreme torrential precipitation in Catalonia
423 (NE Iberia). *Natural Hazards and Earth System Sciences* 20, 2483–2501. [https://doi.org/10.5194/nhess-20-2483-](https://doi.org/10.5194/nhess-20-2483-2020)
424 2020

425 Lopez-Bustins, J.-A., Martin-Vide, J., Sanchez-Lorenzo, A., 2008. Iberia winter rainfall trends based upon changes in
426 teleconnection and circulation patterns. *Global and Planetary Change* 63, 171–176.
427 <https://doi.org/https://doi.org/10.1016/j.gloplacha.2007.09.002>

428 López-Moreno, J.I., Vicente-Serrano, S.M., Morán-Tejeda, E., Lorenzo-Lacruz, J., Kenawy, A., Beniston, M., 2011.
429 Effects of the North Atlantic Oscillation (NAO) on combined temperature and precipitation winter modes in the
430 Mediterranean mountains: Observed relationships and projections for the 21st century. *Global and Planetary*
431 *Change* 77, 62–76. <https://doi.org/https://doi.org/10.1016/j.gloplacha.2011.03.003>

432 Luppichini, M., Barsanti, M., Giannecchini, R., Bini, M., 2021. Statistical relationships between large-scale circulation
433 patterns and local-scale effects: NAO and rainfall regime in a key area of the Mediterranean basin. *Atmospheric*
434 *Research* 248, 105270.

435 Martín, P., Sabatés, A., Lloret, J., Martin-Vide, J., 2012. Climate modulation of fish populations: The role of the
436 Western Mediterranean Oscillation (WeMO) in sardine (*Sardina pilchardus*) and anchovy (*Engraulis encrasicolus*)
437 production in the north-western Mediterranean. *Climatic Change* 110, 925–939. [https://doi.org/10.1007/s10584-](https://doi.org/10.1007/s10584-011-0091-z)
438 [011-0091-z](https://doi.org/10.1007/s10584-011-0091-z)

439 Martínez-Artigas, J., Lemus-Canovas, M., Lopez-Bustins, J.A., 2021. Precipitation in peninsular Spain: Influence of
440 teleconnection indices and spatial regionalisation. *International Journal of Climatology* 41, E1320–E1335.
441 <https://doi.org/https://doi.org/10.1002/joc.6770>

442 Martin-Vide, J., Lopez-Bustins, J.-A., 2006. The Western Mediterranean Oscillation and rainfall in the Iberian
443 Peninsula. *International Journal of Climatology* 26, 1455–1475. <https://doi.org/https://doi.org/10.1002/joc.1388>

444 Mellado-Cano, J., Barriopedro, D., García-Herrera, R., Trigo, R.M., Hernández, A., 2019. Examining the North Atlantic
445 Oscillation, East Atlantic Pattern, and Jet Variability since 1685. *Journal of Climate* 32, 6285–6298.
446 <https://doi.org/10.1175/JCLI-D-19-0135.1>

447 Myhre, G., Alterskjær, K., Stjern, C.W., Hodnebrog, Ø., Marelle, L., Samset, B.H., Sillmann, J., Schaller, N., Fischer,
448 E., Schulz, M., Stohl, A., 2019. Frequency of extreme precipitation increases extensively with event rareness
449 under global warming. *Scientific Reports* 9, 16063. <https://doi.org/10.1038/s41598-019-52277-4>

450 Nalley, D., Adamowski, J., Biswas, A., Gharabaghi, B., Hu, W., 2019. A multiscale and multivariate analysis of
451 precipitation and streamflow variability in relation to ENSO, NAO and PDO. *Journal of Hydrology* 574, 288–
452 307. <https://doi.org/https://doi.org/10.1016/j.jhydrol.2019.04.024>

453 National Center for Atmospheric Research Staff (Eds), 2021. The Climate Data Guide: Hurrell North Atlantic
454 Oscillation (NAO) Index (PC-based). [WWW Document]. <https://climatedataguide.ucar.edu/climate-data/hurrell->

455 north-atlantic-oscillation-nao-index-pc-based. URL [https://climatedataguide.ucar.edu/climate-data/hurrell-north-](https://climatedataguide.ucar.edu/climate-data/hurrell-north-atlantic-oscillation-nao-index-pc-based)
456 [atlantic-oscillation-nao-index-pc-based](https://climatedataguide.ucar.edu/climate-data/hurrell-north-atlantic-oscillation-nao-index-pc-based). (accessed 9.22.21).

457 NOAA, 2021. Extended Reconstructed SST [WWW Document]. URL [https://www.ncei.noaa.gov/products/extended-](https://www.ncei.noaa.gov/products/extended-reconstructed-sst)
458 [reconstructed-sst](https://www.ncei.noaa.gov/products/extended-reconstructed-sst) (accessed 9.28.21).

459 Pastor, F., Valiente, J.A., Khodayar, S., 2020. A warming Mediterranean: 38 years of increasing sea surface
460 temperature. *Remote Sensing* 12. <https://doi.org/10.3390/RS12172687>

461 Philandras, C., Nastos, P., Kapsomenakis, J., Douvis, K., Tselioudis, G., Zerefos, C., 2011. Long Term Precipitation
462 Trends and Variability within the Mediterranean Region. *Natural Hazards and Earth System Sciences* 11, 3235–
463 3250. <https://doi.org/10.5194/nhess-11-3235-2011>

464 Rapetti, F., Vittorini, S., 1994. Le precipitazioni in Toscana: osservazioni sui casi estremi. *RIVISTA GEOGRAFICA*
465 *ITALIANA* 101, 47–76.

466 Riaz, S.M.F., Iqbal, M.J., Hameed, S., 2017. Impact of the North Atlantic Oscillation on winter climate of Germany.
467 *Tellus, Series A: Dynamic Meteorology and Oceanography* 69. <https://doi.org/10.1080/16000870.2017.1406263>

468 Ríos-Cornejo, D., Penas, Á., Álvarez-Esteban, R., del Río, S., 2015. Links between teleconnection patterns and
469 precipitation in Spain. *Atmospheric Research* 156, 14–28.

470 Robertson, A.W., Mechoso, C.R., Kim, Y.-J., 2000. The Influence of Atlantic Sea Surface Temperature Anomalies on
471 the North Atlantic Oscillation. *Journal of Climate* 13, 122–138. [https://doi.org/10.1175/1520-](https://doi.org/10.1175/1520-0442(2000)013<0122:TIOASS>2.0.CO;2)
472 [0442\(2000\)013<0122:TIOASS>2.0.CO;2](https://doi.org/10.1175/1520-0442(2000)013<0122:TIOASS>2.0.CO;2)

473 Rousi, E., Rust, H.W., Ulbrich, U., Anagnostopoulou, C., 2020. Implications of Winter NAO Flavors on Present and
474 Future European Climate. *Climate* 8, 13. <https://doi.org/10.3390/cli8010013>

475 Spearman, C., 1904. The proof and measurement of association between two things. *The American Journal of*
476 *Psychology* 15, 72–101. <https://doi.org/10.2307/1412159>

477 Stagl, J., Mayr, E., Koch, H., Hattermann, F.F., Huang, S., 2014. Effects of Climate Change on the Hydrological Cycle
478 in Central and Eastern Europe BT - Managing Protected Areas in Central and Eastern Europe Under Climate
479 Change, in: Rannow, S., Neubert, M. (Eds.), . Springer Netherlands, Dordrecht, pp. 31–43.

480 Trambly, Y., Llasat, M.C., Randin, C., Coppola, E., 2020. Climate change impacts on water resources in the
481 Mediterranean. *Regional Environmental Change* 20, 83. <https://doi.org/10.1007/s10113-020-01665-y>

482 Trigo, I.F., Bigg, G.R., Davies, T.D., 2002. Climatology of Cyclogenesis Mechanisms in the Mediterranean.

483 Trigo, R.M., Pozo- Vázquez, D., Osborn, T.J., Castro- Díez, Y., Gámiz- Fortis, S., Esteban- Parra, M.J., Pozo-
484 Vázquez, D., Osborn, T.J., Castro-Díez, Y., Gámiz-Fortis, S., Esteban-Parra, M.J., 2004. North Atlantic

485 Oscillation influence on precipitation, river flow and water resources in the Iberian Peninsula. *International*
486 *Journal of Climatology: A Journal of the Royal Meteorological Society* 24, 925–944.
487 <https://doi.org/10.1002/joc.1048>

488 Vergni, L., Chiaudani, A., 2015. RELATIONSHIP BETWEEN THE NAO INDEX AND SOME INDICES OF
489 EXTREME PRECIPITATION IN THE ABRUZZO REGION.

490 Vergni, L., di Lena, B., Chiaudani, A., 2016. Statistical characterisation of winter precipitation in the Abruzzo region
491 (Italy) in relation to the North Atlantic Oscillation (NAO). *Atmospheric Research* 178–179, 279–290.
492 <https://doi.org/https://doi.org/10.1016/j.atmosres.2016.03.028>

493 Vicente-Serrano, S.M., López-Moreno, J.I., 2008. Nonstationary influence of the North Atlantic Oscillation on
494 European precipitation. *Journal of Geophysical Research: Atmospheres* 113.
495 <https://doi.org/10.1029/2008JD010382>

496 Virtanen, P., Gommers, R., Oliphant, T.E., Haberland, M., Reddy, T., Cournapeau, D., Burovski, E., Peterson, P.,
497 Weckesser, W., Bright, J., van der Walt, S.J., Brett, M., Wilson, J., Millman, K.J., Mayorov, N., Nelson, A.R.J.,
498 Jones, E., Kern, R., Larson, E., Carey, C.J., Polat, \.Ilhan, Feng, Y., Moore, E.W., VanderPlas, J., Laxalde, D.,
499 Perktold, J., Cimrman, R., Henriksen, I., Quintero, E.A., Harris, C.R., Archibald, A.M., Ribeiro, A.H., Pedregosa,
500 F., van Mulbregt, P., SciPy 1.0 Contributors, 2020. SciPy 1.0: Fundamental Algorithms for Scientific Computing
501 in Python. *Nature Methods* 17, 261–272. <https://doi.org/10.1038/s41592-019-0686-2>

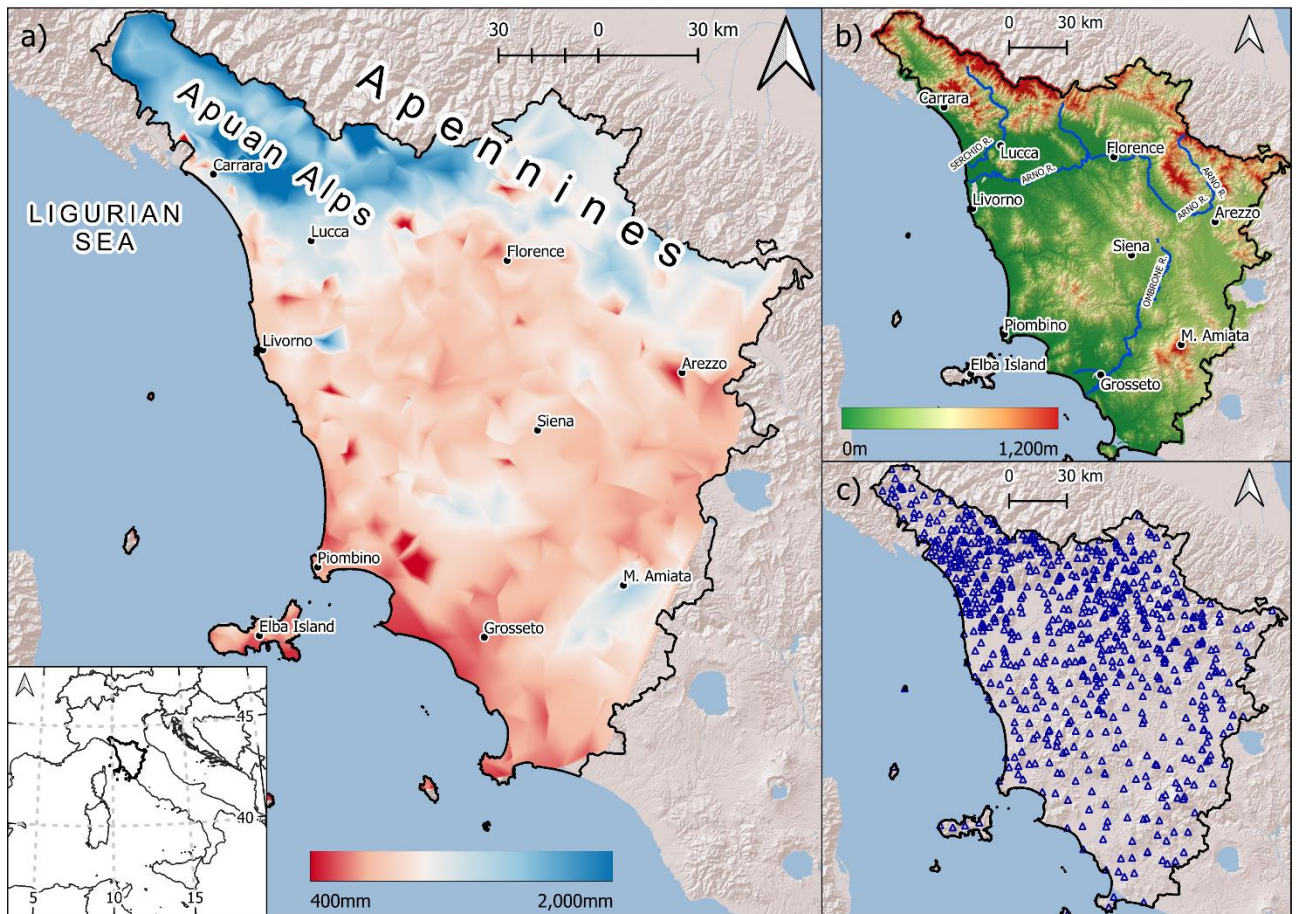
502 Visbeck, M.H., Hurrell, J.W., Polvani, L., Cullen, H.M., 2001. The North Atlantic Oscillation: Past, present, and future.
503 *Proceedings of the National Academy of Sciences* 98, 12876. <https://doi.org/10.1073/pnas.231391598>

504 Wang, C., Dong, S., 2010. Is the basin-wide warming in the North Atlantic Ocean related to atmospheric carbon dioxide
505 and global warming? *Geophysical Research Letters - GEOPHYS RES LETT* 37.
506 <https://doi.org/10.1029/2010GL042743>

507 West, H., Quinn, N., Horswell, M., 2019. Regional rainfall response to the North Atlantic Oscillation (NAO) across
508 Great Britain. *Hydrology Research* 50, 1549–1563. <https://doi.org/10.2166/nh.2019.015>

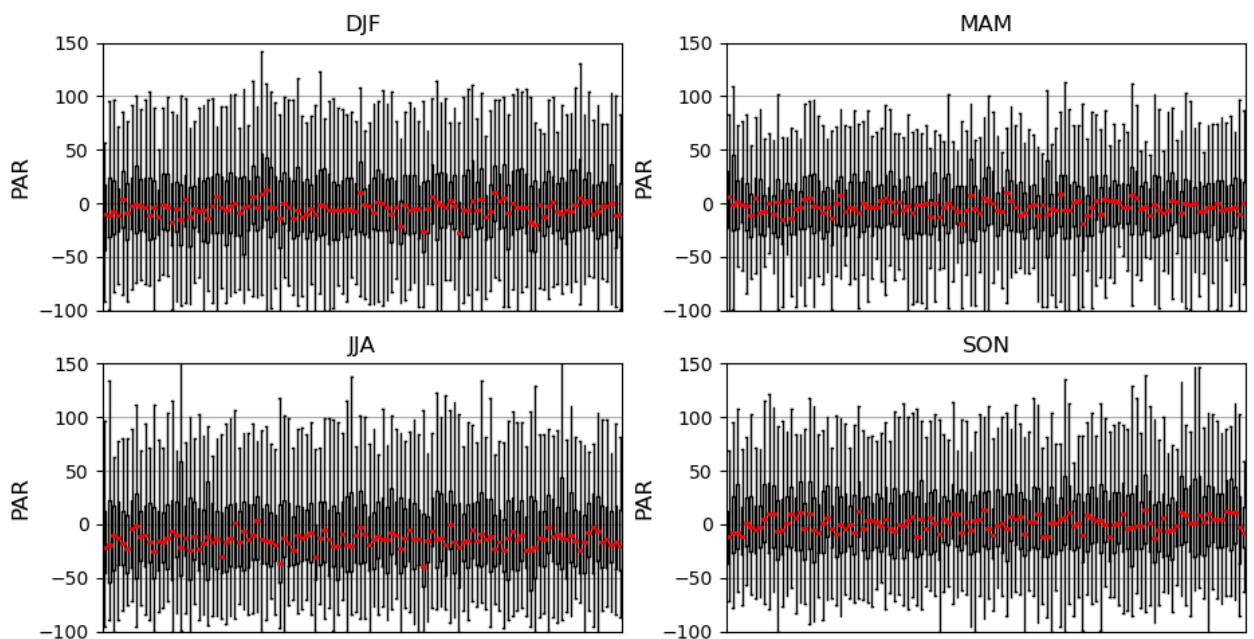
509 Xu, H., Taylor, R.G., Xu, Y., 2011. Quantifying uncertainty in the impacts of climate change on river discharge in sub-
510 catchments of the Yangtze and Yellow River Basins, China. *Hydrol. Earth Syst. Sci.* 15, 333–344.
511 <https://doi.org/10.5194/hess-15-333-2011>

512



514

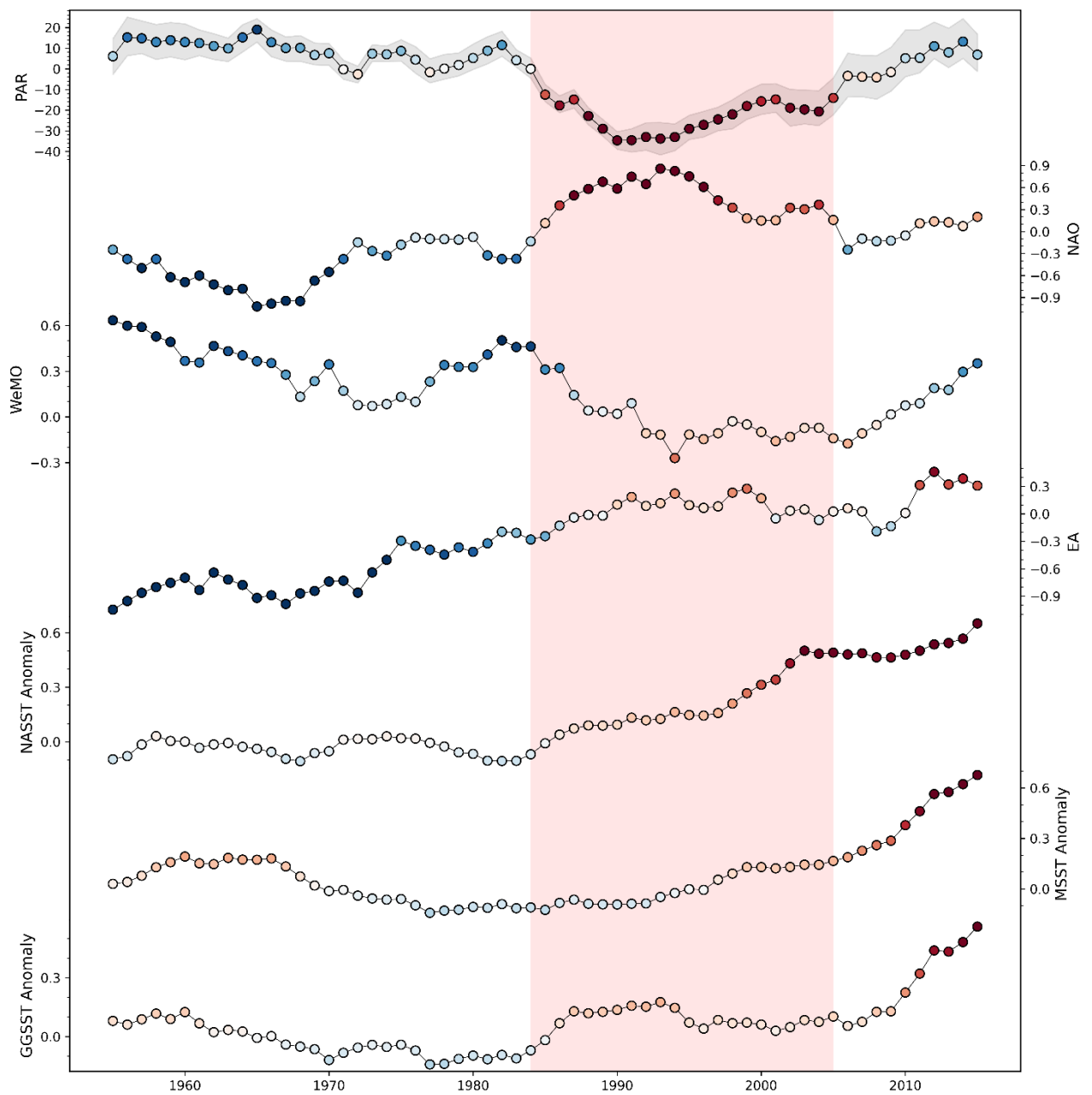
515 **Figure 1.** a) mean annual precipitation (MAP) of Tuscany linked to the morphology: the rainiest areas correspond to
 516 the mountainous areas; b) morphology of Tuscany; c) the 1103 raingauges of the Tuscany Region Hydrologic Service
 517 network used in this work.



518

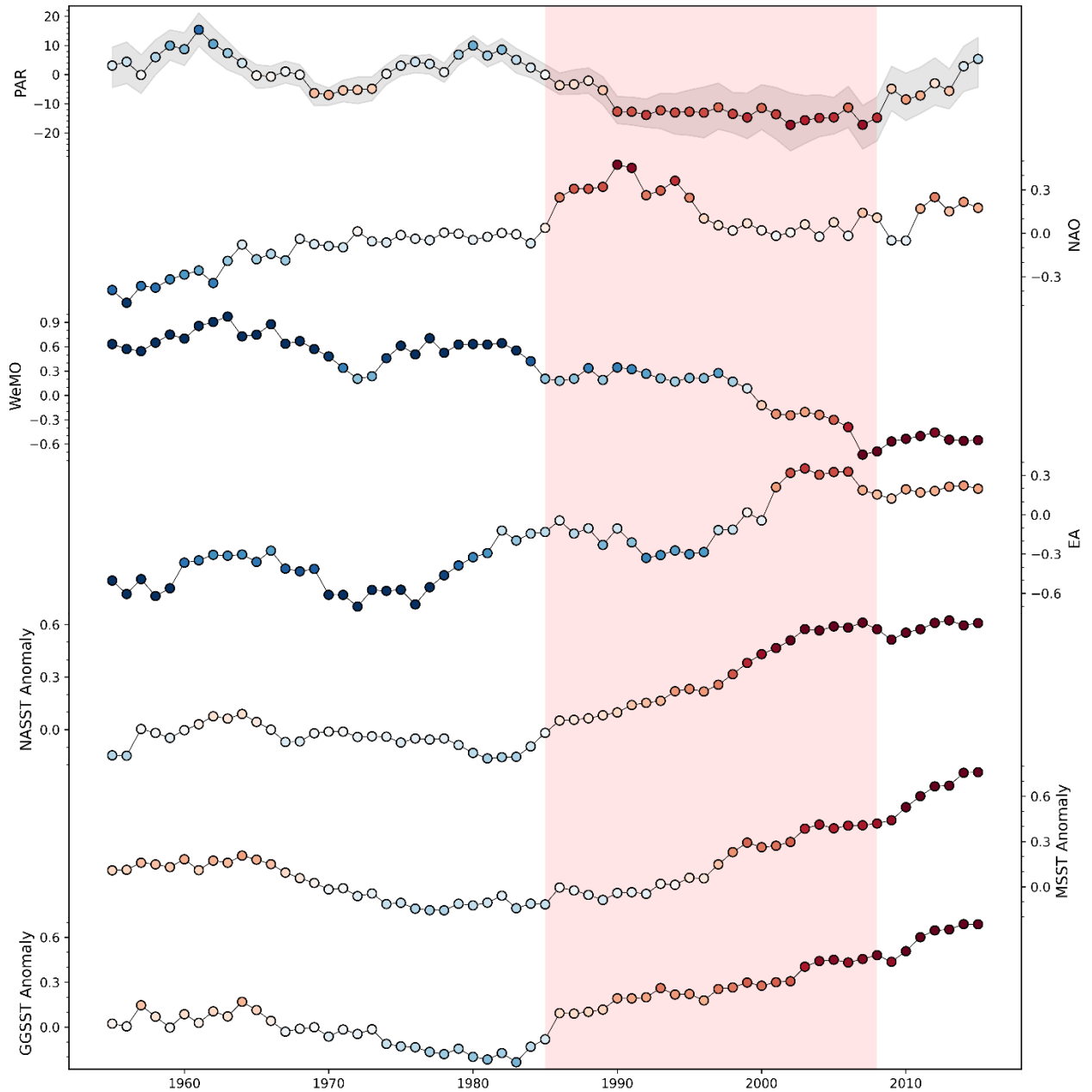
519 **Figure 2.** Percentage Anomaly of Rainfall (PAR) of the 117 rainfall time series used in this work, calculated for the
 520 four seasons. Each boxplot is referred to a rainfall time series. The boxes represent the interval between the 25th and
 521 75th percentiles (Q1 and Q3). IQR is the interquartile range $Q3-Q1$. The upper whisker will extend to the last datum
 522 lower than $Q3 + 1.5 \times IQR$. Similarly, the lower whisker will reach the first datum higher than $Q1 - 1.5 \times IQR$. The red
 523 lines represent the medians (DJF: December-January-February; MAM: March-April-May; JJA: June-July-August;
 524 SON: September-October-November).

525

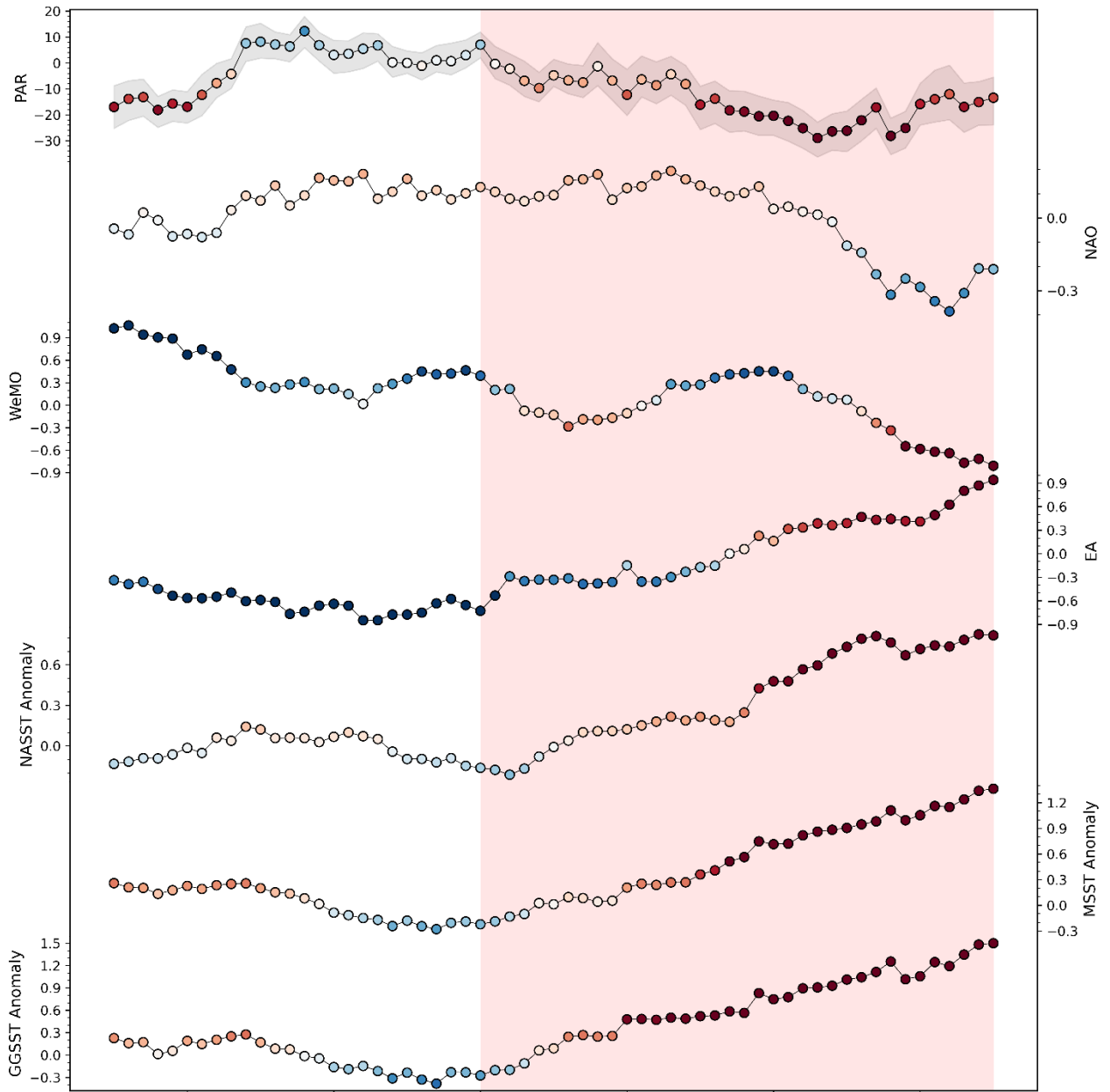


526 **Figure 3.** Trends of Percentage Anomaly Rainfall (PAR), NAO, WeMO, EA, North Atlantic Sea Surface
 527 Temperature (NASST), Mediterranean Sea Surface Temperature (MSST), and Genoa Gulf Sea Surface Temperature
 528

529 (GG SST) for the DJF season. The trends are smoothed by a 10-year mobile window and the colour of the points varies
 530 between blue and red: blue is linked to wet periods, red to dry periods. The grey band on PAR represents the 25th and
 531 75th percentile. The pink band is referred to the main dry period of the time series.

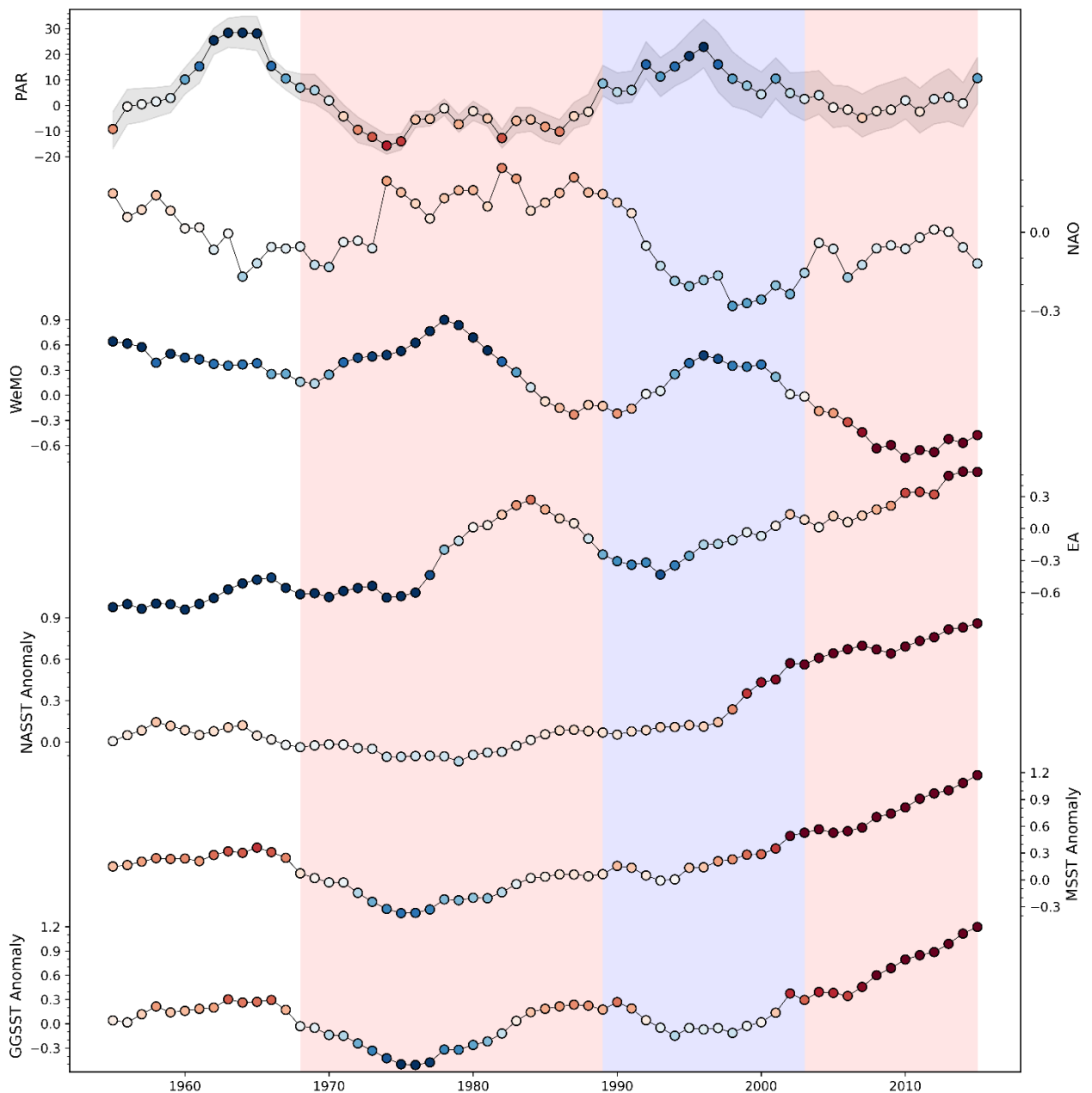


532
 533 **Figure 4.** Trends of Percentage Anomaly Rainfall (PAR), NAO, WeMO, EA, North Atlantic Sea Surface
 534 Temperature (NASST), Mediterranean Sea Surface Temperature (MSST), and Genoa Gulf Sea Surface Temperature
 535 (GG SST) for the MAM season. The trends are smoothed by a 10-year mobile window and the colour of the points goes
 536 from blue to red: blue is linked to wet periods, red to dry periods. The grey band on PAR represents the 25th and
 537 75th percentiles. The pink band refers to the main dry period of the time series.



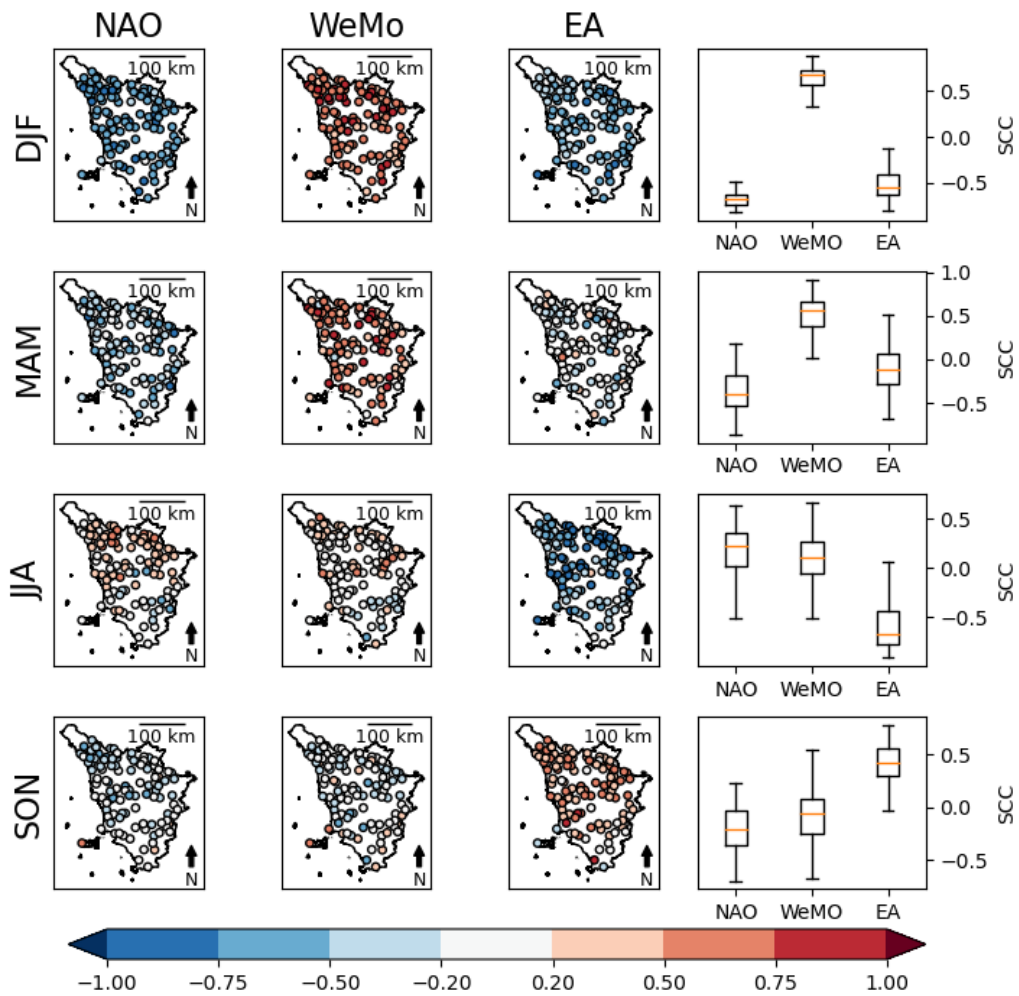
538

539 **Figure 5.** Trends of Percentage Anomaly Rainfall (PAR), NAO, WeMO, EA, North Atlantic Sea Surface
 540 Temperature (NASST), Mediterranean Sea Surface Temperature (MSST), and Genoa Gulf Sea Surface Temperature
 541 (GGSST) for the JJA season. The trends are smoothed with a 10-year mobile window and the colour of the points varies
 542 between blue to red: blue is linked to wet periods, while red is linked to dry periods. The grey band on PAR represents
 543 the 25th and 75th percentile. The pink band refers to the main dry period of the time series.



544

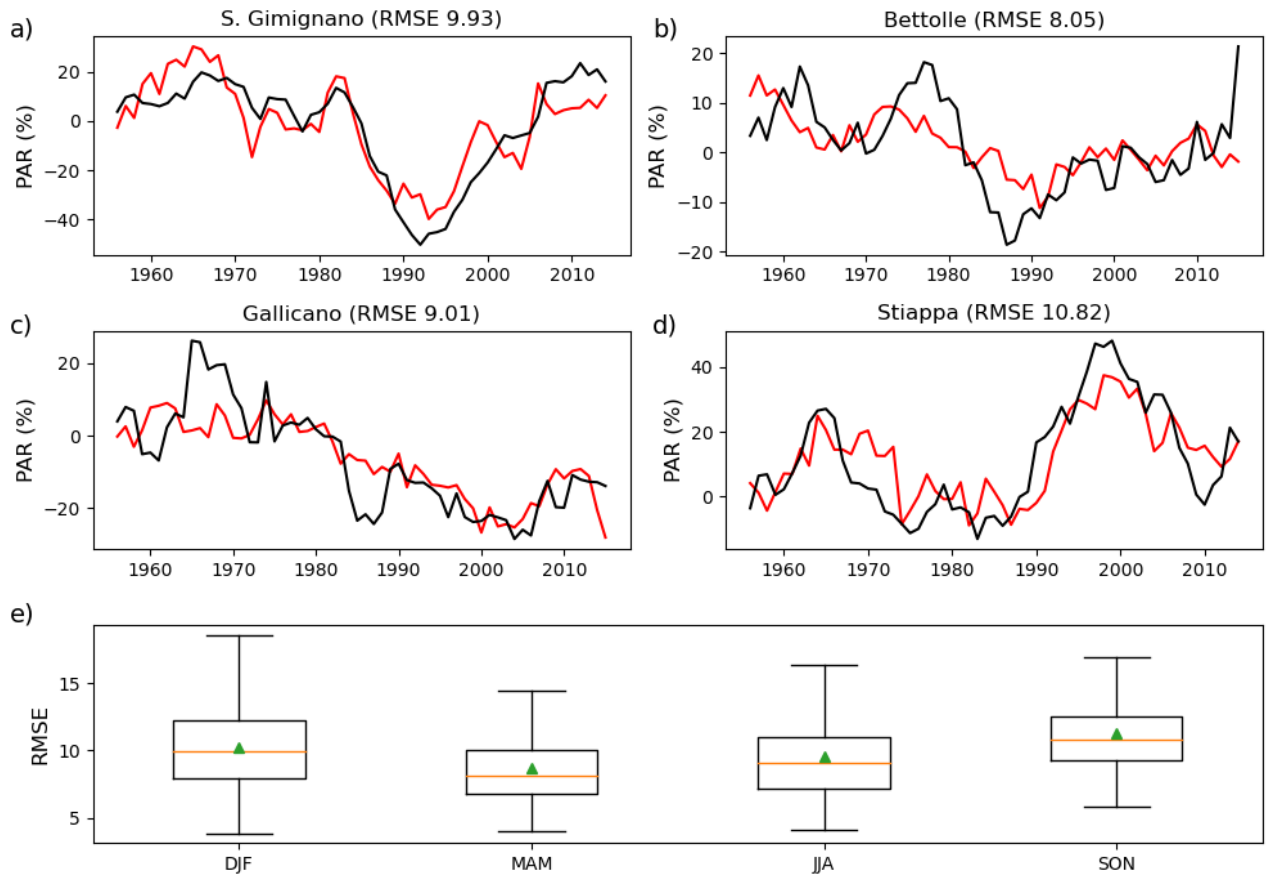
545 **Figure 6** Trends of Percentage Anomaly Rainfall (PAR), NAO, WeMO, EA, North Atlantic Sea Surface
 546 Temperature (NASST), Mediterranean Sea Surface Temperature (MSST), and Genoa Gulf Sea Surface Temperature
 547 (GGSST) for the SON season. The trends are smoothed with a 10-year mobile window and the colour of the points
 548 varies between blue to red: blue indicates wet periods, red indicates dry periods. The grey band on PAR represents the
 549 25th and 75th percentile. The pink band is referred to the main dry period of the time series, while the blue band is
 550 referred to the main wet period of the time series.



551

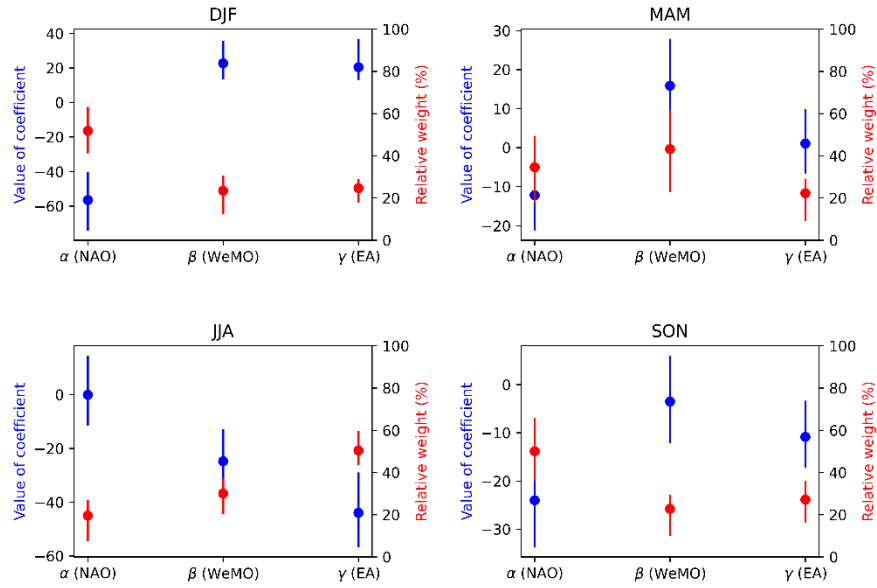
552 **Figure 7.** Spearman's correlation coefficients (SCC) between season rainfall and climatic patterns. For each season,
 553 we report the correlation with NAO, EA and WeMo and the relative boxplots. The boxes represent the interval between
 554 the 25th and 75th percentiles (Q1 and Q3). IQR is the interquartile range Q3-Q1. The upper whisker will extend to the
 555 last datum lower than $Q3 + 1.5 \times IQR$. Similarly, the lower whisker will reach the first datum higher than $Q1 - 1.5 \times IQR$.
 556 The orange lines represent the medians (DJF: December-January-February; MAM: March-April-May; JJA: June-July-
 557 August; SON: September-October-November).

558



559

560 **Figure 8.** a-d) Four examples of observed PAR (black line) and predicted PAR (red line) respectively for the
 561 seasons DJF, MAM, JJA and SON. We selected these examples because they have Root Mean Square Error (RMSE)
 562 values similar to the error medians calculated on the whole dataset; e) the boxplots represent the RMSE of the linear
 563 models for the four seasons. The boxes represent the interval between the 25th and 75th percentiles (Q1 and Q3). IQR is
 564 the interquartile range $Q3 - Q1$. The upper whisker will extend to the last datum lower than $Q3 + 1.5 \times IQR$. Similarly, the
 565 lower whisker will reach the first datum higher than $Q1 - 1.5 \times IQR$. The orange lines represent the medians, while the
 566 green triangles represent the means (DJF: December-January-February; MAM: March-April-May; JJA: June-July-
 567 August; SON: September-October-November).



568

569 **Figure 9.** Setting of the linear model coefficients used to understand the relationship between climate patterns and
 570 rainfall. The blue circle is the mean absolute value of the coefficient, whereas the red circle represents the mean relative
 571 weight of the coefficient on the prediction. The results are reported for each season. The blue and red lines represent the
 572 interval between the 25th and 75th percentiles of the coefficient distributions (DJF: December-January-February; MAM:
 573 March-April-May; JJA: June-July-August; SON: September-October-November).

Declaration of interests

The authors declare that they have no known competing financial interests or personal relationships that could have appeared to influence the work reported in this paper.

The authors declare the following financial interests/personal relationships which may be considered as potential competing interests:

Conflicts of Interest

The authors declare no conflict of interest. The funders had no role in the design of the study; in the collection, analyses, or interpretation of data; in the writing of the manuscript, or in the decision to publish the results.

Cover letter

Dear Editor of Journal of Hydrology,

I am submitting a manuscript for consideration of publication in Journal of Hydrology. The manuscript is entitled “Influence of large-scale atmospheric circulation on the rainfall of a key Mediterranean area: how does current global change affect the rainfall regime?”.

It has not been published elsewhere and that it has not been submitted simultaneously for publication elsewhere.

The work aim is to understand the variation of the rainfall trend in the last 70 years in an important area of the Mediterranean. The study area is influenced by the most important cyclonic and anticyclonic dynamics of the Northern Hemisphere, which are represented by North Atlantic Oscillation, East Atlantic, and Western Mediterranean Oscillations. The study of the influences of these climatic patterns is very important in the contest of the current climate change. The study demonstrated a clear reduction of rainfall during the warm period of the year. This is in accordance with several studies, and the rainfall trend is explained with the pattern trends.

We think that the article may be of interest to your journal as it belongs to the category of hydrometeorology.

Thank you very much for your consideration.

Yours Sincerely,

Dr. Marco Luppichini

University of Pisa

Via Santa Maria 53, 56126 Pisa, Italy

E-mail: marco.luppichini@unifi.it

1 **Seasonal rainfall trends ~~Influence of large-scale atmospheric~~**
2 **circulation on of the rainfall of a key Mediterranean area in**
3 **relationship towith the large-scale atmospheric circulation: how does**
4 **current global change affect the rainfall regime?**

5 Marco Luppichini^{1,2,*}, Monica Bini^{2,3,4}, Michele Barsanti⁵, Roberto Giannecchini^{2,4,6}, Giovanni Zanchetta^{2,4,7}

6 ¹ Department of Earth Sciences, University of Study of Florence, Via La Pira 4, Florence, Italy

7 ² Department of Earth Sciences, University of Pisa, Via S. Maria, 52, 56126 Pisa, Italy

8 ³ Istituto Nazionale di Geofisica e Vulcanologia (INGV), Via Vigna Murata 605, 00143 Roma, Italy

9 ⁴ CIRSEC Centro Interdipartimentale di Ricerca per lo Studio degli Effetti del Cambiamento Climatico
10 dell'Università di Pisa, Via del Borghetto 80, 56124 Pisa, Italy

11 ⁵ Department of Civil and Industrial Engineering, University of Pisa, Largo L. Lazzarino, 56122 Pisa, Italy

12 ⁶ Institute of Geosciences and Earth Resources, IGG-CNR, via Moruzzi 1, 56124 Pisa, Italy

13 ⁷ Istituto di Geologia Ambientale e Geoingegneria, IGAG-CNR, Rome, Italy

14 **Abstract**

15 Current global warming causes a change in atmospheric dynamics, with consequent variations in the rainfall
16 regimes. Understanding the relationship between global climate patterns, global warming, and rainfall regimes is crucial
17 for the creation of future scenarios and for the relative modification of water management. The aim of this study is to
18 improve ~~the~~ knowledge of the relationship ~~of-between~~ North Atlantic Oscillation (NAO), East Atlantic (EA), and
19 Western Mediterranean Oscillation (WeMO) with the seasonal rainfalls in Tuscany, Italy. The study area occupies a
20 strategic position since it lies in a transition zone between the wet area of northern Europe and the dry area of the
21 northern coast of Africa. This research, based on a statistical correlation method and on linear models, is designed to
22 understand the relationship between seasonal rainfalls and climate patterns. ~~The results of this study demonstrate that~~
23 ~~The method ofof the use of~~ linear models ~~innovative in this thematic area~~, can yield more information than ~~traditional~~
24 statistical correlations. The results show a ~~possible~~ decrease in rainfall in the warm period of the year, namely in the
25 summer, when its expression is most visible. This phenomenon is ascribable to current global warming, which causes
26 an increase in sea-surface temperatures. An increase in the Northern Atlantic Sea Surface Temperature (~~SST~~) and in the
27 Mediterranean Sea Surface Temperature (~~SST~~) causes a reduction of the Iceland Low, with an extension of the Azores

28 High. Moreover, an increase in the Genoa Gulf SST induces a weakening of the Genoa Gulf Low, one of the main
29 cyclogenetic systems of the Mediterranean.

30 **Keywords:** Climatic Patterns, Current Global Warming, East Atlantic, North Atlantic Oscillation, Western
31 Mediterranean Oscillation, rainfall trend, Tuscany.

32 **Introduction and goals**

33 Current global warming causes effects at different scale levels, including changes in the hydrological cycle (Allan,
34 2011; Bates et al., 2008). The effects are visible in air temperature trends and, more ~~complexively~~generally, in rainfall,
35 in the form of frequency and intensity of extreme events and changes in soil moisture (Blöschl et al., 2019; Stagl et al.,
36 2014; Xu et al., 2011), with wide implications in terms of ~~socioal~~-economic conditions and financial policy (European
37 Environment Agency, 2019). The Mediterranean region is an ideal research testbed for current climatic changes both
38 for its location ~~and for its~~ historico-cultural importance, and for having been considered a hot spot for future climatic
39 changes (Giorgi, 2006). The Mediterranean, located between the European humid domain and the North African arid
40 belt, provides alternating circulation regimes with large spatial and temporal variability (Dünkeloh and Jacobeit, 2003).
41 ~~Furthermore, the highly populated and industrialized Mediterranean region shows an increase in the demand of water~~
42 ~~supply.~~ In this context, a correct characterization of rainfall regimes can improve the management of water resources
43 (Tramblay et al., 2020) and ~~of~~ extreme events (Cardoso Pereira et al., 2020; Myhre et al., 2019). Several studies have
44 identified a general decrease (although with some exceptions) in the annual rainfall amount in the area of the
45 Mediterranean basin (Bertola et al., 2019; Blöschl et al., 2019; Caloiero et al., 2018, 2011; Colantoni et al., 2015;
46 Deitch et al., 2017; Dünkeloh and Jacobeit, 2003; Halifa-Marín et al., 2021; Longobardi and Villani, 2010; Martin-Vide
47 and Lopez-Bustins, 2006; Philandras et al., 2011; Ríos-Cornejo et al., 2015); and atmospheric patterns related to
48 mesoscale circulation (Brandimarte et al., 2011; Caloiero et al., 2011; Halifa-Marín et al., 2021; Lopez-Bustins et al.,
49 2008; Luppichini et al., 2021; Martinez-Artigas et al., 2021; Ríos-Cornejo et al., 2015; Trigo et al., 2004).

50 During the winter months, one of the main drivers of rainfall variability in southern Europe and in the
51 Mediterranean is the presence of different pressure fields over the Northern Atlantic Ocean and their variability
52 indicated as the North Atlantic Oscillation (NAO) (Hurrell, 1995). NAO is defined by an index measured as a north-
53 southern dipole of pressure anomalies, with one pole located at higher latitudes (Iceland Low 80°N) and the other at the
54 central latitudes of the North Atlantic between 35°N and 40°N (Azores High).

55 The East Atlantic (EA) index is similar to that of NAO but is displaced south-eastward to the approximate nodal
56 lines of the NAO pattern. The EA index is often interpreted as a downward-shifted NAO model, but its strong
57 subtropical link entails a different peculiarity. The EA value is positive when a significant drop in pressure occurs in the

58 Atlantic Ocean; at the same time, the subtropical oceanic anticyclone belt considerably rises in latitude and ~~reinforces~~
59 ~~strengthens itself~~. In response, the African anticyclone gains energy and invasiveness over the Mediterranean, subjecting
60 this area to frequent pulses of hot and dry Saharan air in all seasons (Climate Prediction Center, 2021; Mellado-Cano et
61 al., 2019). The NAO and EA indexes present interannual and annual variabilities with positive and negative phases. The
62 rainfall in the Mediterranean can be associated with a negative phase of NAO and/or EA, when we observe an
63 expansion of the Iceland Low. Instead, during a positive phase of NAO and/or EA, Northern Europe is the rainiest area
64 (Rousi et al., 2020). ~~Both NAO and EA are influenced by the Sea Surface Temperature (SST) of the Northern Atlantic~~
65 ~~Ocean (NASST) and of the Mediterranean (MSST). An increase in NASST and in MSST is correlated to an expansion~~
66 ~~of the Azores High and to a consecutive reduction of the Iceland Low, which cause a formation of the NAO and EA~~
67 ~~positive phases~~ (Frankignoul et al., 2003; Robertson et al., 2000; Visbeck et al., 2001). ~~More recently, NAO has been~~
68 ~~correlated to the Atlantic Multidecadal Oscillation (AMO), a representative index of the NASST trend~~ (Knight et al.,
69 2005). ~~AMO changes the zonal position of the NAO centre of action, moving the cyclonic area closer to Europe or to~~
70 ~~North America. During a positive phase of AMO, the Icelandic Low moves further towards North America, while the~~
71 ~~Azores High moves further towards Europe (and vice versa) for the negative phase of AMO~~ (Börgel et al., 2020). ~~The~~
72 ~~statistical correlation between the NAO and the winter rainfalls in Europe varies over time~~ (Vicente-Serrano and López-
73 ~~Moreno, 2008) and it is a function of NAO and AMO with a different role of the indices from northern Europe to the~~
74 ~~Mediterranean~~ (Luppichini et al., 2021).

75 The Western Mediterranean oscillation (WeMO) is an index often used to study variability in rainfall in alternative
76 to NAO in the Mediterranean region. The WeMO index is the difference of atmospheric pressure in a dipole, with the
77 first pole located in Padua (45.40°N, 11.48°E) in northern Italy and the second one located in San Fernando, Cádiz
78 (36.28°N, 6.12°W) in southwestern Spain (Climatic Research Unit, 2021). Specifically, the former is located in the Po
79 plain (an area with relatively high barometric variability due to the different influence of the central European
80 anticyclone and ~~of~~ the Genoa Gulf Low), while the latter pole is located in the Gulf of Cádiz in the southwest of the
81 Iberian Peninsula, often subject to the influence of the Azores anticyclone and, episodically, to the cut-off of
82 circumpolar lows or to its own cyclogenesis (Halifa-Marín et al., 2021; Lopez-Bustins et al., 2020; Martin-Vide and
83 Lopez-Bustins, 2006). A positive phase of WeMO is associated with a low-pressure area in the Ligurian Sea and with
84 an anticyclone in the Gulf of Cadiz. Instead, a negative phase of the index determines a low in the Gulf of Cadiz and an
85 anticyclone in Central Europe. ~~During the positive phase, in the Iberian Peninsula the winds are typically west and~~
86 ~~northwest coming from the North Atlantic area. These winds cross the continental areas of the peninsula, and become~~
87 ~~dry, causing rainfall on the north-western coasts and the inland. Conversely, a negative WeMO phase is associated with~~
88 ~~humid air masses travelling over the Mediterranean Sea. When these winds reach the eastern side of the Iberian~~

Formatted: Font color: Auto

89 Peninsula, they are laden with moisture, resulting in an increase in rainfall, sometimes torrential, in this WeMO is
90 influenced by NASST and MSST, but also by the Genoa Gulf Sea Surface Temperature (GGSST), with positive values
91 correlating to low values of SST (Martín et al., 2012; Martin-Vide and Lopez-Bustins, 2006).

92 Both NAO and EA are influenced by the Sea Surface Temperature (SST) of the Northern Atlantic Ocean (NASST)
93 and of the Mediterranean (MSST). An increase in NASST and in MSST is correlated to an expansion of the Azores
94 High and to a consecutive reduction of the Iceland Low, which cause a formation of the NAO and EA positive phases.
95 More recently, NAO has been correlated to the Atlantic Multidecadal Oscillation (AMO), a representative index of the
96 NASST trend. AMO changes the zonal position of the NAO center of action, moving the cyclonic area closer to Europe
97 or North America. During a positive phase of AMO, the Icelandic Low moves further towards North America, while the
98 Azores High moves further towards Europe (and viceversa) for the negative phase of AMO. WeMO is also influenced
99 by the NASST and MSST, but also by the Genoa Gulf Sea Surface Temperature (GGSST), with positive values
100 correlating to low values of SST. Current global warming causes a progressive increase in NASST, MSST and
101 GGSST (Pastor et al., 2020; Wang and Dong, 2010) so that NAO and EA are likely to be characterized by more
102 positive phases, and WeMO by more negative phases.

103 The purpose of this study is to understand the rainfall seasonal trends of the last 70 years in Tuscany (central Italy),
104 in relation to mesoscale circulation and to the indices defined above. The region has a strategic location: it is located in
105 the northern sector of the Mediterranean, in the proximity of the Genoa Gulf, by far the most. The rainfall dataset used
106 employed came derives from several raingauges with high spatial density and temporal activity from 1950 to 2020. The
107 large number of raingauges allowed us to which allow us to investigate the rainfall trend in great detail and with direct
108 measurements. The same dataset was used by Luppichini et al. (2020), who employed different types of elaboration to
109 understand the variable influence of NAO on the Tuscany rainfall. The rainfall trends are compared with the NAO, EA
110 and WeMO indices by means of mathematical and statistical methods, so as to understand the climatic trends
111 influencing the rainfall regime in the area. We investigated the link between the different indices by using traditional
112 statistical methods. We investigated the link between the different indices by using traditional statistical methods
113 (Spearman, 1904), but also by introducing in this field an innovative approach, which employs a linear model to
114 understand the influence of each index on the rainfall prediction. The combination of these different methods helped us
115 to comprehend the accuracy and the advantages of the new method proposed.

116 In our study, we compared these SSTs with the atmospheric indices to improve knowledge on the rainfall trend and
117 to understand possible future scenarios.

118

119 Many land dynamics (e.g., drought, floods, solid transport, coastal erosion) are linked to the rainfall regime which
120 can create management criticalities (e.g., Billi and Fazzini, 2017; Bini et al., 2021; Piccarreta et al., 2004). The study of
121 variations in the amount of rainfall related to climatic indices allows to lay the foundations for future studies and land
122 management. The observations put forward in this work and the methods adopted could be extended to other
123 Mediterranean areas by increasing knowledge about these issues.

124 **In our study, we compared these SSTs with the atmospheric indices to improve knowledge on**
125 **the rainfall trend and to understand possible future scenarios.**

126 **Study area** The region has a strategic location: it is located in the northern sector of the
127 Mediterranean, in the proximity of the Genoa Gulf, by far the most active cyclogenetic centre
128 of the Mediterranean.

129 **As expected, the mean annual precipitation (MAP) in Tuscany is influenced by morphology**
130 **(Figure 1a). The rainiest areas are located at the highest altitudes (Apuan Alps and Northern**
131 **Apennines; Figure 1b). In particular, the Apuan Alps in north-western Tuscany show some**
132 **of the highest rainfall amounts in Italy, often characterized by high intensity. In Tuscany,**
133 **MAP is in a range of 400-3000 mm/year with a clear gradient from the northern to the**
134 **southern and it is linked to the morphology (Figure 1a). The main rainy season is autumn,**
135 **with a progressive decrease that generally starts in December. The mean rainfall in the DJF**
136 **season is ca 300 mm, ca 250 mm in MAM, ca 130 mm in JJA, and ca 350 mm in SON.**

137 **FIGURE 1**

138

Formatted: Heading 1

Formatted: Heading 1

Formatted: English (United States)

Field Code Changed

Formatted: English (United States)

Formatted: English (United States)

139 **Materials and Methods** The same dataset was used by Luppichini et al. (2020), who employed
140 different types of elaboration to understand the variable influence of NAO on the Tuscany
141 rainfall.

142 Study area

143 Tuscany has a strategic location because it is located in the northern sector of the Mediterranean, in the proximity of
144 the Genoa Gulf, by far the most active cyclogenetic centre of the Mediterranean (Trigo et al., 2002).

145 As expected, the mean annual precipitation (MAP) in Tuscany is influenced by morphology (Figure 1a). The rainiest
146 areas are located at the highest altitudes (Apuan Alps and Northern Apennines; Figure 1b). In particular, the Apuan
147 Alps in north-western Tuscany show some of the highest rainfall amounts in Italy (Giannecchini and D'Amato Avanzi,
148 2012; Rapetti and Vittorini, 1994), often characterized by high intensity (D'Amato Avanzi et al., 2004; Giannecchini,
149 2006). In Tuscany, MAP is in a range of 400-3000 mm/year with a clear gradient from the northern to the southern and
150 it is linked to the morphology (Figure 1a). The main rainy season is autumn, with a progressive decrease that generally
151 starts in December. The mean rainfall in the DJF season is ca 300 mm, ca 250 mm in MAM, ca 130 mm in JJA, and ca
152 350 mm in SON.

153 **FIGURE 1**

154 Dataset

155 *Rainfall dataset and processing*

156 The raingauge dataset was provided by the Tuscany Region Hydrologic Service (SIR) network and includes 1103
157 raingauges (Figure 1c). The daily data were obtained by an automated download procedure through an HTTP request in
158 March 2021. The dataset is the best one available in this area and it is managed by the SIR which validates and checks
159 the data. The dataset is used in several research works because it is referenced and managed by a public body. In
160 particular, Luppichini et al. 2021 used this dataset to understand the relationship between NAO and winter rainfall in
161 this area. The activity period of each raingauge is variable. The older stations have been monitoring since the beginning
162 of the last century, even if a temporal continuity of the data is not always guaranteed for some stations. SIR provides the
163 daily rainfall data for each raingauge in the operation period. To obtain longer and more complete time series from this
164 dataset, we grouped the stations according to a stringent protocol. This procedure is necessary to reconstruct the time
165 series of the stations that have experienced minor changes in position or that have undergone an administrative variation
166 (e.g., a slight change in name or identification code). In many cases, sThe stations have consecutive intermittent activity

Formatted: Heading 1

Formatted: English (United Kingdom)

167 times due to the decommissioning of one and the subsequent installation of a new one. In these cases, we merged the
168 stations by assigning the same, or part of the same name, with a difference in quote-~~altimetry~~ (less than 20%) of the
169 measurement, and a maximum distance (less than 2 km). The geographic coordinates of the merged stations derived
170 from a cartesian mean of the original coordinates of the origin stations.

171 By using the data available and following the procedure described above, a total of 117 time series were obtained from
172 1950 to 2020. The rainfall data can also be useful for comparison with the results of the linear models (~~see-section~~
173 Linear Models), which predict rainfall anomalies; ~~instead,~~ ~~t~~ the absolute values rainfall values are expressed as
174 percentage anomalies of rainfall (PAR), and are calculated as follows:

$$PAR_{s,i} = \frac{x_{s,i} - \bar{x}_i}{\bar{x}_i} \cdot 100 \quad (1)$$

Formatted: Centered

175 where, $x_{s,i}$ is the annual seasonal rainfall amount of the i-th year and s-th season, \bar{x}_i is the annual rainfall amount
176 mean of the period 1961-1990.

177 ~~The values of PAR are calculated for the four seasons: winter (DJF: December, January and February); spring~~
178 ~~(MAM: March, April and May –); summer (JJA: June, July and August); autumn (SON: September, October and~~
179 ~~November). The PA- Mean Average PAR (MAPAR) is the averaged with a a ten-year mobile window average of PAR
180 calculated for each season, and the values are associated with the central year. We chose to use a ten-year mobile
181 average because this time range is within the standard 10–30 year time scale considered to be decadal variability (Meehl
182 et al., 2009).~~

Formatted: Indent: First line: 0"

184 *Climatic Dataset*

185 The NAO dataset is provided by the Climate Analysis Section of the US National Center for Atmospheric Research
186 (NCAR). This dataset is based on the principal (PC)-based index component of the NAO, which are the time series of
187 the leading Empirical Orthogonal Function (EOF) of SLP anomalies over the Atlantic sector, 20°-80°N, 90°W-40°E.
188 This index is used to measure the yearly NAO, by tracking the seasonal movements of the Icelandic Low and Azores
189 High. The dataset has a monthly frequency from January 1889 to December 2020. PC-based indices are more optimal
190 representations of the full spatial patterns of the NAO (National Center for Atmospheric Research Staff (Eds), 2021).

191 The EA dataset used in this study is provided by the National Weather Service of NOAA. The frequency of the
192 dataset is on a monthly basis, from 1950 to 2020. The index is standardized by ~~the~~-1981-2010 climatology (Climate
193 Prediction Center, 2021).

194 The WeMO index is provided by the Climatic Research Unit (CRU) of the University of East Anglia (Climatic
195 Research Unit, 2021). The time series startsed in 1821 and has a monthly frequency.

196 The trends of NASST, MSST, and GGSST are calculated from the Extended Reconstructed Sea Surface
197 Temperature (ERSST) dataset version 5 (NOAA, 2021), and they are expressed using a 10-year mobile window of
198 anomalies. The anomalies are referred to the mean of the ~~period~~-1961-1990period. NASST is calculated in the area 0N-
199 65N 80W-0E; MSST in the area 38N-49N 0E-28E; and GGSST in the area 42.8N-44.8N 7.6E-10.76E.

200 Statistical Correlation and Linear Models

201 ~~We investigated the link between the different indices by using traditional statistical methods (Spearman, 1904),~~
202 ~~but also by introducing in this field an innovative approach, which employs a linear model to understand the influence~~
203 ~~of each index on the rainfall prediction. The combination of these different methods helped us to comprehend the~~
204 ~~accuracy and the advantages of the new method proposed.~~

205 We calculated the correlation coefficient ~~in order~~ to identify a possible relationship between atmospheric
206 teleconnection and rainfall amount. ~~Several authors use a statistical method of correlation to quantify the relationship~~
207 ~~between atmospheric indices and rainfalls~~ (Brandimarte et al., 2011; Faust et al., 2016; Kalimeris et al., 2017; Kotsias et
208 al., 2020; Koyama and Stroeve, 2019; López-Moreno et al., 2011; Vicente-Serrano and López-Moreno, 2008). ~~In~~
209 ~~particular, S~~some authors (Caloiero et al., 2011; Izquierdo et al., 2014; Luppichini et al., 2021; Nalley et al., 2019;
210 Vergni et al., 2016) use ~~the~~ Spearman's correlation coefficient (SCC) (Spearman, 1904) to understand the relationship
211 between atmospheric index and rainfall amount. This relationship is suitable for monotonically-related variables, even
212 when their relationship is not linear. The range of Spearman's coefficients is between -1 and 1; positive values indicate
213 a tendency of one variable to increase or decrease together with another variable, whereas negative values indicate a
214 trend in which the increase in the values of one variable is associated with the decrease in the values of the other
215 variable, and vice versa. ~~We have divided the time series into four seasons~~~~We calculated the SCC between the three~~
216 ~~atmospheric teleconnections and the rainfall for the four seasons~~: winter from December to February (DJF), spring from
217 March to May (MAM), summer from June to August (JJA) and autumn from September to November (SON). ~~We~~
218 ~~calculated the SCC among the three atmospheric teleconnections and the rainfall for the four seasons using a 10-year~~
219 ~~moving time window from 1950 to 2020. We assigned the correlation result to the year halfway through each ten-years.~~
220 ~~SCC was calculated using a 10-year moving time window from 1950 to 2020. The result of the correlation was assigned~~
221 ~~to the year halfway through each ten-year period.~~

222 ~~However, the trends in the time series can influence the SCC~~ (Arianos and Carbone, 2009; Boris et al., 2009; Iqbal
223 et al., 2020; Podobnik and Stanley, 2008). ~~To exclude the influence of the trends on the results of this study, we~~

Formatted: English (United States)

investigated further using the detrended cross-correlation analysis (DCCA) proposed by (Kristoufek, (2014) in the framework developed by (Ide et al., (2017)). The DCCA results are in perfect agreement with the SCC results. Therefore, we could exclude an influence of the trends on the use of SCC in this study. More information can be found in the supplementary material.

Formatted: English (United States)

Formatted: English (United States)

Formatted: English (United States)

Linear Models

The simplest mathematical model is the linear one. We can create linear models capable to of predicting the rainfall amount by using the NAO, WeMO and EA time series. The equation of a linear model predicting the rainfall (R_p), by using the NAO, WeMO and EA time series, is the following:

$$R_p = \alpha NAO + \beta WeMO + \gamma EA + \delta \quad (12)$$

We can analyse the best estimates setting of the independent variable coefficients of the model parameters (α , β , γ) to understand the role of each input on in the prediction of rainfall. If we want to obtain the best prediction models, we should use models that are more complex than a simple linear model. However, the simplicity of the linear models does not allow to have the best prediction models, but it certainly allows to analyse the influence of the inputs, since one of the tasks of this work is to show that more complex models (for instance with the inclusion of synergies between the input data) are not necessary to explain the rainfall observed. input clearly and to exclude synergy between the inputs and this is the main of this work. We therefore created a linear model for each raingauge time series for each season. We created a linear model for each raingauge time series and for the four seasons. The different dimensionality range of the three atmospheric teleconnections could influence the information expressed by the parameters of models α , β and δ . For this reason, we scaled the time series of NAO, WeMO and EA in the range between 0 and 1 for the studied period (1950-2020), by applying the following equation:

$$Ts = \frac{Ts - Ts_m}{Ts_M - Ts_m} \quad (3)$$

where Ts is the index time series in the range 0- and 1 range, Ts_M is the maximum value of the index, and Ts_m is the minimum value of the index. We fitted a linear model for each time series. The fitting of the linear models is executed using the SciPy library in Python Language and, in more detail, the "curve_fit" method (Virtanen et al., 2020). We validated the fits calculating the Root Mean Square Error (RMSE) and the Correlation Coefficient (r) as follows. The quality valuation of the models is done calculating Root Mean Square Error (RMSE) and Correlation Coefficient (r) as following:

Formatted: Not Highlight

Formatted: Not Highlight

Formatted: Not Highlight

Formatted: Not Highlight

Formatted: Not Highlight

Formatted: Not Highlight

$$RMSE = \left(\frac{1}{N} \sum_{i=0}^N (F_i - V_i)^2 \right)^{0.5} \quad (4)$$

$$r = \frac{\left(\frac{1}{N} \sum_{i=0}^N (F_i * V_i) \right)}{\left(\frac{1}{N} \sum_{i=0}^N F_i^2 \right)^{0.5} * \left(\frac{1}{N} \sum_{i=0}^N V_i^2 \right)^{0.5}} \quad (5)$$

where F_i are the forecast values, V_i are the observed values and N the number of years.

Results

Rainfall Trends

Figure 2 reports the values of PAR calculated for each time series used in this work, and obtained from equation 1. The graphs indicate a small variability of PAR between each time series, excluding the possibility of different influences on the linear model outcomes by the input stations and a significant variability in the study area. The $MAPAR$ of the study area is shown in Figures 3-6 for the four seasons. The rainfall trends expressed in PAR are shown in Figures 3-6. These trends variations of $MAPAR$ over time are very different in the four seasons. From 1950 to 1985, the DJF season was characterized by a slow rainfall reduction followed by a sudden decrease around the 90's. The first years of the 1990's presented a $MAPAR$ reduction of about 30-40%. Starting from 2000, the DJF $MAPAR$ increased we can observe a progressively progressive increase in winter rainfall with until reaching a return of the amount recorded before 1990 (Figure 3). Until the 1990s, the MAM rainfall trend $MAPAR$ was identified characterized by an oscillation. From the 1990's to the 2010's, we observe MAM $MAPAR$ values has the minimum values which are in the range between -10 and -20%. After 2008, MAM $MAPAR$ there was an increased after 2008 in precipitation (Figure 4). The JJA $MAPAR$ started to season was characterized by a progressive reduction decrease of rainfall starting from in 1965 with the minimum values of -30% around 2005. The last years were marked by a weakly increase of JJA $MAPAR$ in rainfall (Figure 5). Finally, rainfall in the SON season presented SON $MAPAR$ had a certain variability over an approximate 20-year period. The maximum rainfall SON $MAPAR$ amount was recorded around 1965 and 1995, while the minimum values were referred those of the period 1970-1990 (Figure 6).

FIGURE 2

Atmospheric Teleconnection Trends

In DJF, NAO was characterized by an intensification of the positive phase, the EA time series was characterized by an intensification of the positive phase starting from 1985 (Figure 3), and WeMO was characterized by a positive phase with a decrease in the 1990-2010 period.

275 In MAM, NAO and EA time series were characterized by a progressive increase with an intensification of the
276 positive phase; WeMO has experienced a progressive decrease from a positive phase to a negative persistence phase
277 since 2005 (Figure 4).

278 In JJA, NAO was characterized by a positive phase until 2005, whereas the index was characterized by a negative
279 phase, except for some years. In this season, EA started to increase progressively in 1995, while WeMO had a
280 progressive decrease with a persistence positive phase since 2005 (Figure 5).

281 In SON, NAO is variable with periods characterized by negative alternated with positive phases. In this season, EA
282 had a higher index fluctuation, with a negative phase until 1980, followed by a more positive ten-year phase and then by
283 a negative phase until 2000. From 2000 to 2020, EA increased reaching its maximum values. WeMO was characterized
284 by two distinct positive phases around 1975 and 1995, but the overall trend has decreased with a negative phase since
285 2005 (Figure 6).

Formatted: English (United States)

286 From 1950 to 2020, NAO was characterized by an intensification of the positive phase in the DJF and
287 MAM seasons (Figures 3 and 4). In the JJA season, NAO was characterized by a positive phase until
288 2005, whereas the index was characterized by a negative phase, except for some years. Finally, NAO
289 was more variable in the SON season with periods characterized by negative alternated with positive
290 phases (Figure 6).

291 From 1950 to 2020, the EA time series was characterized by an intensification of the positive phase
292 starting from 1985 for the DJF period (Figure 3), and from 1995 for the MAM and JJA periods (Figures
293 4 and 5). The SON period presented a higher index fluctuation, with a negative phase until 1980,
294 followed by a more positive ten year phase and then by a negative phase until 2000. From 2000 to 2020,
295 we can observe an increase in the positive phase except for some cases (Figure 6).

296 In DJF, WeMO was characterized by a positive phase with a decrease in the 1990-2010 period (Figure
297 3). Around 2005 we observed a drastic change in the WeMO index in the MAM, JJA and SON seasons
298 with a negative persistence phase (Figures 4-6). Before 2005, the index in these seasons was
299 characterized by positive phases except for some years in which the values of the index were negative
300 (Figures 4-6).

301 Sea surface temperature trends

302 Figures 3-6 show the trends variations of NASST, MSST and GGSST display started to display a clear increasing
303 trend starting in from the 1980's in all seasons. Such increase only started around the 2010's for DJF and GGSST, while
304 it started to increased starting from 1980s in the other seasons. The increase in SST was higher-greater in the
305 summer than in the other seasons (Figures 3-6).

307 **FIGURE 3**

308 **FIGURE 4**

309 **FIGURE 5**

310 **FIGURE 6**

311 Statistical Correlation

312 Figure 7 reports the results obtained from ~~the Spearman's correlation coefficient~~ SCC; and Figure 8 shows the spatial
313 ~~distribution of the p-values obtained~~. In the DJF season, rainfall is correlated with WeMO and anticorrelated with NAO
314 and EA. Rainfall increases during a negative phase of NAO or EA and a positive phase of WeMO. During this period,
315 each atmospheric teleconnection has a similar effect on the rainfall amount. In the MAM season, the strongest
316 correlation is with WeMO, and even in this case a positive phase of the index corresponds to a rainfall increase in the
317 study area. NAO and EA are weakly anticorrelated with the rainfall amount. The strongest correlation is with EA in the
318 JJA season, and a negative phase of this index indicates an increase in rainfall in the area. ~~On other hand, while~~ a
319 positive phase of EA corresponds to reduced precipitation in summer. NAO and WeMO are weakly correlated with ~~the~~
320 rainfall, but do not ~~have show~~ a clear behaviour. Even in the SON season, the strongest correlation is with EA. The
321 correlation in this season is positive, which indicates that a positive EA phase determines increased precipitation in the
322 area. The spatial correlation distribution is homogenous with no clear spatial pattern, especially when the correlations
323 are strong, providing a precise indication of the relationship (Figure 7).

324 **FIGURE 7**

325 **FIGURE 8**

Formatted: Highlight

326 Linear Models

327 In Figure 9a-d, we report four examples of the ~~MAPAR~~ prediction ~~of PAR~~ by means of linear models referred to the
328 DJF, MAM, JJA and SON seasons. The cases shown represent the results of the lineal models because they have ~~Root~~
329 ~~Mean Square Error~~ (RMSE) values similar to the error medians calculated on the ~~whole entire~~ dataset (Figure 9e). ~~For~~
330 ~~the case shown in Figure 9a, α , β and γ are respectively -96.56, 42.53, and 4.85; for the case reported in Figure 9b they~~
331 ~~are -21.39, -15.54 and -15.76, for the case reported in Figure 9c they are -30.71, -56.10 and -1.34; for the case reported~~
332 ~~in Figure 9c they are -48.05, 7.54 and 6.71~~. Figure 9e ~~and 9d~~ also reports the RMSE ~~and r~~ ~~of~~ the entire dataset. SON,
333 followed by MAM, ~~which~~ is the season with the highest average errors.

334 Figure 10 shows the mean values of coefficients α , β and γ for the linear models in each season (blue circles). We
335 can observe a change in the values of the three coefficients from one season to another. ~~In Figure 10, ~~the red circles in~~~~
336 ~~Figure 9~~ show the relative weights of each coefficient. In the DJF season, the coefficient with the greatest weight is α
337 with a mean value of about 55%, followed by β and γ . The coefficients indicate that NAO has more influence on the
338 rainfall trend than WeMO and EA ~~in on~~ DJF. In this season, ~~the coefficient values indicate that -an increase in~~
339 ~~rainfall increased precipitation~~ is linked to a negative phase of NAO (α is negative) and a positive phase of WeMO (β is

Formatted: English (United States)

340 positive). ~~A positive γ is not to be understood as a positive link between rainfall and index, but it works as a~~
341 ~~compensation with respect to the α coefficient in the model.~~ In the MAM season, β (WeMO) has the highest weight in
342 the results of the models, followed by α (NAO) and γ (EA). ~~Therefore, in particular, the coefficients denote that~~
343 ~~the amount of precipitation-rainfall is correlated with a positive phase of WeMO and with a negative phase of NAO.~~
344 ~~Again~~ Also in this season, EA has less influence on the model than the other two indices. In the JJA season EA is ~~the~~
345 ~~index with the most important index, with~~ the greatest coefficient (γ). In particular, ~~the coefficients suggest that~~
346 ~~the summer rainfall is seems to be~~ linked to a negative phase of EA. Less important, ~~the coefficients indicate that~~
347 the summer rainfall is linked to a negative phase of WeMO. In the SON season, NAO has the greatest weight and is
348 followed by WeMO and EA, which have less influence on the rainfall trend. In this case, the coefficients are all
349 negative, so that rainfall is correlated to a negative phase of these indices.

350 **FIGURE 98**

351 **FIGURE 910**

Formatted: Highlight

352 Discussion

353 Mathematical and statistical relationship between atmospheric teleconnections and rainfall

354 The statistical correlation calculated with Spearman's method represents a first indication of the influence of climate
355 patterns on the local rainfall trend (~~Figure 7~~). In accordance with several studies (Caloiero et al., 2011; Deser et al.,
356 2017; Ferrari et al., 2013; George et al., 2004; López-Moreno et al., 2011; Luppichini et al., 2021; Riaz et al., 2017;
357 Vergni and Chiaudani, 2015; Vicente-Serrano and López-Moreno, 2008; West et al., 2019), NAO influence is
358 predominant in winter, with an anticorrelation between index and rainfall amount. In agreement with the obtained SCC,
359 an increase in the Azores High, and consequently a decrease in the Iceland Low, determine reduced winter rainfall in
360 the study area. The correlation between NAO and rainfall decreases during the successive seasons with a minimum
361 correlation in ~~the~~ summer. In winter and in spring, the correlation with WeMO is strong and it is characterized by a
362 positive sign. This implies the formation of the Genoa Gulf Low and its reinforcement increases the amount of rainfall
363 in the study area. This can be ascribed to the direction of the moist air masses coming from the Atlantic Ocean and
364 directed to the north-western coast of Spain and to the Mediterranean (Degeai et al., 2020; Martín et al., 2012; Martin-
365 Vide and Lopez-Bustins, 2006). In this dynamic state the moist air masses can reach Tuscany, enhancing local
366 cyclogenesis and rainfall. The SCC values indicate that the influence of the Genoa Gulf Low decreases in summer and
367 autumn (~~Figure 7~~). The correlation between rainfall and EA is strong in winter and summer; in summer, the ~~main~~
368 correlation with rainfall is ~~particularly-mainly~~ with EA. In winter, the link between EA and rainfall is the same for

369 NAO. In summer, the greater representativeness of EA than of NAO on the Azores High allows a better understanding
370 of the link between rainfall and global climate in this season. In detail, the formation of the Azores High and of the
371 African High results in an increase in the EA index, and this means that there is reduced precipitation in the study area.
372 In autumn, the statistical correlations do not allow to ~~make-create~~ a link between large-scale circulation and rainfall.
373 Indeed, we can observe a weak anticorrelation with NAO, a weak correlation with EA, and no correlation with WeMO.
374 This method seems unsuitable to represent the autumn season with its atmospheric dynamics.

375 The results of the linear models are conformant to the statistical correlation results for the DJF, MAM and JJA
376 seasons, ~~whereas-while~~ we ~~can~~ observe some differences in SON. The strong correspondence between the two methods
377 in DJF, MAM and JJA makes it possible to validate our linear model. In autumn, the analysis of the linear models
378 identifies an important role of NAO, and therefore a link between ~~the-northern~~ Atlantic atmospheric circulation and ~~the~~
379 rainfall in the study area. In autumn, the coefficients of NAO (α) are set negative and this means that an increase in the
380 index is linked to a decrease in rainfall in the study area. This mathematical result is more plausible than that obtained
381 from the analysis of correlations based on the notions of atmospheric physics ~~that-we~~ introduced previously. The linear
382 model-based method ~~has~~ allowed us to refine our investigations and to improve our knowledge of the dynamics in the
383 Mediterranean over the seasons.

384 The use of our linear models offers the advantage of clarifying the role and influence of large-scale atmospheric
385 circulation on rainfall over the study region in different seasons, and this may appear controversial when using only the
386 statistical correlation. These linear methods can also be useful for rainfall prediction, although it is not the ~~intention-aim~~
387 of this paper to produce the best model for predictions. ~~A more complex model may be better suited to reduce the~~
388 ~~overall model; if we wanted to reduce the model errors, we should have chosen a more complex model able to better~~
389 ~~adapt to the variability of the inputs;~~ however, it would have been difficult to understand the influence of each input
390 parameter, which is the main scope of this paper.

391 Long-term rainfall trends and ~~relationship~~ with climate patterns

392 This study ~~has~~ identified a confused trend for the DJF, MAM and SON rainfall, while ~~the~~ JJA rainfall clearly tends
393 to decrease (~~Figures 3-6~~). These results agree with those of other studies based on different rainfall datasets (Caloiero et
394 al., 2018; Deitch et al., 2017; Philandras et al., 2011). More specifically, Deitch et al. (2017) studied the seasonal trend
395 of rainfall in the Mediterranean area, demonstrating a negative trend for summer rainfall and no trend for
396 winter/autumnal rainfall in Tuscany.

397 The DJF seasons are characterized by significantly decreased precipitation between 1984 and 2005 (Figure 3). This
398 period is marked by a positive phase of NAO and EA and a negative phase of WeMO. Starting around 1984, the

399 increase in NAO and EA is due to an increase in NASST (Figure 3). An increase in NASST is correlated to an
400 expansion of the Azores High and a consecutive reduction of the Iceland Low, resulting in the formation of the NAO
401 and EA positive phases (Börgel et al., 2020; Frankignoul et al., 2003; Robertson et al., 2000; Visbeck et al., 2001). The
402 successive increase in rainfall from 2005 to 2020 seems to have been caused by an increase in the WeMO, and therefore
403 by an increase in the Genoa Gulf Low persistence. This could indicate a change of the main climatic driver with respect
404 to the previous period (Figure 3).

405 The MAM season presents a decrease in the amount of rainfall in the period between 1985 and 2008 (Figure 4). The
406 WeMO constantly decreases with progressive intensification of the negative phase. This indicates a gradual reduced
407 intensity of the Genoa Gulf Low. ~~As a matter of fact, the~~ GGSST has progressively increased since 1985.
408 Furthermore, NAO and EA are in a persistent positive phase. Since 2008, there has been a weak increase in the
409 precipitation trend.

410 The JJA rainfall trends have the highest correlation with EA, while NAO and WeMO have a lower influence (Figure
411 7 and 910). The increase in NASST, MSST and GGSST induces the NAO and EA indices to a positive phase, and
412 WeMO to a negative phase. This process induces a progressive reduction of rainfall trends in this season.

413 SON is characterized by rainfall trend variability with two wet periods and two dry periods (Figure 6). Each dry
414 period is marked by an increase in NAO, whereas the wet period results from an increase in WeMO linked to a weak
415 decrease in GGSST (Figure 6).

416 The increase in sea surface temperature is greater in the warm periods of the year and it is caused by current global
417 warming. From these observations, we can evince that the warm periods of the year are marked by a greater decrease in
418 precipitation resulting in less water availability in the environmental system.

419 **Conclusions**

420 This study helps to gain a better knowledge of the rainfall trends of the last 70 years in Tuscany, a key area of the
421 Mediterranean Basin, strongly influenced by the cyclogenetic activity related to the Genoa Gulf Low. These trends are
422 analyzed on the basis of the trend of the main atmospheric drivers of the northern hemisphere. The location of the study
423 area allows to understand the influences of Atlantic atmospheric circulation and of the Mediterranean atmospheric
424 circulation on rainfall. Along with ~~the~~ Spearman's traditional coefficient analysis, this study proposes a new
425 mathematical method to investigate the relationship between climate pattern and rainfall. The method based on the use
426 of linear models has resulted to be valid, with similar results derived from a statistical correlation. This new method has
427 allowed ~~for~~ a more detailed comprehension of the link between climate patterns and precipitation in the study area. In
428 Tuscany, ~~the~~ rainfall amount is influenced by Northern Atlantic atmospheric circulation and by the Genoa Gulf Low.

429 The influences of the two atmospheric systems vary during the year: in winter, rainfall is strongly correlated to the three
430 indices; in spring, the main influence is represented by WeMO, indicating an important role played by the Genoa Gulf
431 Low; in summer, the main driver is EA, which represents better than NAO the influence of the Azores High in this
432 season; in autumn, the strongest correlation is with NAO.

433 The amount of ~~precipitation-rainfall~~ in the study area is influenced by the SSTs ~~that-which~~ induce a variation in the
434 Northern Atlantic and Mediterranean atmospheric circulations (Börgel et al., 2020; Frankignoul et al., 2003; Robertson
435 et al., 2000; Visbeck et al., 2001). Current global warming determines an increase in the SSTs and this increase is
436 higher in the warm seasons of the year (James et al., 2006). The results of this study show that in these seasons there is
437 the greatest reduction of water availability, on account of a direct decrease in precipitation. For this reason,

438 ~~In conclusion,~~ current global warming ~~can-could~~ be responsible for less rainfall in this area, and this occurs mainly
439 in the warm seasons when temperature increase is highest. ~~-These aspects can be deepened by future studies that can~~
440 ~~strengthen the relationships found and the considerations made in this work.~~

441

442 **Conflicts of Interest:** The authors declare no conflict of interest. The funders had no role in the design of the study;
443 in the collection, analyses, or interpretation of data; in the writing of the manuscript, or in the decision to publish the
444 results.

445 **Acknowledgements:** The authors are grateful to the Tuscany Region Hydrologic Service for providing the data
446 used in this work.

447 **Funding:** This research was funded by project no. 249792 “Dalla Preistoria all'Antropocene: Nuove Tecnologie per
448 la valorizzazione dell'eredità culturale della Versilia (PANTAREI)” Tuscany Region (call POR FSE 2014-2020, Resp.
449 M. Bini); by the collaborative research agreement no. 579999-2019 “Autorità di Bacino Distrettuale Appennino
450 Settentrionale” (Resp. Monica Bini and Roberto Gianneccchini); and by the project: “Cambiamenti globali e impatti
451 locali: conoscenza e consapevolezza per uno sviluppo sostenibile della pianura Apuo-versiliese” Fondazione Cassa
452 Risparmio di Lucca, (Resp. M. Bini).

453 Reference

454 Allan, R.P., 2011. Human influence on rainfall. *Nature* 470, 344–345. <https://doi.org/10.1038/470344a>
455 Arianos, S., Carbone, A., 2009. Cross-correlation of long-range correlated series. *Journal of Statistical Mechanics:*
456 *Theory and Experiment* 2009, P03037.

457 Bates, B., Kundzewicz, Z.W., Wu, S., Burkett, V., Doell, P., Gwary, D., Hanson, C., Heij, B., Jiménez, B., Kaser, G.,
458 Kitoh, A., Kovats, S., Kumar, P., Magadza, C.H.D., Martino, D., Mata, L., Medany, M., Miller, K., Arnell, N.,
459 2008. Climate Change and Water. Technical Paper of the Intergovernmental Panel on Climate Change.

460 Bertola, M., Viglione, A., Hall, J., Blöschl, G., 2019. Flood trends in Europe: are changes in small and big floods
461 different? *Hydrology and Earth System Sciences Discussions* 1–23. <https://doi.org/10.5194/hess-2019-523>

462 Billi, P., Fazzini, M., 2017. Global change and river flow in Italy. *Global and Planetary Change* 155, 234–246.
463 <https://doi.org/https://doi.org/10.1016/j.gloplacha.2017.07.008>

464 Bini, M., Casarosa, N., Luppichini, M., 2021. Exploring the relationship between river discharge and coastal erosion:
465 An integrated approach applied to the pisa coastal plain (italy). *Remote Sensing* 13.
466 <https://doi.org/10.3390/rs13020226>

467 Blöschl, G., Hall, J., Viglione, A., Perdigão, R.A.P., Parajka, J., Merz, B., Lun, D., Arheimer, B., Aronica, G.T.,
468 Bilibashi, A., Boháč, M., Bonacci, O., Borgia, M., Čanjevac, I., Castellarin, A., Chirico, G.B., Claps, P., Frolova,
469 N., Ganora, D., Gorbachova, L., Gül, A., Hannaford, J., Harrigan, S., Kireeva, M., Kiss, A., Kjeldsen, T.R.,
470 Kohnová, S., Koskela, J.J., Ledvinka, O., Macdonald, N., Mavrova-Guirguinova, M., Mediero, L., Merz, R.,
471 Molnar, P., Montanari, A., Murphy, C., Osuch, M., Ovcharuk, V., Radevski, I., Salinas, J.L., Sauquet, E., Šraj,
472 M., Szolgay, J., Volpi, E., Wilson, D., Zaimi, K., Živković, N., 2019. Changing climate both increases and
473 decreases European river floods. *Nature* 573, 108–111. <https://doi.org/10.1038/s41586-019-1495-6>

474 Börgel, F., Frauen, C., Neumann, T., Meier, H.E.M., 2020. The Atlantic Multidecadal Oscillation controls the impact of
475 the North Atlantic Oscillation on North European climate. *Environmental Research Letters* 15.

476 Boris, P., Davor, H., M, P.A., Eugene, S.H., 2009. Cross-correlations between volume change and price change.
477 *Proceedings of the National Academy of Sciences* 106, 22079–22084. <https://doi.org/10.1073/pnas.0911983106>

478 Brandimarte, L., di Baldassarre, G., Bruni, G., D’Odorico, P., Montanari, A., D’Odorico, P., Montanari, A., 2011.
479 Relation Between the North-Atlantic Oscillation and Hydroclimatic Conditions in Mediterranean Areas. *Water*
480 *Resources Management* 25, 1269–1279. <https://doi.org/10.1007/s11269-010-9742-5>

481 Caloiero, T., Caloiero, P., Frustaci, F., 2018. Long-term precipitation trend analysis in Europe and in the Mediterranean
482 basin. *Water and Environment Journal* 32, 433–445. <https://doi.org/https://doi.org/10.1111/wej.12346>

483 Caloiero, T., Coscarelli, R., Ferrari, E., Mancini, M., 2011. Precipitation change in Southern Italy linked to global scale
484 oscillation indexes. *Nat. Hazards Earth Syst. Sci.* 11, 1683–1694. <https://doi.org/10.5194/nhess-11-1683-2011>

485 Cardoso Pereira, S., Marta-Almeida, M., Carvalho, A.C., Rocha, A., 2020. Extreme precipitation events under climate
486 change in the Iberian Peninsula. *International Journal of Climatology* 40, 1255–1278.
487 <https://doi.org/https://doi.org/10.1002/joc.6269>

488 Climate Prediction Center, 2021. East Atlantic [WWW Document]. URL
489 <https://www.cpc.ncep.noaa.gov/data/teledoc/ea.shtml> (accessed 9.22.21).

490 Climatic Research Unit, 2021. Mediterranean Oscillation Indices (MOI) [WWW Document]. URL
491 <https://crudata.uea.ac.uk/cru/data/moi/> (accessed 9.22.21).

492 Colantoni, A., Delfanti, L., Cossio, F., Baciotti, B., Salvati, L., Perini, L., Lord, R., 2015. Soil Aridity under Climate
493 Change and Implications for Agriculture in Italy. *Applied Mathematical Sciences* 9, 2467–2475.
494 <https://doi.org/10.12988/ams.2015.52112>

495 D'Amato Avanzi, G., Giannecchini, R., Puccinelli, A., 2004. The influence of the geological and geomorphological
496 settings on shallow landslides. An example in a temperate climate environment: the June 19, 1996 event in
497 northwestern Tuscany (Italy). *Engineering Geology* 73, 215–228.
498 <https://doi.org/https://doi.org/10.1016/j.enggeo.2004.01.005>

499 Deitch, M.J., Sapundjieff, M.J., Feirer, S.T., 2017. Characterizing Precipitation Variability and Trends in the World's
500 Mediterranean-Climate Areas. *Water (Basel)* 9. <https://doi.org/10.3390/w9040259>

501 Deser, C., Hurrell, J.W., Phillips, A.S., 2017. The role of the North Atlantic Oscillation in European climate projections.
502 *Climate Dynamics* 49, 3141–3157. <https://doi.org/10.1007/s00382-016-3502-z>

503 Dünkloh, A., Jacobeit, J., 2003. Circulation dynamics of Mediterranean precipitation variability 1948–98. *International*
504 *Journal of Climatology* 23, 1843–1866. <https://doi.org/https://doi.org/10.1002/joc.973>

505 European Environment Agency, 2019. Economic losses from climate -related extremes in Europe. Indicator
506 Assessment.

507 Faust, J.C., Fabian, K., Milzer, G., Giraudeau, J., Knies, J., 2016. Norwegian fjord sediments reveal NAO related winter
508 temperature and precipitation changes of the past 2800 years. *Earth and Planetary Science Letters* 435, 84–93.
509 <https://doi.org/https://doi.org/10.1016/j.epsl.2015.12.003>

510 Ferrari, E., Caloiero, T., Coscarelli, R., 2013. Influence of the North Atlantic Oscillation on winter rainfall in Calabria
511 (southern Italy). *Theoretical and Applied Climatology* 114, 479–494. <https://doi.org/10.1007/s00704-013-0856-6>

512 Frankignoul, C., Friederichs, P., Kestenare, E., 2003. Influence of Atlantic SST anomalies on the atmospheric
513 circulation in the Atlantic-European sector. *Annals of Geophysics* 46.

Formatted: English (United States)

Formatted: English (United States)

514 George, D.G., Järvinen, M., Arvola, L., 2004. The influence of the North Atlantic Oscillation on the winter
515 characteristics of Windermere (UK) and Pääjärvi (Finland).

516 Giannecchini, R., 2006. Relationship between rainfall and shallow landslides in the southern Apuan Alps (Italy).
517 *Natural Hazards and Earth System Science* 6, 357–364. <https://doi.org/10.5194/nhess-6-357-2006>

518 Giannecchini, R., D'Amato Avanzi, G., 2012. [Historical research as a tool in estimating hydrogeological hazard in a](#)
519 [typical small alpine-like area: The example of the Versilia River basin \(Apuan Alps, Italy\)](#). *Physics and*
520 *Chemistry of the Earth, Parts A/B/C* 49, 32–43. <https://doi.org/10.1016/J.PCE.2011.12.005>

521 Giorgi, F., 2006. Climate change hot-spots. *Geophysical Research Letters* 33.
522 <https://doi.org/https://doi.org/10.1029/2006GL025734>

523 Halifa-Marín, A., Lorente-Plazas, R., Pravia-Sarabia, E., Montávez, J.P., Jiménez-Guerrero, P., 2021. [Atlantic and](#)
524 [Mediterranean influence promoting an abrupt change in winter precipitation over the southern Iberian Peninsula](#).
525 *Atmospheric Research* 253. <https://doi.org/10.1016/j.atmosres.2021.105485>

526 Hurrell, J.W., 1995. Decadal Trends in the North Atlantic Oscillation: Regional Temperatures and Precipitation.
527 *Science* (1979) 269, 676 LP – 679. <https://doi.org/10.1126/science.269.5224.676>

528 Ide, J.S., Cappabianco, F.A., Faria, F.A., Li, C.-S.R., 2017. [Detrended Partial Cross Correlation for Brain Connectivity](#)
529 [Analysis](#).

530 Iqbal, J., Lone, K.J., Hussain, L., Rafique, M., 2020. Detrended cross correlation analysis (DCCA) of radon, thoron,
531 temperature and pressure time series data. *Physica Scripta* 95, 085213. <https://doi.org/10.1088/1402-4896/ab9fb1>

532 Izquierdo, R., Alarcón, M., Aguilhaume, L., Àvila, A., 2014. [Effects of teleconnection patterns on the atmospheric](#)
533 [routes, precipitation and deposition amounts in the north-eastern Iberian Peninsula](#). *Atmospheric Environment* 89,
534 482–490. <https://doi.org/https://doi.org/10.1016/j.atmosenv.2014.02.057>

535 James, H., Makiko, S., Reto, R., Ken, L., W, L.D., Martin, M.-E., 2006. Global temperature change. *Proceedings of the*
536 *National Academy of Sciences* 103, 14288–14293. <https://doi.org/10.1073/pnas.0606291103>

537 Kalimeris, A., Ranieri, E., Founda, D., Norrant, C., 2017. [Variability modes of precipitation along a Central](#)
538 [Mediterranean area and their relations with ENSO, NAO, and other climatic patterns](#). *Atmospheric Research* 198,
539 56–80. <https://doi.org/https://doi.org/10.1016/j.atmosres.2017.07.031>

540 Knight, J.R., Allan, R.J., Folland, C.K., Vellinga, M., Mann, M.E., 2005. A signature of persistent natural thermohaline
541 circulation cycles in observed climate. *Geophysical Research Letters* 32. <https://doi.org/10.1029/2005GL024233>

Formatted: English (United States)

Formatted: English (United States)

Formatted: English (United States)

Formatted: English (United States)

Formatted: English (United States)

- 542 Kotsias, G., Lolis, C.J., Hatzianastassiou, N., Levizzani, V., Bartzokas, A., 2020. On the connection between large-scale
543 atmospheric circulation and winter GPCP precipitation over the Mediterranean region for the period 1980-2017.
544 Atmospheric Research 233, 104714. <https://doi.org/https://doi.org/10.1016/j.atmosres.2019.104714>
- 545 Koyama, T., Stroeve, J., 2019. Greenland monthly precipitation analysis from the Arctic System Reanalysis (ASR):
546 2000–2012. Polar Science 19, 1–12. <https://doi.org/https://doi.org/10.1016/j.polar.2018.09.001>
- 547 Kristoufek, L., 2014. Measuring correlations between non-stationary series with DCCA coefficient. Physica A:
548 Statistical Mechanics and its Applications 402, 291–298.
549 <https://doi.org/https://doi.org/10.1016/j.physa.2014.01.058>
- 550 Longobardi, A., Villani, P., 2010. Trend analysis of annual and seasonal rainfall time series in the Mediterranean area.
551 International Journal of Climatology 30, 1538–1546. <https://doi.org/https://doi.org/10.1002/joc.2001>
- 552 Lopez-Bustins, J.A., Arbiol-Roca, L., Martin-Vide, J., Barrera-Escoda, A., Prohom, M., 2020. Intra-annual variability
553 of the Western Mediterranean Oscillation (WeMO) and occurrence of extreme torrential precipitation in Catalonia
554 (NE Iberia). Natural Hazards and Earth System Sciences 20, 2483–2501. [https://doi.org/10.5194/nhess-20-2483-](https://doi.org/10.5194/nhess-20-2483-2020)
555 2020
- 556 Lopez-Bustins, J.-A., Martin-Vide, J., Sanchez-Lorenzo, A., 2008. Iberia winter rainfall trends based upon changes in
557 teleconnection and circulation patterns. Global and Planetary Change 63, 171–176.
558 <https://doi.org/https://doi.org/10.1016/j.gloplacha.2007.09.002>
- 559 López-Moreno, J.I., Vicente-Serrano, S.M., Morán-Tejeda, E., Lorenzo-Lacruz, J., Kenawy, A., Beniston, M., 2011.
560 Effects of the North Atlantic Oscillation (NAO) on combined temperature and precipitation winter modes in the
561 Mediterranean mountains: Observed relationships and projections for the 21st century. Global and Planetary
562 Change 77, 62–76. <https://doi.org/https://doi.org/10.1016/j.gloplacha.2011.03.003>
- 563 Luppichini, M., Barsanti, M., Giannecchini, R., Bini, M., 2021. Statistical relationships between large-scale circulation
564 patterns and local-scale effects: NAO and rainfall regime in a key area of the Mediterranean basin. Atmospheric
565 Research 248, 105270.
- 566 Martín, P., Sabatés, A., Lloret, J., Martin-Vide, J., 2012. Climate modulation of fish populations: The role of the
567 Western Mediterranean Oscillation (WeMO) in sardine (*Sardina pilchardus*) and anchovy (*Engraulis encrasicolus*)
568 production in the north-western Mediterranean. Climatic Change 110, 925–939. [https://doi.org/10.1007/s10584-](https://doi.org/10.1007/s10584-011-0091-z)
569 011-0091-z

Formatted: English (United States)

Formatted: English (United States)

Formatted: English (United States)

570 Martinez-Artigas, J., Lemus-Canovas, M., Lopez-Bustins, J.A., 2021. Precipitation in peninsular Spain: Influence of
571 teleconnection indices and spatial regionalisation. *International Journal of Climatology* 41, E1320–E1335.
572 <https://doi.org/https://doi.org/10.1002/joc.6770>

573 Martin-Vide, J., Lopez-Bustins, J.-A., 2006. The Western Mediterranean Oscillation and rainfall in the Iberian
574 Peninsula. *International Journal of Climatology* 26, 1455–1475. <https://doi.org/https://doi.org/10.1002/joc.1388>

575 Meehl, G., Goddard, L., Murphy, J., Boer, G., Danabasoglu, G., Dixon, K., Giorgetta, M., Greene, A., Hawkins, E.,
576 Hegerl, G., Karoly, D., Kimoto, M., 2009. Decadal Prediction: Can It Be Skillful? *Bull Am Meteorol Soc* 90,
577 1467–1485. <https://doi.org/10.1175/2009BAMS2778.1>

578 Mellado-Cano, J., Barriopedro, D., García-Herrera, R., Trigo, R.M., Hernández, A., 2019. Examining the North Atlantic
579 Oscillation, East Atlantic Pattern, and Jet Variability since 1685. *Journal of Climate* 32, 6285–6298.
580 <https://doi.org/10.1175/JCLI-D-19-0135.1>

581 Myhre, G., Alterskjær, K., Stjern, C.W., Hodnebrog, Ø., Marelle, L., Samset, B.H., Sillmann, J., Schaller, N., Fischer,
582 E., Schulz, M., Stohl, A., 2019. Frequency of extreme precipitation increases extensively with event rareness
583 under global warming. *Scientific Reports* 9, 16063. <https://doi.org/10.1038/s41598-019-52277-4>

584 Nalley, D., Adamowski, J., Biswas, A., Gharabaghi, B., Hu, W., 2019. A multiscale and multivariate analysis of
585 precipitation and streamflow variability in relation to ENSO, NAO and PDO. *Journal of Hydrology* 574, 288–
586 307. <https://doi.org/https://doi.org/10.1016/j.jhydrol.2019.04.024>

587 National Center for Atmospheric Research Staff (Eds), 2021. The Climate Data Guide: Hurrell North Atlantic
588 Oscillation (NAO) Index (PC-based). [WWW Document]. [https://climatedataguide.ucar.edu/climate-data/hurrell-](https://climatedataguide.ucar.edu/climate-data/hurrell-north-atlantic-oscillation-nao-index-pc-based)
589 [north-atlantic-oscillation-nao-index-pc-based](https://climatedataguide.ucar.edu/climate-data/hurrell-north-atlantic-oscillation-nao-index-pc-based).

590 NOAA, 2021. Extended Reconstructed SST [WWW Document]. URL [https://www.ncei.noaa.gov/products/extended-](https://www.ncei.noaa.gov/products/extended-reconstructed-sst)
591 [reconstructed-sst](https://www.ncei.noaa.gov/products/extended-reconstructed-sst) (accessed 9.28.21).

592 Pastor, F., Valiente, J.A., Khodayar, S., 2020. A warming Mediterranean: 38 years of increasing sea surface
593 temperature. *Remote Sensing* 12. <https://doi.org/10.3390/RS12172687>

594 Philandras, C., Nastos, P., Kapsomenakis, J., Douvis, K., Tselioudis, G., Zerefos, C., 2011. Long Term Precipitation
595 Trends and Variability within the Mediterranean Region. *Natural Hazards and Earth System Sciences* 11, 3235–
596 3250. <https://doi.org/10.5194/nhess-11-3235-2011>

597 Piccarreta, M., Capolongo, D., Boenzi, F., 2004. Trend analysis of precipitation and drought in Basilicata from 1923 to
598 2000 within a southern Italy context. *International Journal of Climatology* 24, 907–922.
599 <https://doi.org/https://doi.org/10.1002/joc.1038>

Formatted: English (United States)

Formatted: English (United States)

Formatted: English (United States)

600 Podobnik, B., Stanley, H.E., 2008. Detrended Cross-Correlation Analysis: A New Method for Analyzing Two
601 Nonstationary Time Series. *Physical Review Letters* 100, 84102.
602 <https://doi.org/10.1103/PhysRevLett.100.084102>

603 Rapetti, F., Vittorini, S., 1994. Le precipitazioni in Toscana: osservazioni sui casi estremi. *RIVISTA GEOGRAFICA*
604 *ITALIANA* 101, 47–76.

605 Riaz, S.M.F., Iqbal, M.J., Hameed, S., 2017. Impact of the North Atlantic Oscillation on winter climate of Germany.
606 *Tellus, Series A: Dynamic Meteorology and Oceanography* 69. <https://doi.org/10.1080/16000870.2017.1406263>

607 Ríos-Cornejo, D., Penas, Á., Álvarez-Esteban, R., del Río, S., 2015. Links between teleconnection patterns and
608 precipitation in Spain. *Atmospheric Research* 156, 14–28.

609 Robertson, A.W., Mechoso, C.R., Kim, Y.-J., 2000. The Influence of Atlantic Sea Surface Temperature Anomalies on
610 the North Atlantic Oscillation. *Journal of Climate* 13, 122–138. [https://doi.org/10.1175/1520-0442\(2000\)013<0122:TIOASS>2.0.CO;2](https://doi.org/10.1175/1520-0442(2000)013<0122:TIOASS>2.0.CO;2)

612 Rousi, E., Rust, H.W., Ulbrich, U., Anagnostopoulou, C., 2020. Implications of Winter NAO Flavors on Present and
613 Future European Climate. *Climate* 8, 13. <https://doi.org/10.3390/cli8010013>

614 Spearman, C., 1904. The proof and measurement of association between two things. *The American Journal of*
615 *Psychology* 15, 72–101. <https://doi.org/10.2307/1412159>

616 Stagl, J., Mayr, E., Koch, H., Hattermann, F.F., Huang, S., 2014. Effects of Climate Change on the Hydrological Cycle
617 in Central and Eastern Europe BT - *Managing Protected Areas in Central and Eastern Europe Under Climate*
618 *Change*, in: Rannow, S., Neubert, M. (Eds.), . Springer Netherlands, Dordrecht, pp. 31–43.

619 Tramblay, Y., Llasat, M.C., Randin, C., Coppola, E., 2020. Climate change impacts on water resources in the
620 Mediterranean. *Regional Environmental Change* 20, 83. <https://doi.org/10.1007/s10113-020-01665-y>

621 Trigo, I.F., Bigg, G.R., Davies, T.D., 2002. Climatology of Cyclogenesis Mechanisms in the Mediterranean.

622 Trigo, R.M., Pozo- Vázquez, D., Osborn, T.J., Castro- Díez, Y., Gámiz- Fortis, S., Esteban- Parra, M.J., Pozo-
623 Vázquez, D., Osborn, T.J., Castro-Díez, Y., Gámiz-Fortis, S., Esteban-Parra, M.J., 2004. North Atlantic
624 Oscillation influence on precipitation, river flow and water resources in the Iberian Peninsula. *International*
625 *Journal of Climatology: A Journal of the Royal Meteorological Society* 24, 925–944.
626 <https://doi.org/10.1002/joc.1048>

627 Vergni, L., Chiaudani, A., 2015. RELATIONSHIP BETWEEN THE NAO INDEX AND SOME INDICES OF
628 EXTREME PRECIPITATION IN THE ABRUZZO REGION.

Formatted: English (United States)

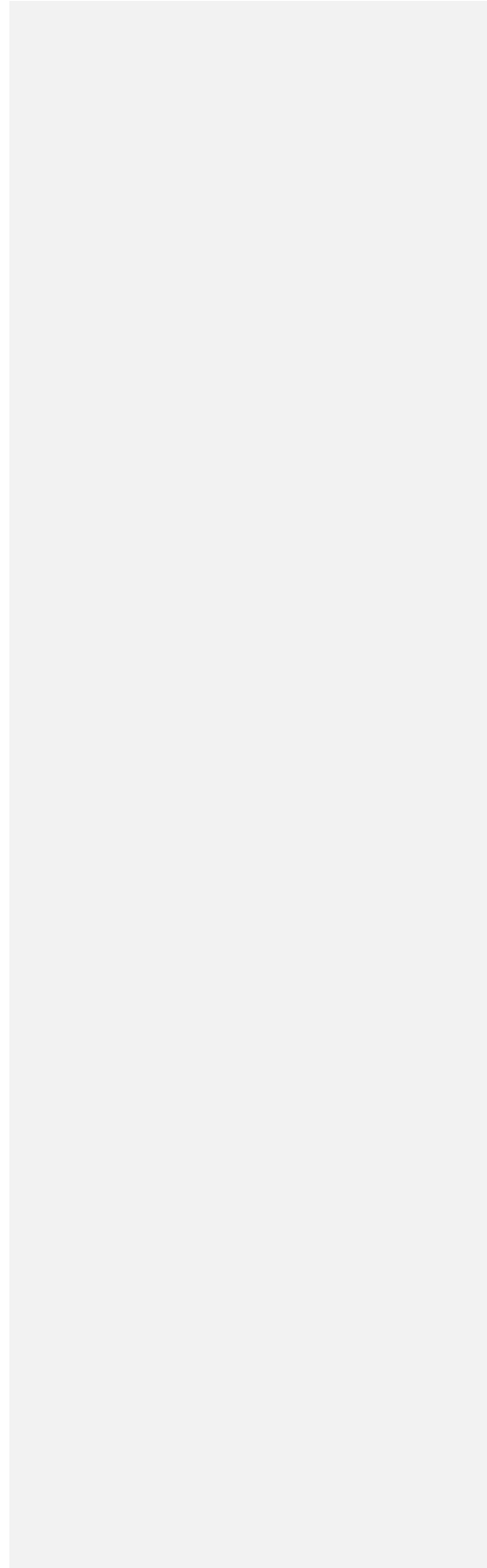
Formatted: English (United States)

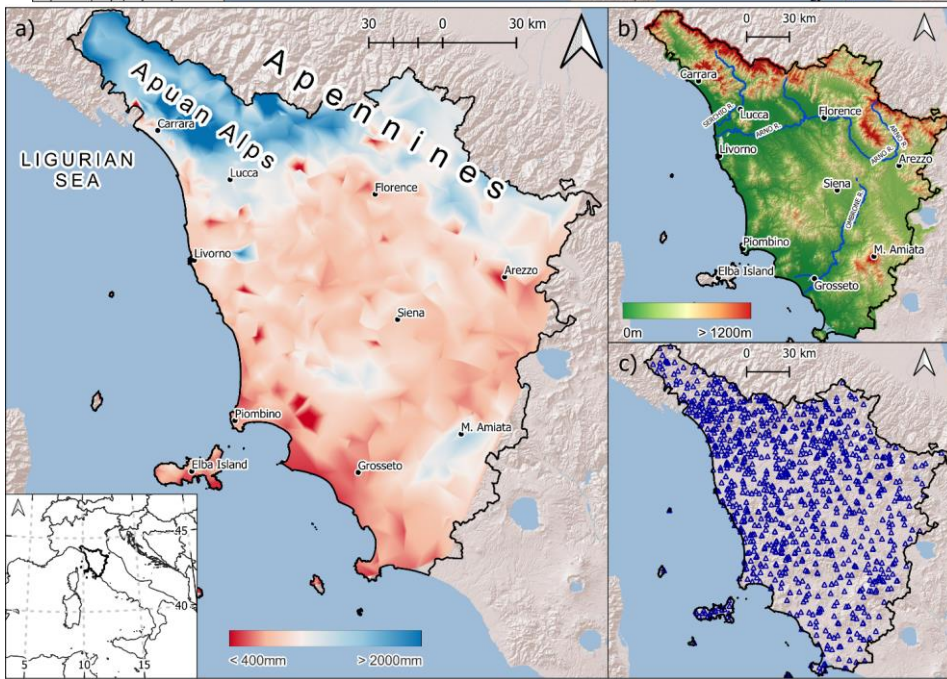
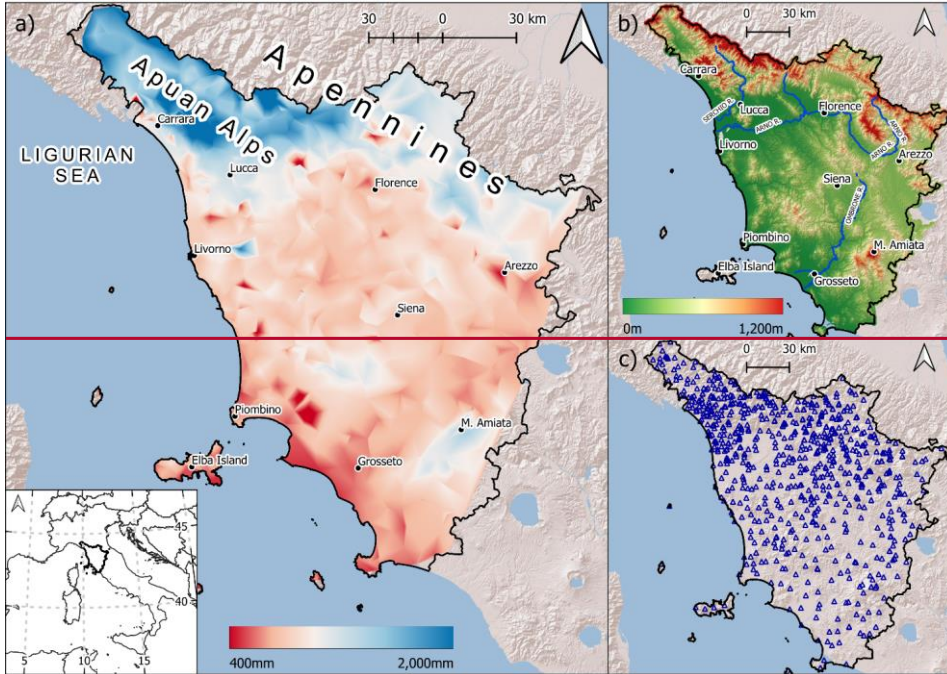
- 629 Vergni, L., di Lena, B., Chiaudani, A., 2016. Statistical characterisation of winter precipitation in the Abruzzo region
630 (Italy) in relation to the North Atlantic Oscillation (NAO). *Atmospheric Research* 178–179, 279–290.
631 <https://doi.org/https://doi.org/10.1016/j.atmosres.2016.03.028>
- 632 Vicente-Serrano, S.M., López-Moreno, J.I., 2008. Nonstationary influence of the North Atlantic Oscillation on
633 European precipitation. *Journal of Geophysical Research: Atmospheres* 113.
634 <https://doi.org/10.1029/2008JD010382>
- 635 Virtanen, P., Gommers, R., Oliphant, T.E., Haberland, M., Reddy, T., Cournapeau, D., Burovski, E., Peterson, P.,
636 Weckesser, W., Bright, J., van der Walt, S.J., Brett, M., Wilson, J., Millman, K.J., Mayorov, N., Nelson, A.R.J.,
637 Jones, E., Kern, R., Larson, E., Carey, C.J., Polat, İlhan, Feng, Y., Moore, E.W., VanderPlas, J., Laxalde, D.,
638 Perktold, J., Cimrman, R., Henriksen, I., Quintero, E.A., Harris, C.R., Archibald, A.M., Ribeiro, A.H., Pedregosa,
639 F., van Mulbregt, P., SciPy 1.0 Contributors, 2020. SciPy 1.0: Fundamental Algorithms for Scientific Computing
640 in Python. *Nature Methods* 17, 261–272. <https://doi.org/10.1038/s41592-019-0686-2>
- 641 Visbeck, M.H., Hurrell, J.W., Polvani, L., Cullen, H.M., 2001. The North Atlantic Oscillation: Past, present, and future.
642 *Proceedings of the National Academy of Sciences* 98, 12876. <https://doi.org/10.1073/pnas.231391598>
- 643 Wang, C., Dong, S., 2010. Is the basin-wide warming in the North Atlantic Ocean related to atmospheric carbon dioxide
644 and global warming? *Geophysical Research Letters - GEOPHYS RES LETT* 37.
645 <https://doi.org/10.1029/2010GL042743>
- 646 West, H., Quinn, N., Horswell, M., 2019. Regional rainfall response to the North Atlantic Oscillation (NAO) across
647 Great Britain. *Hydrology Research* 50, 1549–1563. <https://doi.org/10.2166/nh.2019.015>
- 648 Xu, H., Taylor, R.G., Xu, Y., 2011. Quantifying uncertainty in the impacts of climate change on river discharge in sub-
649 catchments of the Yangtze and Yellow River Basins, China. *Hydrol. Earth Syst. Sci.* 15, 333–344.
650 <https://doi.org/10.5194/hess-15-333-2011>

Formatted: English (United States)

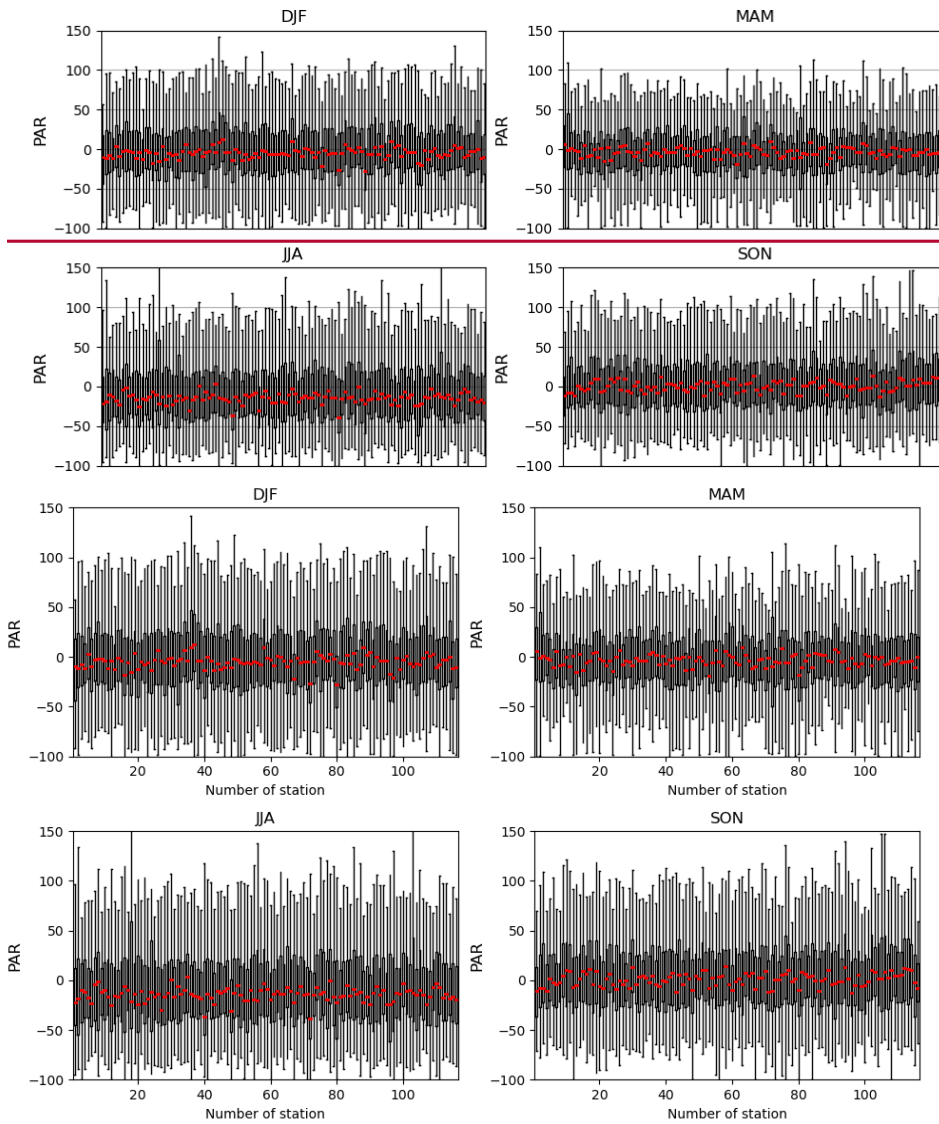
Formatted: English (United States)

651



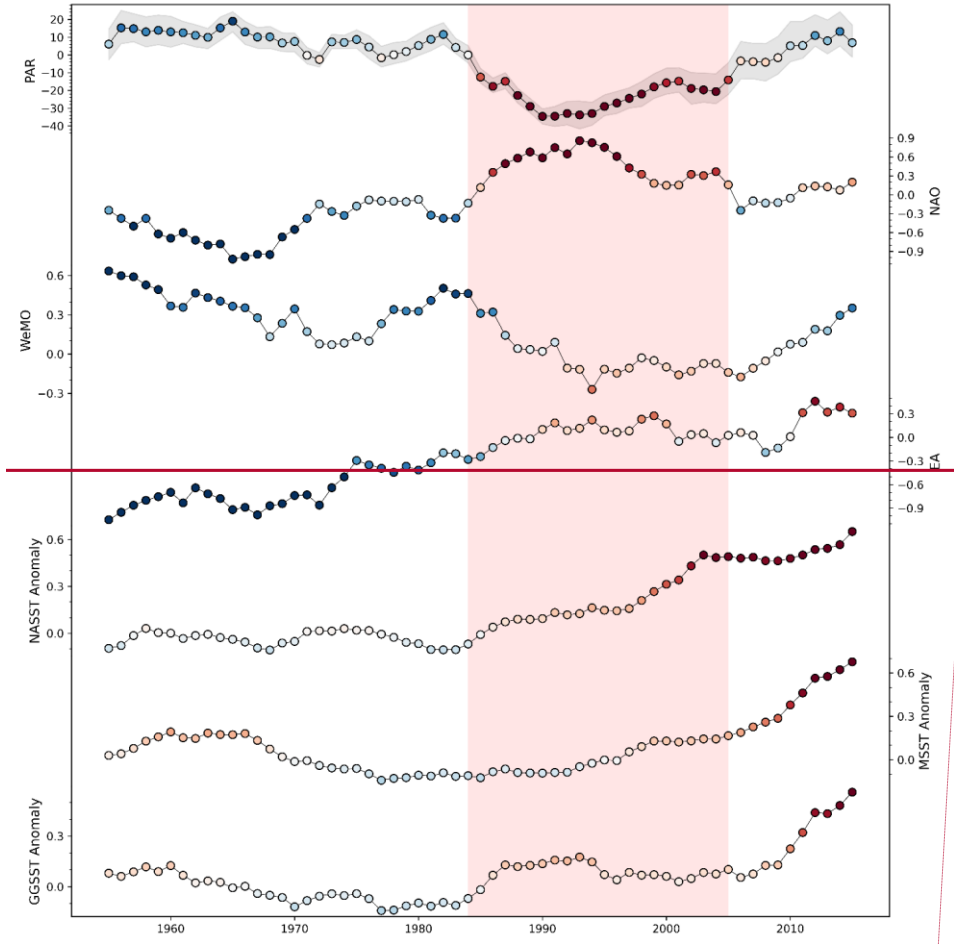


655 **Figure 1.** a) mean annual precipitation (MAP) of Tuscany linked to the morphology: the rainiest areas correspond to
656 the mountainous areas; b) morphology of Tuscany; c) the 1103 raingauges of the Tuscany Region Hydrologic Service
657 network used in this work.

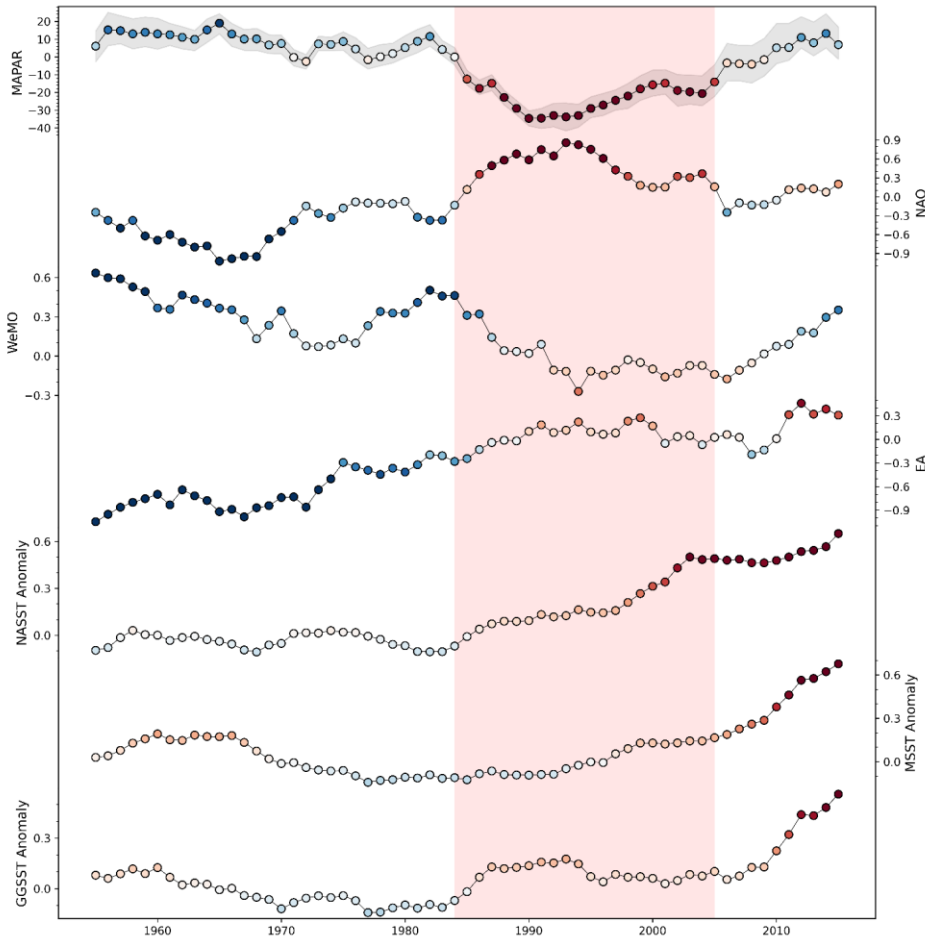


659
660 **Figure 2.** For the four seasons, Percentage Anomaly of Rainfall (PAR) of the 117 rainfall time series used in this
661 work, calculated for the four seasons. Each boxplot is referred to a rainfall time series and represents the distribution of

662 [rainfall anomaly values with respect to the annual rainfall amount of the 1961-1990 period, in agreement with the](#)
663 [equation 1 in the text](#). The boxes represent the interval between the 25th and 75th percentiles (Q1 and Q3). IQR is the
664 interquartile range $Q3-Q1$. The upper whisker will extend to the last datum lower than $Q3 + 1.5 \times IQR$. Similarly, the
665 lower whisker will reach the first datum higher than $Q1 - 1.5 \times IQR$. The red lines represent the medians (DJF:
666 December-January-February; MAM: March-April-May; JJA: June-July-August; SON: September-October-November).
667



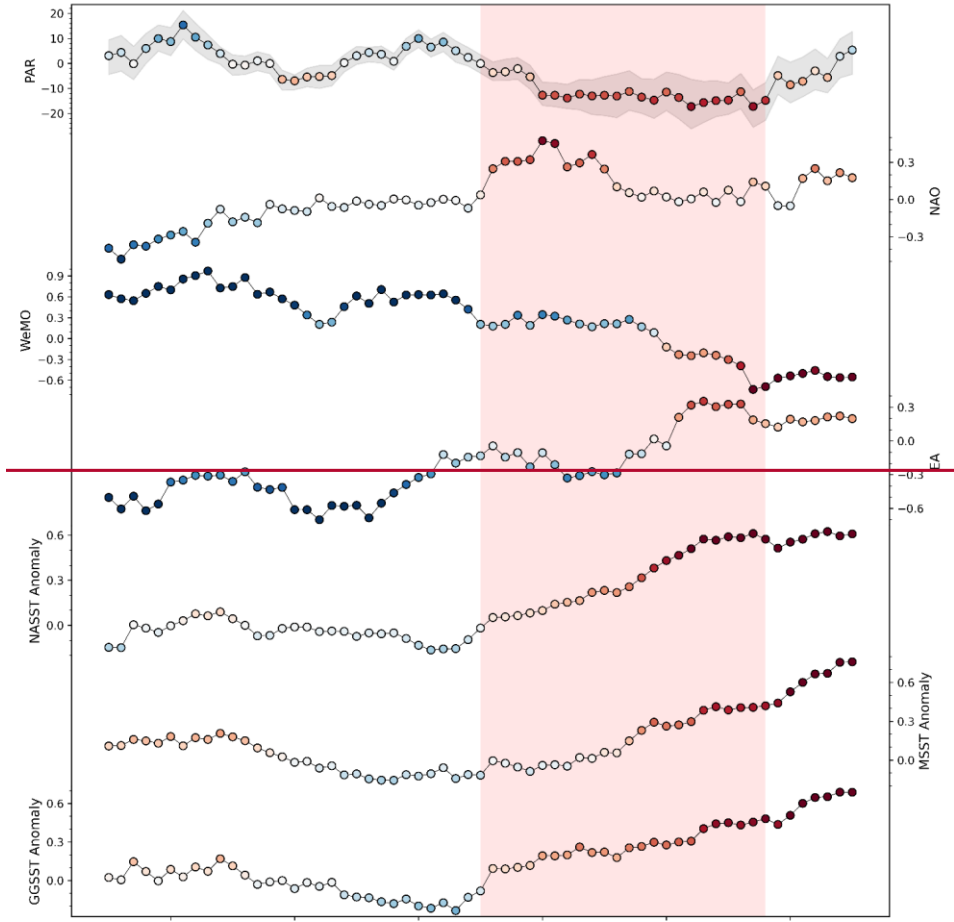
Commented [m1]: Cambiare fig MAPAR

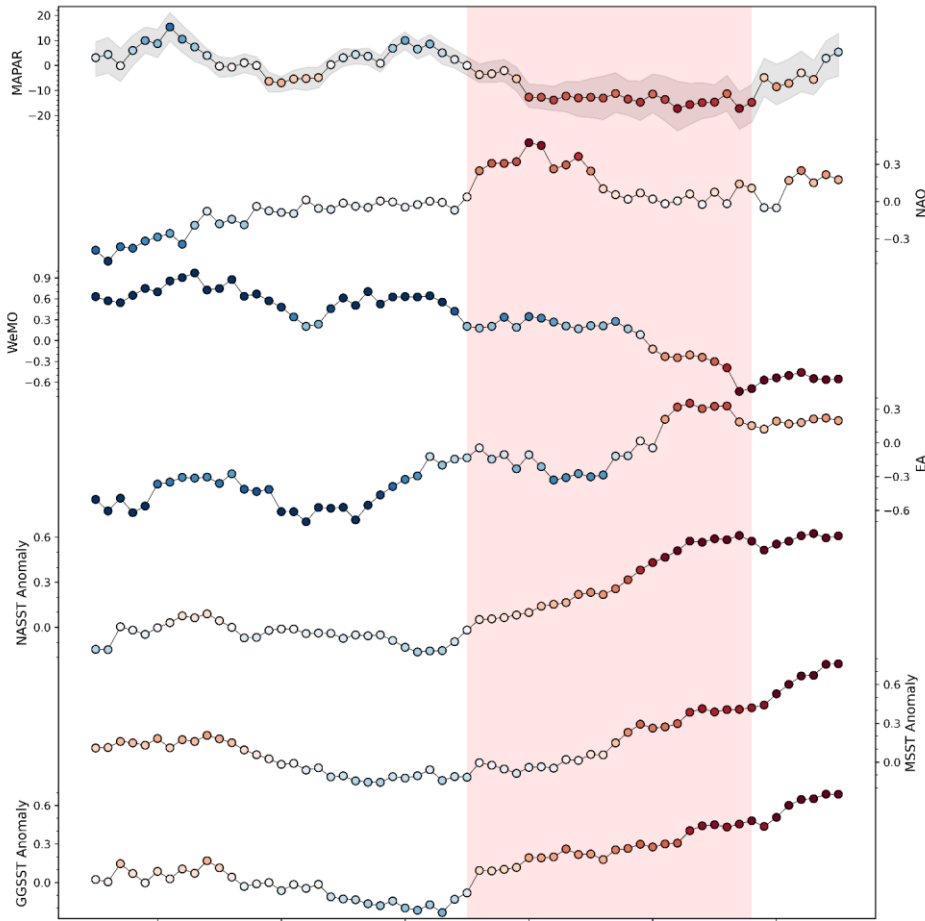


669

670 **Figure 3.** DJF season, trends of Mobile Average Percentage Anomaly Rainfall (MAPAR), NAO, WeMO, EA,
 671 North Atlantic Sea Surface Temperature (NASST), Mediterranean Sea Surface Temperature (MSST), and Genoa Gulf
 672 Sea Surface Temperature (GGSST) for the DJF season. The trends are smoothed by a 10-year mobile window and the
 673 colour of the points varies between blue and red: blue is linked to wet periods, red to dry periods. The grey band on
 674 MAPAR represents the 25th and 75th percentile, the dots represent the mean value. The pink band is referred to the
 675 main dry period of the time series.

Formatted: Font: Not Bold

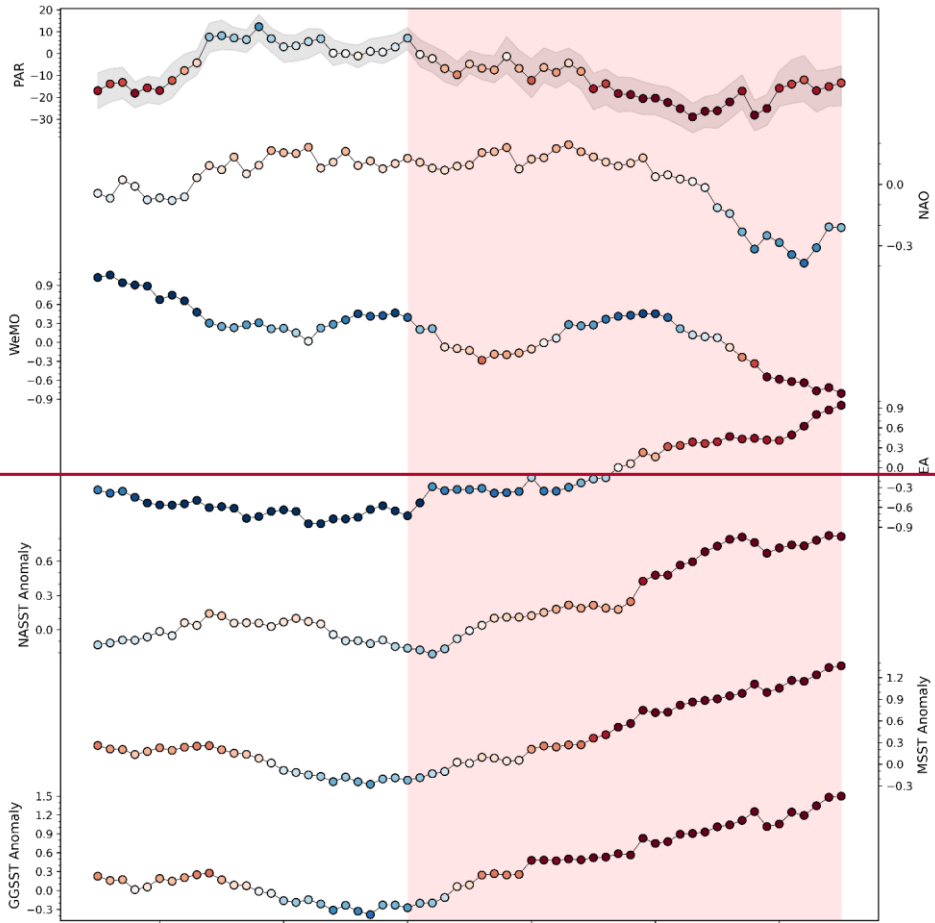




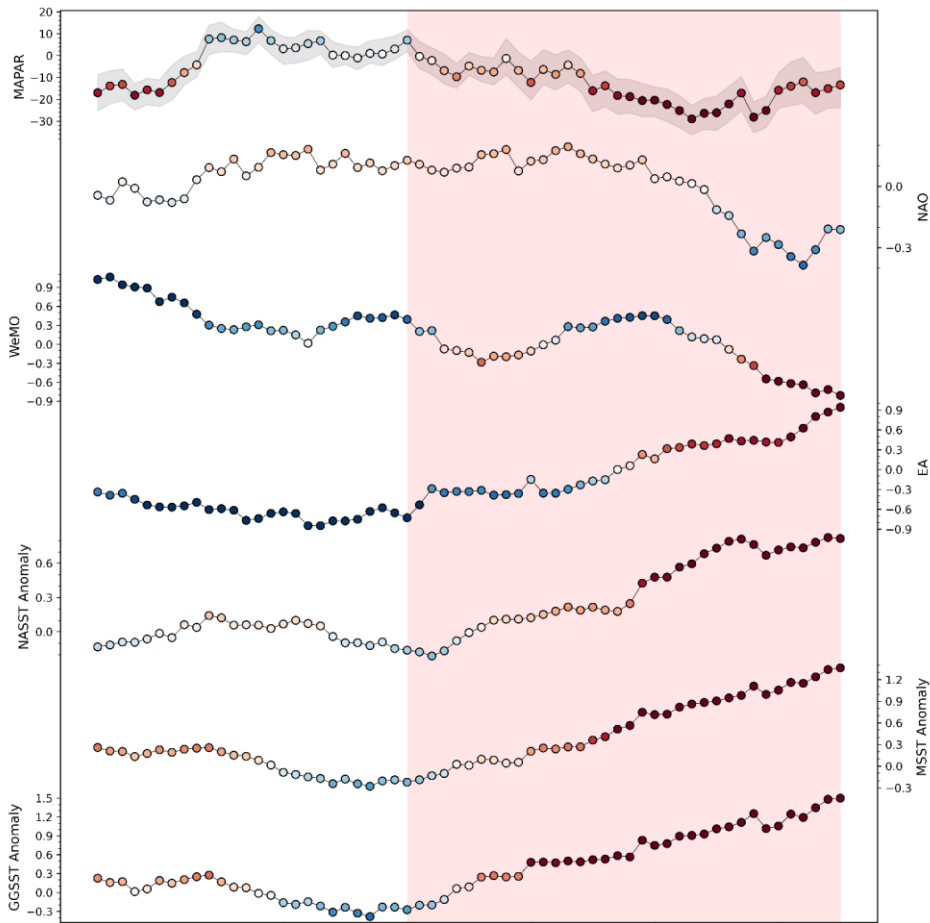
677

678 **Figure 4.** MAM season. Trends of Mobile Average -Percentage Anomaly Rainfall (MAPAR), NAO, WeMO, EA,
 679 North Atlantic Sea Surface Temperature (NASST), Mediterranean Sea Surface Temperature (MSST), and Genoa Gulf
 680 Sea Surface Temperature (GGSST) for the MAM season. The trends are smoothed by a 10-year mobile window and the
 681 colour of the points goes from blue to red: blue is linked to wet periods, red to dry periods. The grey band on MAPAR
 682 represents the 25th and 75th percentiles, the dots represent the mean value. The pink band refers to the main dry period
 683 of the time series.

Formatted: Font: Not Bold



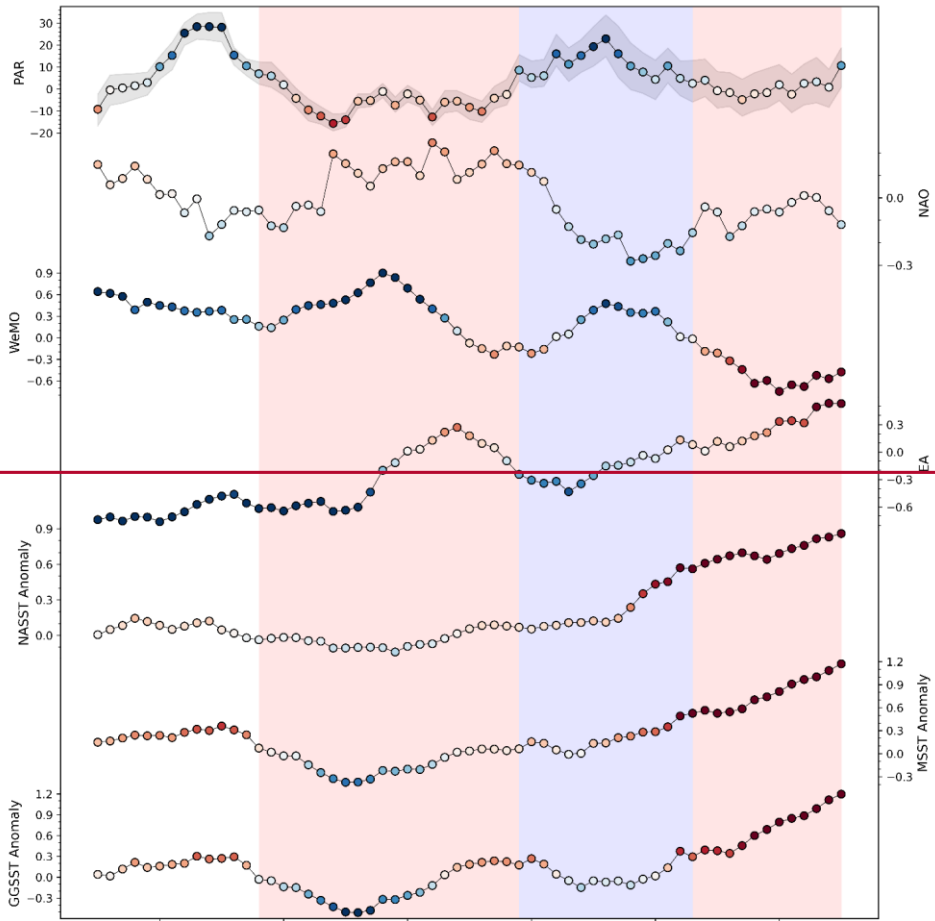
684



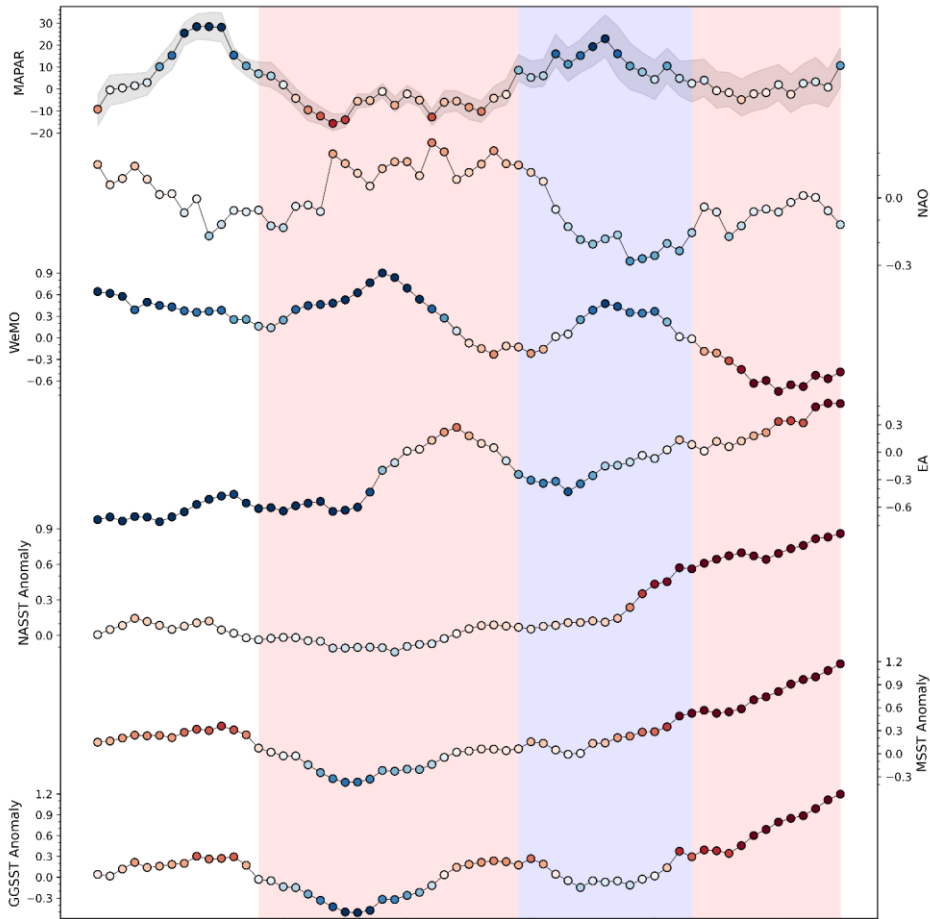
685

686 **Figure 5.** JJA trends of Mobile Average Percentage Anomaly Rainfall (MAPAR), NAO, WeMO, EA, North
 687 Atlantic Sea Surface Temperature (NASST), Mediterranean Sea Surface Temperature (MSST), and Genoa Gulf Sea
 688 Surface Temperature (GGST) for the JJA season. The trends are smoothed with a 10-year mobile window and the
 689 colour of the points varies between blue to red: blue is linked to wet periods, while red is linked to dry periods. The grey
 690 band on MAPAR represents the 25th and 75th percentile, the dots represent the mean value. The pink band refers to the
 691 main dry period of the time series.

Formatted: Font: Not Bold



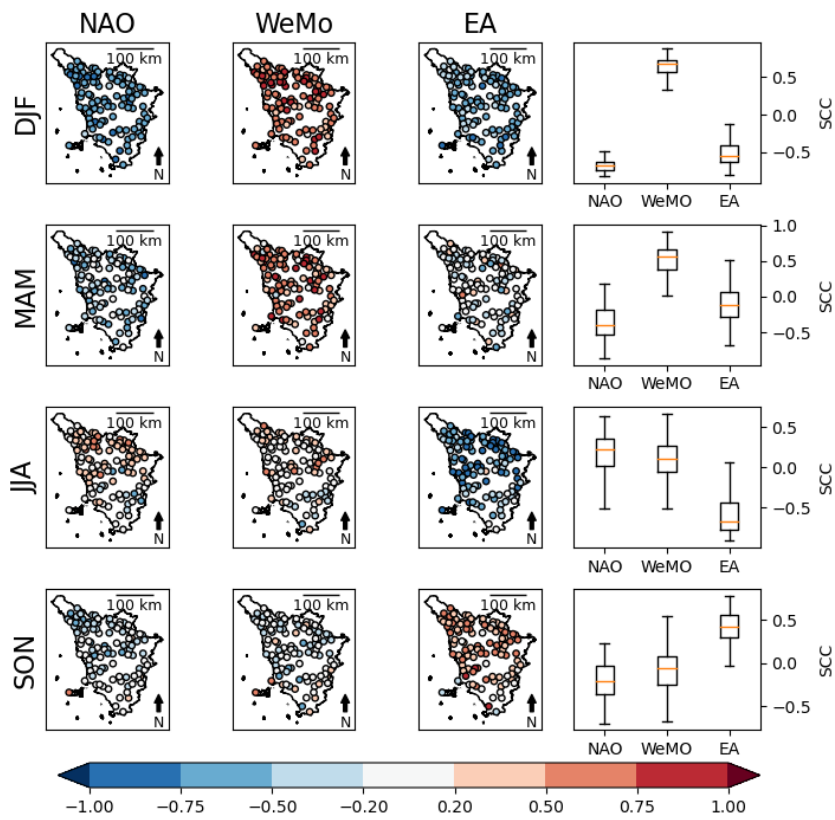
692



693

694 **Figure 6** SON season. Trends of Mobile Average Percentage Anomaly Rainfall (MAPAR), NAO, WeMO, EA,
 695 North Atlantic Sea Surface Temperature (NASST), Mediterranean Sea Surface Temperature (MSST), and Genoa Gulf
 696 Sea Surface Temperature (GGST) for the SON season. The trends are smoothed with a 10-year mobile window and
 697 the colour of the points varies between blue to red: blue indicates wet periods, red indicates dry periods. The grey band
 698 on MAPAR represents the 25th and 75th percentile, the dots represent the mean value. The pink band is referred to the
 699 main dry period of the time series, while the blue band is referred to the main wet period of the time series.

Formatted: Font: Not Bold



700

701 **Figure 7.** Spearman's correlation coefficients (SCC) between season rainfall and climatic patterns. For each season,
 702 we report the correlation with NAO, EA and WeMo and the relative boxplots. The boxes represent the interval between
 703 the 25th and 75th percentiles (Q1 and Q3). IQR is the interquartile range Q3-Q1. The upper whisker will extend to the
 704 last datum lower than $Q3 + 1.5 \times IQR$. Similarly, the lower whisker will reach the first datum higher than $Q1 - 1.5 \times IQR$.
 705 The orange lines represent the medians. (DJF: December-January-February; MAM: March-April-May; JJA: June-July-
 706 August; SON: September-October-November).

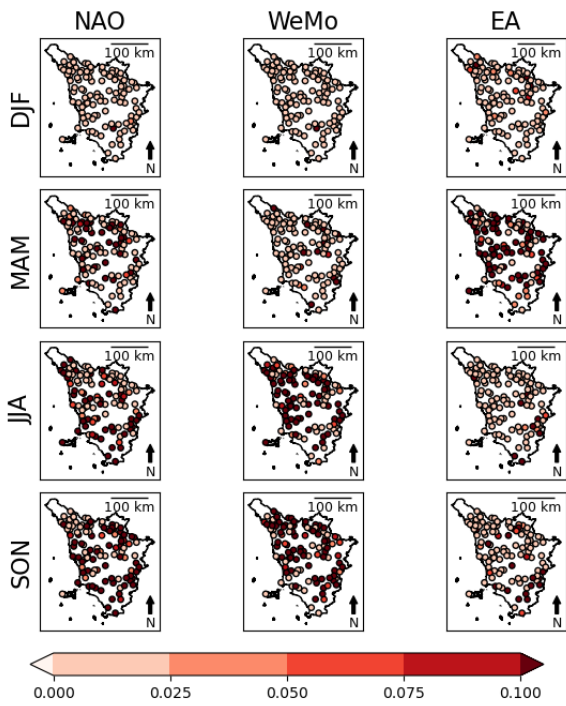


Figure 8. P-values of Spearman's correlation coefficients (SCC).

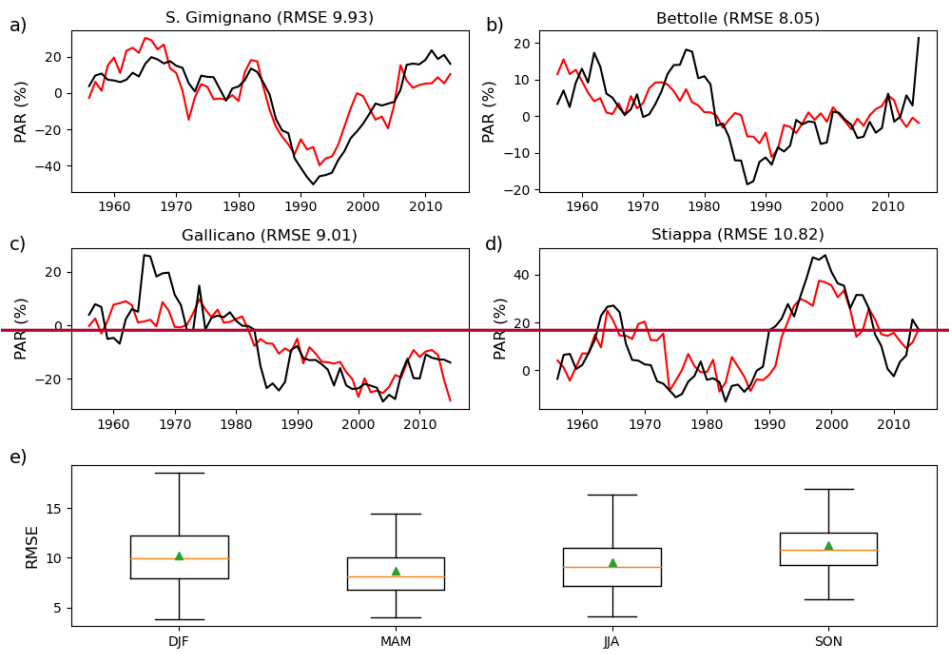
Formatted: Centered

Formatted: Font: Bold, English (United Kingdom)

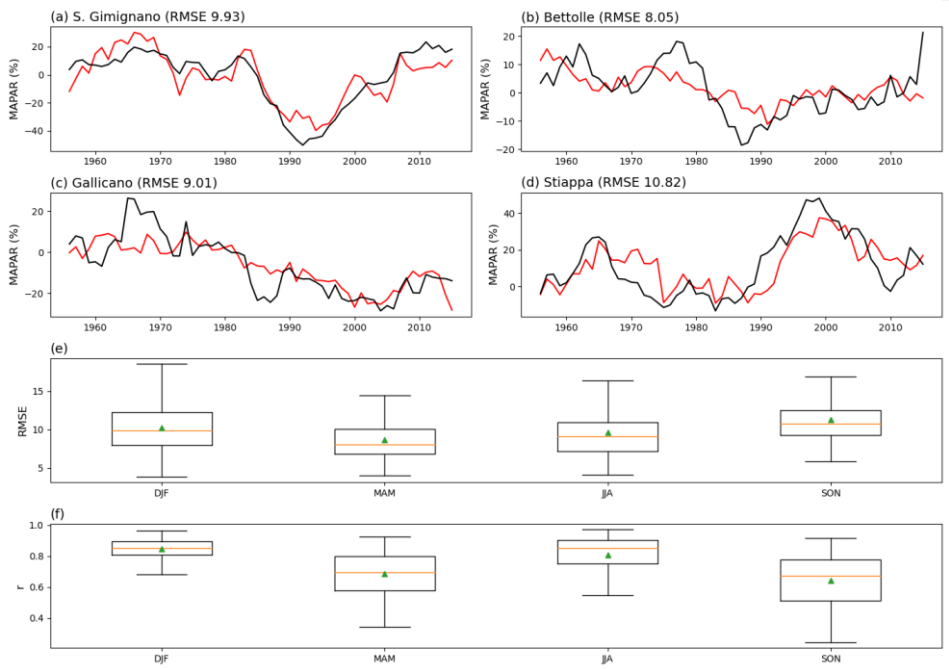
Formatted: Font: Not Bold

Formatted: English (United States)

Formatted: Normal



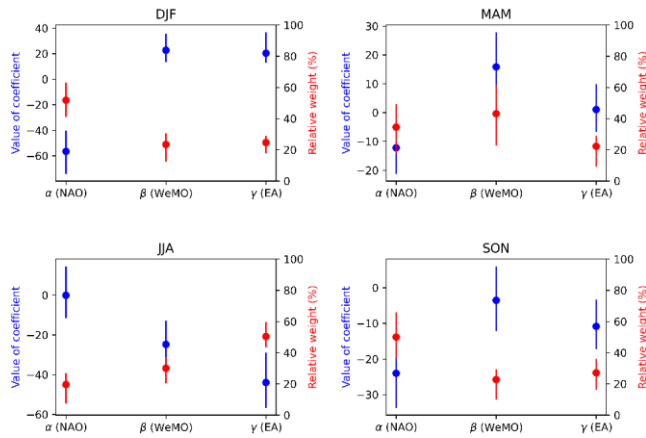
711



712

713 **Figure 9.** a-d) Four examples of observed MAPAR (black line) and predicted MAPAR (red line) respectively for
 714 the seasons DJF, MAM, JJA and SON. ~~We selected these examples because they have Root Mean Square Error~~
 715 ~~(RMSE) values similar to the error medians calculated on the whole dataset;~~ e) the boxplots represent the RMSE_Root
 716 Mean Square Error (RMSE) of the linear models for the four seasons. f) the boxplots represent the Correlation
 717 Coefficient (r) of the linear models for the four seasons. The boxes represent the interval between the 25th and 75th
 718 percentiles (Q1 and Q3). IQR is the interquartile range Q3-Q1. The upper whisker will extend to the last datum lower
 719 than $Q3 + 1.5 \times IQR$. Similarly, the lower whisker will reach the first datum higher than $Q1 - 1.5 \times IQR$. The orange lines
 720 represent the medians, while the green triangles represent the means. (DJF: December-January-February; MAM: March-
 721 April-May; JJA: June-July-August; SON: September-October-November).

Commented [m12]: In tutte le figure semplificare questa scritta che al primo editor non piace è troppo lunga



722
 723 **Figure 10.** Setting of the linear model coefficients used to understand the relationship between climate patterns and
 724 rainfall. The blue circle is the mean absolute value of the coefficient, whereas the red circle represents the mean relative
 725 weight of the coefficient on the prediction. The results are reported for each season. The blue and red lines represent the
 726 interval between the 25th and 75th percentiles of the coefficient distributions (DJF: December-January-February; MAM:
 727 March-April-May; JJA: June-July-August; SON: September-October-November).

1 **Seasonal rainfall trends of a key Mediterranean area in relation to**
2 **large-scale atmospheric circulation: how does current global change**
3 **affect the rainfall regime?**

4 Marco Luppichini^{1,2,*}, Monica Bini^{2,3,4}, Michele Barsanti⁵, Roberto Gianecchini^{2,4,6}, Giovanni Zanchetta^{2,4,7}

5 ¹Department of Earth Sciences, University of Study of Florence, Via La Pira 4, Florence, Italy

6 ²Department of Earth Sciences, University of Pisa, Via S. Maria, 52, 56126 Pisa, Italy

7 ³Istituto Nazionale di Geofisica e Vulcanologia (INGV), Via Vigna Murata 605, 00143 Roma, Italy

8 ⁴CIRSEC Centro Interdipartimentale di Ricerca per lo Studio degli Effetti del Cambiamento Climatico
9 dell'Università di Pisa, Via del Borghetto 80, 56124 Pisa, Italy

10 ⁵Department of Civil and Industrial Engineering, University of Pisa, Largo L. Lazzarino, 56122 Pisa, Italy

11 ⁶Institute of Geosciences and Earth Resources, IGG-CNR, via Moruzzi 1, 56124 Pisa, Italy

12 ⁷Istituto di Geologia Ambientale e Geoingegneria, IGAG-CNR, Rome, Italy

13 **Abstract**

14 Current global warming causes a change in atmospheric dynamics, with consequent variations in the rainfall regimes.
15 Understanding the relationship between global climate patterns, global warming, and rainfall regimes is crucial for the
16 creation of future scenarios and for the relative modification of water management. The aim of this study is to improve
17 knowledge of the relationship between North Atlantic Oscillation (NAO), East Atlantic (EA), and Western Mediterranean
18 Oscillation (WeMO) with the seasonal rainfalls in Tuscany, Italy. The study area occupies a strategic position since it lies
19 in a transition zone between the wet area of northern Europe and the dry area of the northern coast of Africa. This research,
20 based on a statistical correlation method and on linear models, is designed to understand the relationship between seasonal
21 rainfalls and climate patterns. The results of this study demonstrate that the use of linear models can yield more
22 information than traditional statistical correlations. The results show a decrease in rainfall in the warm period of the year,
23 namely in the summer, when its expression is most visible. This phenomenon is ascribable to current global warming,
24 which causes an increase in sea-surface temperatures. An increase in the Northern Atlantic Sea Surface Temperature and
25 in the Mediterranean Sea Surface Temperature causes a reduction of the Iceland Low, with an extension of the Azores
26 High. Moreover, an increase in the Genoa Gulf SST induces a weakening of the Genoa Gulf Low, one of the main
27 cyclogenetic systems of the Mediterranean.

28 **Keywords:** Climatic Patterns, Current Global Warming, East Atlantic, North Atlantic Oscillation, Western
29 Mediterranean Oscillation, rainfall trend, Tuscany.

30 **Introduction**

31 Current global warming causes effects at different scale levels, including changes in the hydrological cycle (Allan,
32 2011; Bates et al., 2008). The effects are visible in air temperature trends and, more generally, in rainfall, in the form of
33 frequency and intensity of extreme events and changes in soil moisture (Blöschl et al., 2019; Stagl et al., 2014; Xu et al.,
34 2011), with wide implications in terms of socio-economic conditions and financial policy (European Environment
35 Agency, 2019). The Mediterranean region is an ideal research testbed for current climatic changes both for its location
36 for its historico-cultural importance, and for having been considered a hot spot for future climatic changes (Giorgi, 2006).
37 The Mediterranean, located between the European humid domain and the North African arid belt, provides alternating
38 circulation regimes with large spatial and temporal variability (Dükeloh and Jacobeit, 2003). In this context, a correct
39 characterization of rainfall regimes can improve the management of water resources (Tramblay et al., 2020) and of
40 extreme events (Cardoso Pereira et al., 2020; Myhre et al., 2019). Several studies have identified a general decrease
41 (although with some exceptions) in the annual rainfall amount in the area of the Mediterranean basin (Bertola et al., 2019;
42 Blöschl et al., 2019; Caloiero et al., 2018, 2011; Colantoni et al., 2015; Deitch et al., 2017; Dükeloh and Jacobeit, 2003;
43 Halifa-Marín et al., 2021; Longobardi and Villani, 2010; Martin-Vide and Lopez-Bustins, 2006; Philandras et al., 2011;
44 Ríos-Cornejo et al., 2015); and atmospheric patterns related to mesoscale circulation (Brandimarte et al., 2011; Caloiero
45 et al., 2011; Halifa-Marín et al., 2021; Lopez-Bustins et al., 2008; Luppichini et al., 2021; Martinez-Artigas et al., 2021;
46 Ríos-Cornejo et al., 2015; Trigo et al., 2004).

47 During the winter months, one of the main drivers of rainfall variability in southern Europe and in the Mediterranean
48 is the presence of different pressure fields over the Northern Atlantic Ocean and their variability indicated as the North
49 Atlantic Oscillation (NAO) (Hurrell, 1995). NAO is defined by an index measured as a north-southern dipole of pressure
50 anomalies, with one pole located at higher latitudes (Iceland Low 80°N) and the other at the central latitudes of the North
51 Atlantic between 35°N and 40°N (Azores High). The East Atlantic (EA) index is similar to that of NAO but is displaced
52 south-eastward to the approximate nodal lines of the NAO pattern. The EA index is often interpreted as a downward-
53 shifted NAO model, but its strong subtropical link entails a different peculiarity. The EA value is positive when a
54 significant drop in pressure occurs in the Atlantic Ocean; at the same time, the subtropical oceanic anticyclone belt
55 considerably rises in latitude and strengthens. In response, the African anticyclone gains energy and invasiveness over
56 the Mediterranean, subjecting this area to frequent pulses of hot and dry Saharan air in all seasons (Climate Prediction
57 Center, 2021; Mellado-Cano et al., 2019). The NAO and EA indexes present interannual and annual variabilities with

58 positive and negative phases. The rainfall in the Mediterranean can be associated with a negative phase of NAO and/or
59 EA, when we observe an expansion of the Iceland Low. Instead, during a positive phase of NAO and/or EA, Northern
60 Europe is the rainiest area (Rousi et al., 2020). Both NAO and EA are influenced by the Sea Surface Temperature (SST)
61 of the Northern Atlantic Ocean (NASST) and of the Mediterranean (MSST). An increase in NASST and in MSST is
62 correlated to an expansion of the Azores High and to a consecutive reduction of the Iceland Low, which cause a formation
63 of the NAO and EA positive phases (Frankignoul et al., 2003; Robertson et al., 2000; Visbeck et al., 2001). More recently,
64 NAO has been correlated to the Atlantic Multidecadal Oscillation (AMO), a representative index of the NASST trend
65 (Knight et al., 2005). AMO changes the zonal position of the NAO centre of action, moving the cyclonic area closer to
66 Europe or to North America. During a positive phase of AMO, the Icelandic Low moves further towards North America,
67 while the Azores High moves further towards Europe (and vice versa) for the negative phase of AMO (Börgel et al.,
68 2020). The statistical correlation between the NAO and the winter rainfalls in Europe varies over time (Vicente-Serrano
69 and López-Moreno, 2008) and it is a function of NAO and AMO with a different role of the indices from northern Europe
70 to the Mediterranean (Luppichini et al., 2021).

71 The Western Mediterranean oscillation (WeMO) is an index often used to study variability in rainfall in alternative to
72 NAO in the Mediterranean region. The WeMO index is the difference of atmospheric pressure in a dipole, with the first
73 pole located in Padua (45.40°N, 11.48°E) in northern Italy and the second one located in San Fernando, Cádiz (36.28°N,
74 6.12°W) in southwestern Spain (Climatic Research Unit, 2021). Specifically, the former is located in the Po plain (an area
75 with relatively high barometric variability due to the different influence of the central European anticyclone and of the
76 Genoa Gulf Low), while the latter pole is located in the Gulf of Cádiz in the southwest of the Iberian Peninsula, often
77 subject to the influence of the Azores anticyclone and, episodically, to the cut-off of circumpolar lows or to its own
78 cyclogenesis (Halifa-Marín et al., 2021; Lopez-Bustins et al., 2020; Martin-Vide and Lopez-Bustins, 2006). A positive
79 phase of WeMO is associated with a low-pressure area in the Ligurian Sea and with an anticyclone in the Gulf of Cadiz.
80 Instead, a negative phase of the index determines a low in the Gulf of Cadiz and an anticyclone in Central Europe. WeMO
81 is influenced by NASST and MSST, but also by the Genoa Gulf Sea Surface Temperature (GGSST), with positive values
82 correlating to low values of SST (Martín et al., 2012; Martin-Vide and Lopez-Bustins, 2006).

83 Current global warming causes a progressive increase in NASST, MSST and GGSST (Pastor et al., 2020; Wang and
84 Dong, 2010) so that NAO and EA are likely to be characterized by more positive phases, and WeMO by more negative
85 phases.

86 The purpose of this study is to understand the rainfall seasonal trends of the last 70 years in Tuscany (central Italy),
87 in relation to mesoscale circulation and to the indices defined above. The rainfall dataset employed derives from several
88 raingauges with high spatial density and temporal activity which allow us to investigate the rainfall trend in great detail

89 and with direct measurements. The rainfall trends are compared with the NAO, EA and WeMO indices by means of
90 mathematical and statistical methods, so as to understand the climatic trends influencing the rainfall regime in the area
91 We investigated the link between the different indices by using traditional statistical methods (Spearman, 1904)

92 Many land dynamics (e.g., drought, floods, solid transport, coastal erosion) are linked to the rainfall regime which can
93 create management criticalities (e.g., Billi and Fazzini, 2017; Bini et al., 2021; Piccarreta et al., 2004). The study of
94 variations in the amount of rainfall related to climatic indices allows to lay the foundations for future studies and land
95 management. The observations put forward in this work and the methods adopted could be extended to other
96 Mediterranean areas by increasing knowledge about these issues.

97 **Methods**

98 Study area

99 Tuscany has a strategic location because it is located in the northern sector of the Mediterranean, in the proximity of
100 the Genoa Gulf, by far the most active cyclogenetic centre of the Mediterranean (Trigo et al., 2002).

101 As expected, the mean annual precipitation (MAP) in Tuscany is influenced by morphology (Figure 1a). The rainiest
102 areas are located at the highest altitudes (Apuan Alps and Northern Apennines; Figure 1b). In particular, the Apuan Alps
103 in north-western Tuscany show some of the highest rainfall amounts in Italy (Giannecchini and D'Amato Avanzi, 2012;
104 Rapetti and Vittorini, 1994), often characterized by high intensity (D'Amato Avanzi et al., 2004; Giannecchini, 2006). In
105 Tuscany, MAP is in a range of 400-3000 mm/year with a clear gradient from the northern to the southern and it is linked
106 to the morphology (Figure 1a). The main rainy season is autumn, with a progressive decrease that generally starts in
107 December. The mean rainfall in the DJF season is ca 300 mm, ca 250 mm in MAM, ca 130 mm in JJA, and ca 350 mm
108 in SON.

109 **FIGURE 1**

110 Dataset

111 *Rainfall dataset and processing*

112 The raingauge dataset was provided by the Tuscany Region Hydrologic Service (SIR) network and includes 1103
113 raingauges (Figure 1c). The daily data were obtained by an automated download procedure through an HTTP request in
114 March 2021. The dataset is the best one available in this area and it is managed by the SIR which validates and checks
115 the data. The dataset is used in several research works because it is referenced and managed by a public body. In particular,
116 Luppichini et al. 2021 used this dataset to understand the relationship between NAO and winter rainfall in this area. The

117 activity period of each raingauge is variable. The older stations have been monitoring since the beginning of the last
118 century, even if a temporal continuity of the data is not always guaranteed for some stations. SIR provides the daily
119 rainfall data for each raingauge in the operation period. To obtain longer and more complete time series from this dataset,
120 we grouped the stations according to a stringent protocol. This procedure is necessary to reconstruct the time series of the
121 stations that have experienced minor changes in position or that have undergone an administrative variation (e.g., a slight
122 change in name or identification code). The stations have consecutive intermittent activity times due to the
123 decommissioning of one and the subsequent installation of a new one. In these cases, we merged the stations by assigning
124 the same, or part of the same name, with a difference in altimetry (less than 20%) of the measurement, and a maximum
125 distance (less than 2 km). The geographic coordinates of the merged stations derived from a cartesian mean of the original
126 coordinates of the origin stations.

127 By using the data available and following the procedure described above, a total of 117 time series were obtained from
128 1950 to 2020. The rainfall data can also be useful for comparison with the results of the linear models which predict
129 rainfall anomalies. The rainfall values are expressed as percentage anomalies of rainfall (PAR), and are calculated as
130 follows:

$$PAR_{s,i} = \frac{x_{s,i} - \bar{x}_i}{\bar{x}_i} \cdot 100 \quad (1)$$

131 where, $x_{s,i}$ is the annual seasonal rainfall amount of the i -th year and s -th season, \bar{x}_i is the annual rainfall amount mean
132 of the period 1961-1990.

133 The values of PAR are calculated for the four seasons: winter (DJF: December, January and February); spring (MAM:
134 March, April and May –); summer (JJA: June, July and August); autumn (SON: September, October and November).
135 Mean Average PAR (MAPAR) is a ten-year mobile average of PAR calculated for each season, and the values are
136 associated with the central year. We chose to use a ten-year mobile average because this time range is within the standard
137 10–30 year time scale considered to be decadal variability (Meehl et al., 2009).

138 *Climatic Dataset*

139 The NAO dataset is provided by the Climate Analysis Section of the US National Center for Atmospheric Research
140 (NCAR). This dataset is based on the principal (PC)-based index component of the NAO, which are the time series of the
141 leading Empirical Orthogonal Function (EOF) of SLP anomalies over the Atlantic sector, 20°-80°N, 90°W-40°E. This
142 index is used to measure the yearly NAO, by tracking the seasonal movements of the Icelandic Low and Azores High.
143 The dataset has a monthly frequency from January 1889 to December 2020. PC-based indices are more optimal
144 representations of the full spatial patterns of the NAO (National Center for Atmospheric Research Staff (Eds), 2021).

145 The EA dataset used in this study is provided by the National Weather Service of NOAA. The frequency of the dataset
146 is on a monthly basis, from 1950 to 2020. The index is standardized by 1981-2010 climatology (Climate Prediction
147 Center, 2021).

148 The WeMO index is provided by the Climatic Research Unit (CRU) of the University of East Anglia (Climatic
149 Research Unit, 2021). The time series started in 1821 and has a monthly frequency.

150 The trends of NASST, MSST, and GGSST are calculated from the Extended Reconstructed Sea Surface Temperature
151 (ERSST) dataset version 5 (NOAA, 2021), and they are expressed using a 10-year mobile window of anomalies. The
152 anomalies are referred to the mean of the 1961-1990 period. NASST is calculated in the area 0N-65N 80W-0E; MSST in
153 the area 38N-49N 0E-28E; and GGSST in the area 42.8N-44.8N 7.6E-10.76E.

154 Statistical Correlation and Linear Models

155 . We investigated the link between the different indices by using traditional statistical methods (Spearman, 1904), but
156 also by introducing in this field an innovative approach, which employs a linear model to understand the influence of
157 each index on the rainfall prediction. The combination of these different methods helped us to comprehend the accuracy
158 and the advantages of the new method proposed.

159 We calculated the correlation coefficient to identify a possible relationship between atmospheric teleconnection and
160 rainfall amount. Several authors use a statistical method of correlation to quantify the relationship between atmospheric
161 indices and rainfalls (Brandimarte et al., 2011; Faust et al., 2016; Kalimeris et al., 2017; Kotsias et al., 2020; Koyama and
162 Stroeve, 2019; López-Moreno et al., 2011; Vicente-Serrano and López-Moreno, 2008). In particular, some authors
163 (Caloiero et al., 2011; Izquierdo et al., 2014; Luppichini et al., 2021; Nalley et al., 2019; Vergni et al., 2016) use
164 Spearman's correlation coefficient (SCC) (Spearman, 1904) to understand the relationship between atmospheric index
165 and rainfall amount. This relationship is suitable for monotonically-related variables, even when their relationship is not
166 linear. The range of Spearman's coefficients is between -1 and 1; positive values indicate a tendency of one variable to
167 increase or decrease together with another variable, whereas negative values indicate a trend in which the increase in the
168 values of one variable is associated with the decrease in the values of the other variable, and vice versa. We have divided
169 the time series into four seasons: winter from December to February (DJF), spring from March to May (MAM), summer
170 from June to August (JJA) and autumn from September to November (SON). We calculated the SCC among the three
171 atmospheric teleconnections and the rainfall for the four seasons using a 10-year moving time window from 1950 to 2020.
172 We assigned the correlation result to the year halfway through each ten-years.

173 However, the trends in the time series can influence the SCC (Arianos and Carbone, 2009; Boris et al., 2009; Iqbal et
174 al., 2020; Podobnik and Stanley, 2008). To exclude the influence of the trends on the results of this study, we investigated

175 further using the detrended cross-correlation analysis (DCCA) proposed by Kristoufek, (2014) in the framework
 176 developed by Ide et al. (2017). The DCCA results are in perfect agreement with the SCC results. Therefore, we could
 177 exclude an influence of the trends on the use of SCC in this study. More information can be found in the supplementary
 178 material.

179 We can create linear models capable of predicting the rainfall amount by using the NAO, WeMO and EA time series.
 180 The equation of a linear model predicting the rainfall (R_p), is the following:

$$R_p = \alpha NAO + \beta WeMO + \gamma EA + \delta \quad (2)$$

181 We can analyse the best estimates of the model parameters (α , β , γ) to understand the role of each input in the prediction
 182 of rainfall. If we want to obtain the best prediction models, we should use models that are more complex than a simple
 183 linear model. However, the simplicity of the linear models allows to analyse the influence of the inputs, since one of the
 184 tasks of this work is to show that more complex models (for instance with the inclusion of synergies between the input
 185 data) are not necessary to explain the rainfall observed. We therefore created a linear model for each raingauge time series
 186 for each season. The different range of the three atmospheric teleconnections could influence the information expressed
 187 by the parameters of models α , β and δ . For this reason, we scaled the time series of NAO, WeMO and EA in the range
 188 between 0 and 1 for the studied period (1950-2020), by applying the following equation:

$$T = \frac{T_s - T_{s_m}}{T_{s_M} - T_{s_m}} \quad (3)$$

189 where T is the index time series in the 0-1 range, T_{s_M} is the maximum value of the index, and T_{s_m} is the minimum
 190 value of the index. We fitted a linear model for each time series, using the SciPy library in Python Language and, in more
 191 detail, the “curve_fit” method (Virtanen et al., 2020). We validated the fits calculating the Root Mean Square Error
 192 ($RMSE$) and the Correlation Coefficient (r) as follows:

$$RMSE = \left(\frac{1}{N} \sum_{i=0}^N (F_i - V_i)^2 \right)^{0.5} \quad (4)$$

$$r = \frac{\left(\frac{1}{N} \sum_{i=0}^N (F_i * V_i) \right)}{\left(\frac{1}{N} \sum_{i=0}^N F_i^2 \right)^{0.5} \cdot \left(\frac{1}{N} \sum_{i=0}^N V_i^2 \right)^{0.5}} \quad (5)$$

193 where F_i are the forecast values, V_i are the observed values and N the number of years.

194 **Results**

195 **Rainfall Trends**

196 Figure 2 reports the values of *PAR* calculated for each time series used in this work, and obtained from equation 1.
197 The graphs indicate a small variability of *PAR* between each time series, excluding the possibility of different influences
198 on the linear model outcomes by the input stations and a significant variability in the study area. The *MAPAR* of the
199 study area is shown in Figures 3-6 for the four seasons. These variations of *MAPAR* over time are different in the four
200 seasons. From 1950 to 1985, the DJF season was characterized by a slow rainfall reduction followed by a sudden decrease
201 around the 90's. The first years of the 1990's presented a *MAPAR* reduction of 40%. Starting from 2000, the DJF *MAPAR*
202 increased progressively until reaching the amount recorded before 1990 (Figure 3). Until the 1990s, the MAM *MAPAR*
203 was characterized by an oscillation, from the 1990's to the 2010's, MAM *MAPAR* has the minimum values which are in
204 the range between -10 and -20%. MAM *MAPAR* increased after 2008 (Figure 4). The JJA *MAPAR* started to decrease
205 in 1965 with minimum values of -30% around 2005. The last years were marked by a weakly increase of JJA *MAPAR*
206 (Figure 5). SON *MAPAR* had a certain variability over an approximate 20-year period. The maximum SON *MAPAR*
207 amount was recorded around 1965 and 1995, while the minimum values were those of the period 1970-1990 (Figure 6).

208 **FIGURE 2**

209 **Atmospheric Teleconnection Trends**

210 In DJF, NAO was characterized by an intensification of the positive phase, the EA time series was characterized by
211 an intensification of the positive phase starting from 1985 (Figure 3), and WeMO was characterized by a positive phase
212 with a decrease in the 1990-2010 period.

213 In MAM, NAO and EA time series were characterized by a progressive increase with an intensification of the positive
214 phase; WeMO has experienced a progressive decrease from a positive phase to a negative persistence phase since 2005
215 (Figure 4).

216 In JJA, NAO was characterized by a positive phase until 2005, whereas the index was characterized by a negative
217 phase, except for some years. In this season, EA started to increase progressively in 1995, while WeMO had a progressive
218 decrease with a persistence positive phase since 2005 (Figure 5).

219 In SON, NAO is variable with periods characterized by negative alternated with positive phases. In this season, EA
220 had a higher index fluctuation, with a negative phase until 1980, followed by a more positive ten-year phase and then by
221 a negative phase until 2000. From 2000 to 2020, EA increased reaching its maximum values. WeMO was characterized

222 by two distinct positive phases around 1975 and 1995, but the overall trend has decreased with a negative phase since
223 2005 (Figure 6).

224 Sea surface temperature trends

225 The variations of NASST, MSST and GGSST started to display a clear increasing trend in the 1980's in all seasons.
226 Such increase only started around the 2010's for DJF and GGSST, while it started to increase in the 1980s in the other
227 seasons. The increase in SST was greater in the summer than in the other seasons (Figures 3-6).

228

229 **FIGURE 3**

230 **FIGURE 4**

231 **FIGURE 5**

232 **FIGURE 6**

233 Statistical Correlation

234 Figure 7 reports the results obtained from SCC and Figure 8 shows the spatial distribution of the p-values obtained.
235 In the DJF season, rainfall is correlated with WeMO and anticorrelated with NAO and EA. Rainfall increases during a
236 negative phase of NAO or EA and a positive phase of WeMO. During this period, each atmospheric teleconnection has a
237 similar effect on the rainfall amount. In the MAM season, the strongest correlation is with WeMO, and even in this case
238 a positive phase of the index corresponds to a rainfall increase in the study area. NAO and EA are weakly anticorrelated
239 with the rainfall amount. The strongest correlation is with EA in the JJA season, and a negative phase of this index
240 indicates an increase in rainfall in the area, while a positive phase of EA corresponds to reduced precipitation in summer.
241 NAO and WeMO are weakly correlated with rainfall, but do not show a clear behaviour. Even in the SON season, the
242 strongest correlation is with EA. The correlation in this season is positive, which indicates that a positive EA phase
243 determines increased precipitation in the area. The spatial correlation distribution is homogenous with no clear spatial
244 pattern, especially when the correlations are strong, providing a precise indication of the relationship (Figure 7).

245 **FIGURE 7**

246 **FIGURE 8**

247 **Linear Models**

248 In Figure 9a-d, we report four examples of the MAPAR prediction by means of linear models referred to the DJF,
249 MAM, JJA and SON seasons. The cases shown represent the results of the lineal models because they have RMSE values
250 similar to the error medians calculated on the entire dataset (Figure 9e). For the case shown in Figure 9a, α , β and γ are
251 respectively -96.56, 42.53, and 4.85; for the case reported in Figure 9b they are -21.39, -15.54 and -15.76, for the case
252 reported in Figure 9c they are -30.71, -56.10 and -1.34; for the case reported in Figure 9d they are -48.05, 7.54 and 6.71.
253 Figure 9e and 9d also report the RMSE and r of the entire dataset. SON, followed by MAM, which is the season with the
254 highest average errors.

255 Figure 10 shows the mean values of coefficients α , β and γ for the linear models in each season (blue circles). We
256 can observe a change in the values of the three coefficients from one season to another. In Figure 10, the red circles show
257 the relative weights of each coefficient. In the DJF season, the coefficient with the greatest weight is α with a mean value
258 of about 55%, followed by β and γ . The coefficients indicate that NAO has more influence on the rainfall trend than
259 WeMO and EA on DJF. In this season, the coefficient values indicate that an increase in rainfall is linked to a negative
260 phase of NAO (α is negative) and a positive phase of WeMO (β is positive). In the MAM season, β (WeMO) has the
261 highest weight in the results of the models, followed by α (NAO) and γ (EA). Therefore, the coefficients denote that the
262 amount of rainfall is correlated with a positive phase of WeMO and with a negative phase of NAO. Also in this season,
263 EA has less influence on the model than the other two indices. In the JJA season EA is the index with the greatest
264 coefficient (γ). In particular, the coefficients suggest that the summer rainfall is linked to a negative phase of EA. Less
265 important, the coefficients indicate that the summer rainfall is linked to a negative phase of WeMO. In the SON season,
266 NAO has the greatest weight and is followed by WeMO and EA, which have less influence on the rainfall trend. In this
267 case, the coefficients are all negative, so that rainfall is correlated to a negative phase of these indices.

268 **FIGURE 9**

269 **FIGURE 10**

270 **Discussion**

271 **Mathematical and statistical relationship between atmospheric teleconnections and rainfall**

272 The statistical correlation calculated with Spearman's method represents a first indication of the influence of climate
273 patterns on the local rainfall trend. In accordance with several studies (Caloiero et al., 2011; Deser et al., 2017; Ferrari et
274 al., 2013; George et al., 2004; López-Moreno et al., 2011; Luppichini et al., 2021; Riaz et al., 2017; Vergni and Chiaudani,

275 2015; Vicente-Serrano and López-Moreno, 2008; West et al., 2019), NAO influence is predominant in winter, with an
276 anticorrelation between index and rainfall amount. In agreement with the obtained SCC, an increase in the Azores High,
277 and consequently a decrease in the Iceland Low, determine reduced winter rainfall in the study area. The correlation
278 between NAO and rainfall decreases during the successive seasons with a minimum correlation in summer. In winter and
279 in spring, the correlation with WeMO is strong and it is characterized by a positive sign. This implies the formation of
280 the Genoa Gulf Low and its reinforcement increases the amount of rainfall in the study area. This can be ascribed to the
281 direction of the moist air masses coming from the Atlantic Ocean and directed to the north-western coast of Spain and to
282 the Mediterranean (Degeai et al., 2020; Martín et al., 2012; Martin-Vide and Lopez-Bustins, 2006). In this dynamic state
283 the moist air masses can reach Tuscany, enhancing local cyclogenesis and rainfall. The SCC values indicate that the
284 influence of the Genoa Gulf Low decreases in summer and autumn . The correlation between rainfall and EA is strong in
285 winter and summer; in summer, the correlation with rainfall is mainly with EA. In winter, the link between EA and rainfall
286 is the same for NAO. In summer, the greater representativeness of EA than of NAO on the Azores High allows a better
287 understanding of the link between rainfall and global climate in this season. In detail, the formation of the Azores High
288 and of the African High results in an increase in the EA index, and this means that there is reduced precipitation in the
289 study area. In autumn, the statistical correlations do not allow to create a link between large-scale circulation and rainfall.
290 Indeed, we can observe a weak anticorrelation with NAO, a weak correlation with EA, and no correlation with WeMO.
291 This method seems unsuitable to represent the autumn season with its atmospheric dynamics.

292 The results of the linear models are conformant to the statistical correlation results for the DJF, MAM and JJA seasons,
293 while we observe some differences in SON. The strong correspondence between the two methods in DJF, MAM and JJA
294 makes it possible to validate our linear model. In autumn, the analysis of the linear models identifies an important role of
295 NAO, and therefore a link between northern Atlantic atmospheric circulation and rainfall in the study area. In autumn,
296 the coefficients of NAO (α) are set negative and this means that an increase in the index is linked to a decrease in rainfall
297 in the study area. This mathematical result is more plausible than that obtained from the analysis of correlations based on
298 the notions of atmospheric physics introduced previously. The linear model-based method has allowed us to refine our
299 investigations and to improve our knowledge of the dynamics in the Mediterranean over the seasons.

300 The use of our linear models offers the advantage of clarifying the role and influence of large-scale atmospheric
301 circulation on rainfall over the study region in different seasons, and this may appear controversial when using only the
302 statistical correlation. These linear methods can also be useful for rainfall prediction, although it is not the aim of this
303 paper to produce the best model for predictions. A more complex model may be better suited to reduce the overall model;
304 however, it would have been difficult to understand the influence of each input parameter, which is the main scope of this
305 paper.

306 Long-term rainfall trends and relation with climate patterns

307 This study has identified a confused trend for the DJF, MAM and SON rainfall, while the JJA rainfall clearly tends to
308 decrease. These results agree with those of other studies based on different rainfall datasets (Caloiero et al., 2018; Deitch
309 et al., 2017; Philandras et al., 2011). More specifically, Deitch et al. (2017) studied the seasonal trend of rainfall in the
310 Mediterranean area, demonstrating a negative trend for summer rainfall and no trend for winter/autumnal rainfall in
311 Tuscany.

312 The DJF seasons are characterized by significantly decreased precipitation between 1984 and 2005 (Figure 3). This
313 period is marked by a positive phase of NAO and EA and a negative phase of WeMO. Starting around 1984, the increase
314 in NAO and EA is due to an increase in NASST (Figure 3). An increase in NASST is correlated to an expansion of the
315 Azores High and a consecutive reduction of the Iceland Low, resulting in the formation of the NAO and EA positive
316 phases (Börgel et al., 2020; Frankignoul et al., 2003; Robertson et al., 2000; Visbeck et al., 2001). The successive increase
317 in rainfall from 2005 to 2020 seems to have been caused by an increase in the WeMO, and therefore by an increase in the
318 Genoa Gulf Low persistence. This could indicate a change of the main climatic driver with respect to the previous period
319 (Figure 3).

320 The MAM season presents a decrease in the amount of rainfall in the period between 1985 and 2008 (Figure 4). The
321 WeMO constantly decreases with progressive intensification of the negative phase. This indicates a gradual reduced
322 intensity of the Genoa Gulf Low. The GGSST has progressively increased since 1985. Furthermore, NAO and EA are in
323 a persistent positive phase. Since 2008, there has been a weak increase in the precipitation trend. The JJA rainfall trends
324 have the highest correlation with EA, while NAO and WeMO have a lower influence (Figure 7 and 10). The increase in
325 NASST, MSST and GGSST induces the NAO and EA indices to a positive phase, and WeMO to a negative phase. This
326 process induces a progressive reduction of rainfall trends in this season. SON is characterized by rainfall trend variability
327 with two wet periods and two dry periods (Figure 6). Each dry period is marked by an increase in NAO, whereas the wet
328 period results from an increase in WeMO linked to a weak decrease in GGSST (Figure 6). The increase in sea surface
329 temperature is greater in the warm periods of the year and it is caused by current global warming. From these observations,
330 we can evince that the warm periods of the year are marked by a greater decrease in precipitation resulting in less water
331 availability in the environmental system.

332 **Conclusions**

333 This study helps to gain a better knowledge of the rainfall trends of the last 70 years in Tuscany, a key area of the
334 Mediterranean Basin, strongly influenced by the cyclogenetic activity related to the Genoa Gulf Low. These trends are
335 analyzed on the basis of the trend of the main atmospheric drivers of the northern hemisphere. The location of the study

336 area allows to understand the influences of Atlantic atmospheric circulation and of the Mediterranean atmospheric
337 circulation on rainfall. Along with Spearman's traditional coefficient analysis, this study proposes a new mathematical
338 method to investigate the relationship between climate pattern and rainfall. The method based on the use of linear models
339 has resulted to be valid, with similar results derived from a statistical correlation. This new method has allowed for a
340 more detailed comprehension of the link between climate patterns and precipitation in the study area. In Tuscany, the
341 rainfall amount is influenced by Northern Atlantic atmospheric circulation and by the Genoa Gulf Low. The influences
342 of the two atmospheric systems vary during the year: in winter, rainfall is strongly correlated to the three indices; in
343 spring, the main influence is represented by WeMO, indicating an important role played by the Genoa Gulf Low; in
344 summer, the main driver is EA, which represents better than NAO the influence of the Azores High in this season; in
345 autumn, the strongest correlation is with NAO.

346 The amount of rainfall in the study area is influenced by the SSTs which induce a variation in the Northern Atlantic
347 and Mediterranean atmospheric circulations (Börgel et al., 2020; Frankignoul et al., 2003; Robertson et al., 2000; Visbeck
348 et al., 2001). Current global warming determines an increase in the SSTs and this increase is higher in the warm seasons
349 of the year (James et al., 2006). The results of this study show that in these seasons there is the greatest reduction of water
350 availability, on account of a direct decrease in precipitation. For this reason, current global warming could be responsible
351 for less rainfall in this area, and this occurs mainly in the warm seasons when temperature increase is highest. These
352 aspects can be deepened by future studies that can strengthen the relationships found and the considerations made in this
353 work.

354

355 **Conflicts of Interest:** The authors declare no conflict of interest. The funders had no role in the design of the study;
356 in the collection, analyses, or interpretation of data; in the writing of the manuscript, or in the decision to publish the
357 results.

358 **Acknowledgements:** The authors are grateful to the Tuscany Region Hydrologic Service for providing the data used
359 in this work.

360 **Funding:** This research was funded by project no. 249792 "Dalla Preistoria all'Antropocene: Nuove Tecnologie per
361 la valorizzazione dell'eredità culturale della Versilia (PANTAREI)" Tuscany Region (call POR FSE 2014-2020, Resp.
362 M. Bini); by the collaborative research agreement no. 579999-2019 "Autorità di Bacino Distrettuale Appennino
363 Settentrionale" (Resp. Monica Bini and Roberto Gianecchini); and by the project: "Cambiamenti globali e impatti locali:
364 conoscenza e consapevolezza per uno sviluppo sostenibile della pianura Apuo-versiliese" Fondazione Cassa Risparmio
365 di Lucca, (Resp. M. Bini).

366 **Reference**

- 367 Allan, R.P., 2011. Human influence on rainfall. *Nature* 470, 344–345. <https://doi.org/10.1038/470344a>
- 368 Arianos, S., Carbone, A., 2009. Cross-correlation of long-range correlated series. *Journal of Statistical Mechanics: Theory*
369 *and Experiment* 2009, P03037.
- 370 Bates, B., Kundzewicz, Z.W., Wu, S., Burkett, V., Doell, P., Gwary, D., Hanson, C., Heij, B., Jiménez, B., Kaser, G.,
371 Kitoh, A., Kovats, S., Kumar, P., Magadza, C.H.D., Martino, D., Mata, L., Medany, M., Miller, K., Arnell, N.,
372 2008. *Climate Change and Water*. Technical Paper of the Intergovernmental Panel on Climate Change.
- 373 Bertola, M., Viglione, A., Hall, J., Blöschl, G., 2019. Flood trends in Europe: are changes in small and big floods different?
374 *Hydrology and Earth System Sciences Discussions* 1–23. <https://doi.org/10.5194/hess-2019-523>
- 375 Billi, P., Fazzini, M., 2017. Global change and river flow in Italy. *Global and Planetary Change* 155, 234–246.
376 <https://doi.org/https://doi.org/10.1016/j.gloplacha.2017.07.008>
- 377 Bini, M., Casarosa, N., Luppichini, M., 2021. Exploring the relationship between river discharge and coastal erosion: An
378 integrated approach applied to the pisa coastal plain (italy). *Remote Sensing* 13. <https://doi.org/10.3390/rs13020226>
- 379 Blöschl, G., Hall, J., Viglione, A., Perdigão, R.A.P., Parajka, J., Merz, B., Lun, D., Arheimer, B., Aronica, G.T., Bilbashi,
380 A., Boháč, M., Bonacci, O., Borga, M., Čanjevac, I., Castellarin, A., Chirico, G.B., Claps, P., Frolova, N., Ganora,
381 D., Gorbachova, L., Gül, A., Hannaford, J., Harrigan, S., Kireeva, M., Kiss, A., Kjeldsen, T.R., Kohnová, S.,
382 Koskela, J.J., Ledvinka, O., Macdonald, N., Mavrova-Guirguinova, M., Mediero, L., Merz, R., Molnar, P.,
383 Montanari, A., Murphy, C., Osuch, M., Ovcharuk, V., Radevski, I., Salinas, J.L., Sauquet, E., Šraj, M., Szolgay, J.,
384 Volpi, E., Wilson, D., Zaimi, K., Živković, N., 2019. Changing climate both increases and decreases European river
385 floods. *Nature* 573, 108–111. <https://doi.org/10.1038/s41586-019-1495-6>
- 386 Börgel, F., Frauen, C., Neumann, T., Meier, H.E.M., 2020. The Atlantic Multidecadal Oscillation controls the impact of
387 the North Atlantic Oscillation on North European climate. *Environmental Research Letters* 15.
- 388 Boris, P., Davor, H., M, P.A., Eugene, S.H., 2009. Cross-correlations between volume change and price change.
389 *Proceedings of the National Academy of Sciences* 106, 22079–22084. <https://doi.org/10.1073/pnas.0911983106>
- 390 Brandimarte, L., di Baldassarre, G., Bruni, G., D’Odorico, P., Montanari, A., D’Odorico, P., Montanari, A., 2011.
391 *Relation Between the North-Atlantic Oscillation and Hydroclimatic Conditions in Mediterranean Areas*. *Water*
392 *Resources Management* 25, 1269–1279. <https://doi.org/10.1007/s11269-010-9742-5>
- 393 Caloiero, T., Caloiero, P., Frustaci, F., 2018. Long-term precipitation trend analysis in Europe and in the Mediterranean
394 basin. *Water and Environment Journal* 32, 433–445. <https://doi.org/https://doi.org/10.1111/wej.12346>

395 Caloiero, T., Coscarelli, R., Ferrari, E., Mancini, M., 2011. Precipitation change in Southern Italy linked to global scale
396 oscillation indexes. *Nat. Hazards Earth Syst. Sci.* 11, 1683–1694. <https://doi.org/10.5194/nhess-11-1683-2011>

397 Cardoso Pereira, S., Marta-Almeida, M., Carvalho, A.C., Rocha, A., 2020. Extreme precipitation events under climate
398 change in the Iberian Peninsula. *International Journal of Climatology* 40, 1255–1278.
399 <https://doi.org/https://doi.org/10.1002/joc.6269>

400 Climate Prediction Center, 2021. East Atlantic [WWW Document]. URL
401 <https://www.cpc.ncep.noaa.gov/data/teledoc/ea.shtml> (accessed 9.22.21).

402 Climatic Research Unit, 2021. Mediterranean Oscillation Indices (MOI) [WWW Document]. URL
403 <https://crudata.uea.ac.uk/cru/data/moi/> (accessed 9.22.21).

404 Colantoni, A., Delfanti, L., Cossio, F., Baciotti, B., Salvati, L., Perini, L., Lord, R., 2015. Soil Aridity under Climate
405 Change and Implications for Agriculture in Italy. *Applied Mathematical Sciences* 9, 2467–2475.
406 <https://doi.org/10.12988/ams.2015.52112>

407 D'Amato Avanzi, G., Gianecchini, R., Puccinelli, A., 2004. The influence of the geological and geomorphological
408 settings on shallow landslides. An example in a temperate climate environment: the June 19, 1996 event in
409 northwestern Tuscany (Italy). *Engineering Geology* 73, 215–228.
410 <https://doi.org/https://doi.org/10.1016/j.enggeo.2004.01.005>

411 Deitch, M.J., Sapundjieff, M.J., Feirer, S.T., 2017. Characterizing Precipitation Variability and Trends in the World's
412 Mediterranean-Climate Areas. *Water (Basel)* 9. <https://doi.org/10.3390/w9040259>

413 Deser, C., Hurrell, J.W., Phillips, A.S., 2017. The role of the North Atlantic Oscillation in European climate projections.
414 *Climate Dynamics* 49, 3141–3157. <https://doi.org/10.1007/s00382-016-3502-z>

415 Dünkloh, A., Jacobeit, J., 2003. Circulation dynamics of Mediterranean precipitation variability 1948–98. *International*
416 *Journal of Climatology* 23, 1843–1866. <https://doi.org/https://doi.org/10.1002/joc.973>

417 European Environment Agency, 2019. Economic losses from climate -related extremes in Europe. Indicator Assessment.

418 Faust, J.C., Fabian, K., Milzer, G., Giraudeau, J., Knies, J., 2016. Norwegian fjord sediments reveal NAO related winter
419 temperature and precipitation changes of the past 2800 years. *Earth and Planetary Science Letters* 435, 84–93.
420 <https://doi.org/https://doi.org/10.1016/j.epsl.2015.12.003>

421 Ferrari, E., Caloiero, T., Coscarelli, R., 2013. Influence of the North Atlantic Oscillation on winter rainfall in Calabria
422 (southern Italy). *Theoretical and Applied Climatology* 114, 479–494. <https://doi.org/10.1007/s00704-013-0856-6>

423 Frankignoul, C., Friederichs, P., Kestenare, E., 2003. Influence of Atlantic SST anomalies on the atmospheric circulation
424 in the Atlantic-European sector. *Annals of Geophysics* 46.

425 George, D.G., Järvinen, M., Arvola, L., 2004. The influence of the North Atlantic Oscillation on the winter characteristics
426 of Windermere (UK) and Pääjärvi (Finland).

427 Giannecchini, R., 2006. Relationship between rainfall and shallow landslides in the southern Apuan Alps (Italy). *Natural*
428 *Hazards and Earth System Science* 6, 357–364. <https://doi.org/10.5194/nhess-6-357-2006>

429 Giannecchini, R., D'Amato Avanzi, G., 2012. Historical research as a tool in estimating hydrogeological hazard in a
430 typical small alpine-like area: The example of the Versilia River basin (Apuan Alps, Italy). *Physics and Chemistry*
431 *of the Earth, Parts A/B/C* 49, 32–43. <https://doi.org/10.1016/J.PCE.2011.12.005>

432 Giorgi, F., 2006. Climate change hot-spots. *Geophysical Research Letters* 33.
433 <https://doi.org/https://doi.org/10.1029/2006GL025734>

434 Halifa-Marín, A., Lorente-Plazas, R., Pravia-Sarabia, E., Montávez, J.P., Jiménez-Guerrero, P., 2021. Atlantic and
435 Mediterranean influence promoting an abrupt change in winter precipitation over the southern Iberian Peninsula.
436 *Atmospheric Research* 253. <https://doi.org/10.1016/j.atmosres.2021.105485>

437 Hurrell, J.W., 1995. Decadal Trends in the North Atlantic Oscillation: Regional Temperatures and Precipitation. *Science*
438 (1979) 269, 676 LP – 679. <https://doi.org/10.1126/science.269.5224.676>

439 Ide, J.S., Cappabianco, F.A., Faria, F.A., Li, C.-S.R., 2017. Detrended Partial Cross Correlation for Brain Connectivity
440 Analysis.

441 Iqbal, J., Lone, K.J., Hussain, L., Rafique, M., 2020. Detrended cross correlation analysis (DCCA) of radon, thoron,
442 temperature and pressure time series data. *Physica Scripta* 95, 085213. <https://doi.org/10.1088/1402-4896/ab9fb1>

443 Izquierdo, R., Alarcón, M., Aguilauame, L., Àvila, A., 2014. Effects of teleconnection patterns on the atmospheric routes,
444 precipitation and deposition amounts in the north-eastern Iberian Peninsula. *Atmospheric Environment* 89, 482–
445 490. <https://doi.org/https://doi.org/10.1016/j.atmosenv.2014.02.057>

446 James, H., Makiko, S., Reto, R., Ken, L., W, L.D., Martin, M.-E., 2006. Global temperature change. *Proceedings of the*
447 *National Academy of Sciences* 103, 14288–14293. <https://doi.org/10.1073/pnas.0606291103>

448 Kalimeris, A., Ranieri, E., Founda, D., Norrant, C., 2017. Variability modes of precipitation along a Central
449 Mediterranean area and their relations with ENSO, NAO, and other climatic patterns. *Atmospheric Research* 198,
450 56–80. <https://doi.org/https://doi.org/10.1016/j.atmosres.2017.07.031>

451 Knight, J.R., Allan, R.J., Folland, C.K., Vellinga, M., Mann, M.E., 2005. A signature of persistent natural thermohaline
452 circulation cycles in observed climate. *Geophysical Research Letters* 32. <https://doi.org/10.1029/2005GL024233>

453 Kotsias, G., Lolis, C.J., Hatzianastassiou, N., Levizzani, V., Bartzokas, A., 2020. On the connection between large-scale
454 atmospheric circulation and winter GPCP precipitation over the Mediterranean region for the period 1980-2017.
455 Atmospheric Research 233, 104714. <https://doi.org/https://doi.org/10.1016/j.atmosres.2019.104714>

456 Koyama, T., Stroeve, J., 2019. Greenland monthly precipitation analysis from the Arctic System Reanalysis (ASR): 2000–
457 2012. Polar Science 19, 1–12. <https://doi.org/https://doi.org/10.1016/j.polar.2018.09.001>

458 Kristoufek, L., 2014. Measuring correlations between non-stationary series with DCCA coefficient. Physica A: Statistical
459 Mechanics and its Applications 402, 291–298. <https://doi.org/https://doi.org/10.1016/j.physa.2014.01.058>

460 Longobardi, A., Villani, P., 2010. Trend analysis of annual and seasonal rainfall time series in the Mediterranean area.
461 International Journal of Climatology 30, 1538–1546. <https://doi.org/https://doi.org/10.1002/joc.2001>

462 Lopez-Bustins, J.A., Arbiol-Roca, L., Martin-Vide, J., Barrera-Escoda, A., Prohom, M., 2020. Intra-annual variability of
463 the Western Mediterranean Oscillation (WeMO) and occurrence of extreme torrential precipitation in Catalonia
464 (NE Iberia). Natural Hazards and Earth System Sciences 20, 2483–2501. [https://doi.org/10.5194/nhess-20-2483-](https://doi.org/10.5194/nhess-20-2483-2020)
465 2020

466 Lopez-Bustins, J.-A., Martin-Vide, J., Sanchez-Lorenzo, A., 2008. Iberia winter rainfall trends based upon changes in
467 teleconnection and circulation patterns. Global and Planetary Change 63, 171–176.
468 <https://doi.org/https://doi.org/10.1016/j.gloplacha.2007.09.002>

469 López-Moreno, J.I., Vicente-Serrano, S.M., Morán-Tejeda, E., Lorenzo-Lacruz, J., Kenawy, A., Beniston, M., 2011.
470 Effects of the North Atlantic Oscillation (NAO) on combined temperature and precipitation winter modes in the
471 Mediterranean mountains: Observed relationships and projections for the 21st century. Global and Planetary
472 Change 77, 62–76. <https://doi.org/https://doi.org/10.1016/j.gloplacha.2011.03.003>

473 Luppichini, M., Barsanti, M., Giannecchini, R., Bini, M., 2021. Statistical relationships between large-scale circulation
474 patterns and local-scale effects: NAO and rainfall regime in a key area of the Mediterranean basin. Atmospheric
475 Research 248, 105270.

476 Martín, P., Sabatés, A., Lloret, J., Martin-Vide, J., 2012. Climate modulation of fish populations: The role of the Western
477 Mediterranean Oscillation (WeMO) in sardine (*Sardina pilchardus*) and anchovy (*Engraulis encrasicolus*)
478 production in the north-western Mediterranean. Climatic Change 110, 925–939. [https://doi.org/10.1007/s10584-](https://doi.org/10.1007/s10584-011-0091-z)
479 011-0091-z

480 Martinez-Artigas, J., Lemus-Canovas, M., Lopez-Bustins, J.A., 2021. Precipitation in peninsular Spain: Influence of
481 teleconnection indices and spatial regionalisation. International Journal of Climatology 41, E1320–E1335.
482 <https://doi.org/https://doi.org/10.1002/joc.6770>

483 Martin-Vide, J., Lopez-Bustins, J.-A., 2006. The Western Mediterranean Oscillation and rainfall in the Iberian Peninsula.
484 International Journal of Climatology 26, 1455–1475. <https://doi.org/https://doi.org/10.1002/joc.1388>

485 Meehl, G., Goddard, L., Murphy, J., Boer, G., Danabasoglu, G., Dixon, K., Giorgetta, M., Greene, A., Hawkins, E.,
486 Hegerl, G., Karoly, D., Kimoto, M., 2009. Decadal Prediction: Can It Be Skillful? Bull Am Meteorol Soc 90, 1467–
487 1485. <https://doi.org/10.1175/2009BAMS2778.1>

488 Mellado-Cano, J., Barriopedro, D., García-Herrera, R., Trigo, R.M., Hernández, A., 2019. Examining the North Atlantic
489 Oscillation, East Atlantic Pattern, and Jet Variability since 1685. Journal of Climate 32, 6285–6298.
490 <https://doi.org/10.1175/JCLI-D-19-0135.1>

491 Myhre, G., Alterskjær, K., Stjern, C.W., Hodnebrog, Ø., Marelle, L., Samset, B.H., Sillmann, J., Schaller, N., Fischer, E.,
492 Schulz, M., Stohl, A., 2019. Frequency of extreme precipitation increases extensively with event rareness under
493 global warming. Scientific Reports 9, 16063. <https://doi.org/10.1038/s41598-019-52277-4>

494 Nalley, D., Adamowski, J., Biswas, A., Gharabaghi, B., Hu, W., 2019. A multiscale and multivariate analysis of
495 precipitation and streamflow variability in relation to ENSO, NAO and PDO. Journal of Hydrology 574, 288–307.
496 <https://doi.org/https://doi.org/10.1016/j.jhydrol.2019.04.024>

497 National Center for Atmospheric Research Staff (Eds), 2021. The Climate Data Guide: Hurrell North Atlantic Oscillation
498 (NAO) Index (PC-based). [WWW Document]. [https://climatedataguide.ucar.edu/climate-data/hurrell-north-](https://climatedataguide.ucar.edu/climate-data/hurrell-north-atlantic-oscillation-nao-index-pc-based)
499 [atlantic-oscillation-nao-index-pc-based](https://climatedataguide.ucar.edu/climate-data/hurrell-north-atlantic-oscillation-nao-index-pc-based).

500 NOAA, 2021. Extended Reconstructed SST [WWW Document]. URL [https://www.ncei.noaa.gov/products/extended-](https://www.ncei.noaa.gov/products/extended-reconstructed-sst)
501 [reconstructed-sst](https://www.ncei.noaa.gov/products/extended-reconstructed-sst) (accessed 9.28.21).

502 Pastor, F., Valiente, J.A., Khodayar, S., 2020. A warming Mediterranean: 38 years of increasing sea surface temperature.
503 Remote Sensing 12. <https://doi.org/10.3390/RS12172687>

504 Philandras, C., Nastos, P., Kapsomenakis, J., Douvis, K., Tselioudis, G., Zerefos, C., 2011. Long Term Precipitation
505 Trends and Variability within the Mediterranean Region. Natural Hazards and Earth System Sciences 11, 3235–
506 3250. <https://doi.org/10.5194/nhess-11-3235-2011>

507 Piccarreta, M., Capolongo, D., Boenzi, F., 2004. Trend analysis of precipitation and drought in Basilicata from 1923 to
508 2000 within a southern Italy context. International Journal of Climatology 24, 907–922.
509 <https://doi.org/https://doi.org/10.1002/joc.1038>

510 Podobnik, B., Stanley, H.E., 2008. Detrended Cross-Correlation Analysis: A New Method for Analyzing Two
511 Nonstationary Time Series. Physical Review Letters 100, 84102. <https://doi.org/10.1103/PhysRevLett.100.084102>

512 Rapetti, F., Vittorini, S., 1994. Le precipitazioni in Toscana: osservazioni sui casi estremi. RIVISTA GEOGRAFICA
513 ITALIANA 101, 47–76.

514 Riaz, S.M.F., Iqbal, M.J., Hameed, S., 2017. Impact of the North Atlantic Oscillation on winter climate of Germany.
515 Tellus, Series A: Dynamic Meteorology and Oceanography 69. <https://doi.org/10.1080/16000870.2017.1406263>

516 Ríos-Cornejo, D., Penas, Á., Álvarez-Esteban, R., del Río, S., 2015. Links between teleconnection patterns and
517 precipitation in Spain. Atmospheric Research 156, 14–28.

518 Robertson, A.W., Mechoso, C.R., Kim, Y.-J., 2000. The Influence of Atlantic Sea Surface Temperature Anomalies on
519 the North Atlantic Oscillation. Journal of Climate 13, 122–138. [https://doi.org/10.1175/1520-0442\(2000\)013<0122:TIOASS>2.0.CO;2](https://doi.org/10.1175/1520-0442(2000)013<0122:TIOASS>2.0.CO;2)

521 Rousi, E., Rust, H.W., Ulbrich, U., Anagnostopoulou, C., 2020. Implications of Winter NAO Flavors on Present and
522 Future European Climate. Climate 8, 13. <https://doi.org/10.3390/cli8010013>

523 Spearman, C., 1904. The proof and measurement of association between two things. The American Journal of Psychology
524 15, 72–101. <https://doi.org/10.2307/1412159>

525 Stagl, J., Mayr, E., Koch, H., Hattermann, F.F., Huang, S., 2014. Effects of Climate Change on the Hydrological Cycle
526 in Central and Eastern Europe BT - Managing Protected Areas in Central and Eastern Europe Under Climate
527 Change, in: Rannow, S., Neubert, M. (Eds.), . Springer Netherlands, Dordrecht, pp. 31–43.

528 Trambly, Y., Llasat, M.C., Randin, C., Coppola, E., 2020. Climate change impacts on water resources in the
529 Mediterranean. Regional Environmental Change 20, 83. <https://doi.org/10.1007/s10113-020-01665-y>

530 Trigo, I.F., Bigg, G.R., Davies, T.D., 2002. Climatology of Cyclogenesis Mechanisms in the Mediterranean.

531 Trigo, R.M., Pozo- Vázquez, D., Osborn, T.J., Castro- Díez, Y., Gámiz- Fortis, S., Esteban- Parra, M.J., Pozo-Vázquez,
532 D., Osborn, T.J., Castro-Díez, Y., Gámiz-Fortis, S., Esteban-Parra, M.J., 2004. North Atlantic Oscillation influence
533 on precipitation, river flow and water resources in the Iberian Peninsula. International Journal of Climatology: A
534 Journal of the Royal Meteorological Society 24, 925–944. <https://doi.org/10.1002/joc.1048>

535 Vergni, L., Chiaudani, A., 2015. RELATIONSHIP BETWEEN THE NAO INDEX AND SOME INDICES OF
536 EXTREME PRECIPITATION IN THE ABRUZZO REGION.

537 Vergni, L., di Lena, B., Chiaudani, A., 2016. Statistical characterisation of winter precipitation in the Abruzzo region
538 (Italy) in relation to the North Atlantic Oscillation (NAO). Atmospheric Research 178–179, 279–290.
539 <https://doi.org/https://doi.org/10.1016/j.atmosres.2016.03.028>

540 Vicente-Serrano, S.M., López-Moreno, J.I., 2008. Nonstationary influence of the North Atlantic Oscillation on European
541 precipitation. Journal of Geophysical Research: Atmospheres 113. <https://doi.org/10.1029/2008JD010382>

542 Virtanen, P., Gommers, R., Oliphant, T.E., Haberland, M., Reddy, T., Cournapeau, D., Burovski, E., Peterson, P.,
543 Weckesser, W., Bright, J., van der Walt, S.J., Brett, M., Wilson, J., Millman, K.J., Mayorov, N., Nelson, A.R.J.,
544 Jones, E., Kern, R., Larson, E., Carey, C.J., Polat, \.Ilhan, Feng, Y., Moore, E.W., VanderPlas, J., Laxalde, D.,
545 Perktold, J., Cimrman, R., Henriksen, I., Quintero, E.A., Harris, C.R., Archibald, A.M., Ribeiro, A.H., Pedregosa,
546 F., van Mulbregt, P., SciPy 1.0 Contributors, 2020. SciPy 1.0: Fundamental Algorithms for Scientific Computing
547 in Python. *Nature Methods* 17, 261–272. <https://doi.org/10.1038/s41592-019-0686-2>

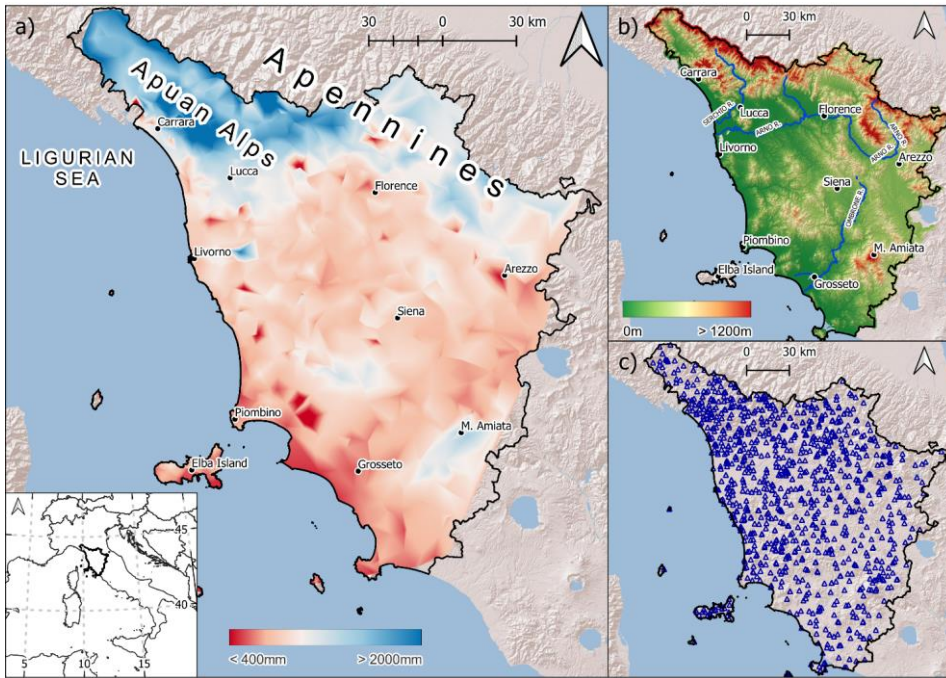
548 Visbeck, M.H., Hurrell, J.W., Polvani, L., Cullen, H.M., 2001. The North Atlantic Oscillation: Past, present, and future.
549 *Proceedings of the National Academy of Sciences* 98, 12876. <https://doi.org/10.1073/pnas.231391598>

550 Wang, C., Dong, S., 2010. Is the basin-wide warming in the North Atlantic Ocean related to atmospheric carbon dioxide
551 and global warming? *Geophysical Research Letters - GEOPHYS RES LETT* 37.
552 <https://doi.org/10.1029/2010GL042743>

553 West, H., Quinn, N., Horswell, M., 2019. Regional rainfall response to the North Atlantic Oscillation (NAO) across Great
554 Britain. *Hydrology Research* 50, 1549–1563. <https://doi.org/10.2166/nh.2019.015>

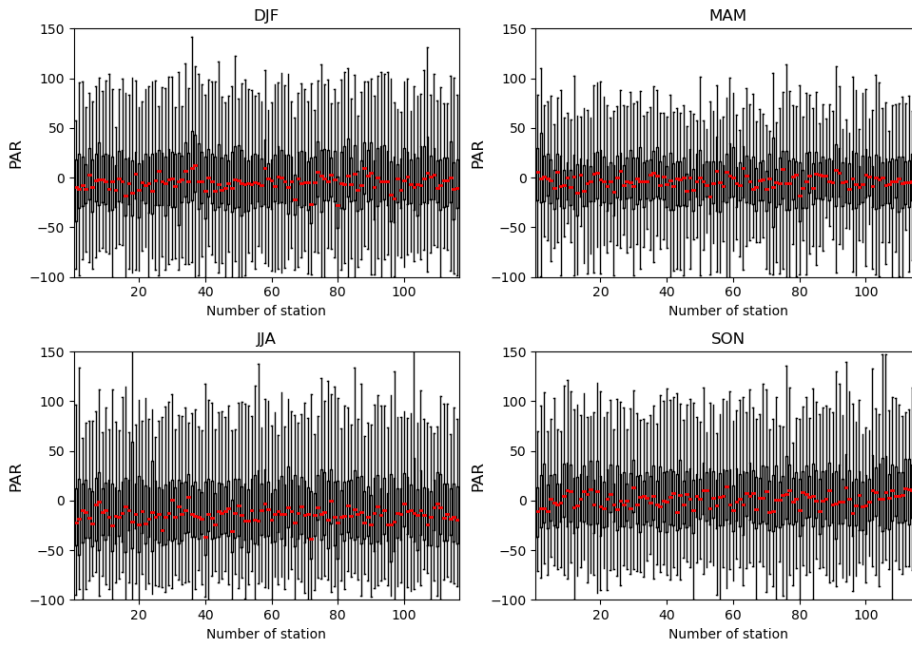
555 Xu, H., Taylor, R.G., Xu, Y., 2011. Quantifying uncertainty in the impacts of climate change on river discharge in sub-
556 catchments of the Yangtze and Yellow River Basins, China. *Hydrol. Earth Syst. Sci.* 15, 333–344.
557 <https://doi.org/10.5194/hess-15-333-2011>

558



560

561 **Figure 1.** a) mean annual precipitation (MAP) of Tuscany linked to the morphology: the rainiest areas correspond to
562 the mountainous areas; b) morphology of Tuscany; c) the 1103 raingauges of the Tuscany Region Hydrologic Service
563 network used in this work.



564

565 **Figure 2.** For the four seasons, Percentage Anomaly of Rainfall (PAR) of the 117 rainfall time series used in this work.

566 Each boxplot is referred to a rainfall time series and represents the distribution of rainfall anomaly values with respect to

567 the annual rainfall amount of the 1961-1990 period, in agreement with the equation 1 in the text. The boxes represent the

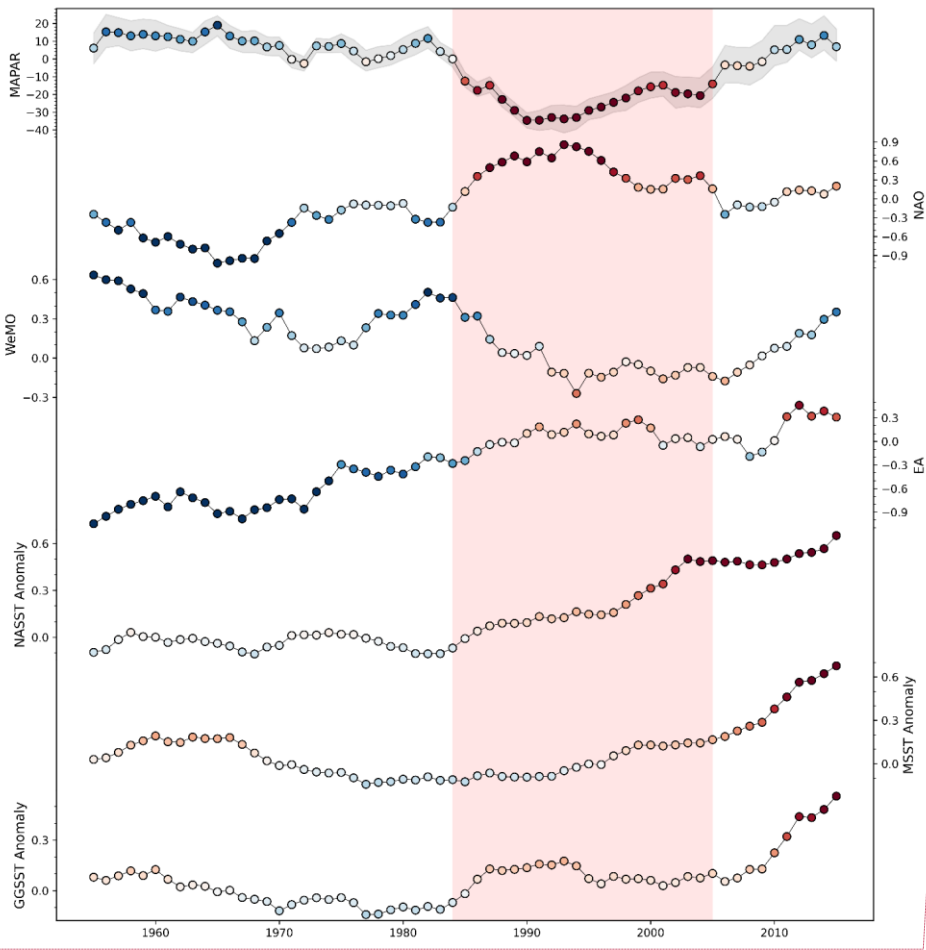
568 interval between the 25th and 75th percentiles (Q1 and Q3). IQR is the interquartile range $Q3-Q1$. The upper whisker will

569 extend to the last datum lower than $Q3 + 1.5 \times IQR$. Similarly, the lower whisker will reach the first datum higher than $Q1$

570 $-1.5 \times IQR$. The red lines represent the medians (DJF: December-January-February; MAM: March-April-May; JJA: June-

571 July-August; SON: September-October-November).

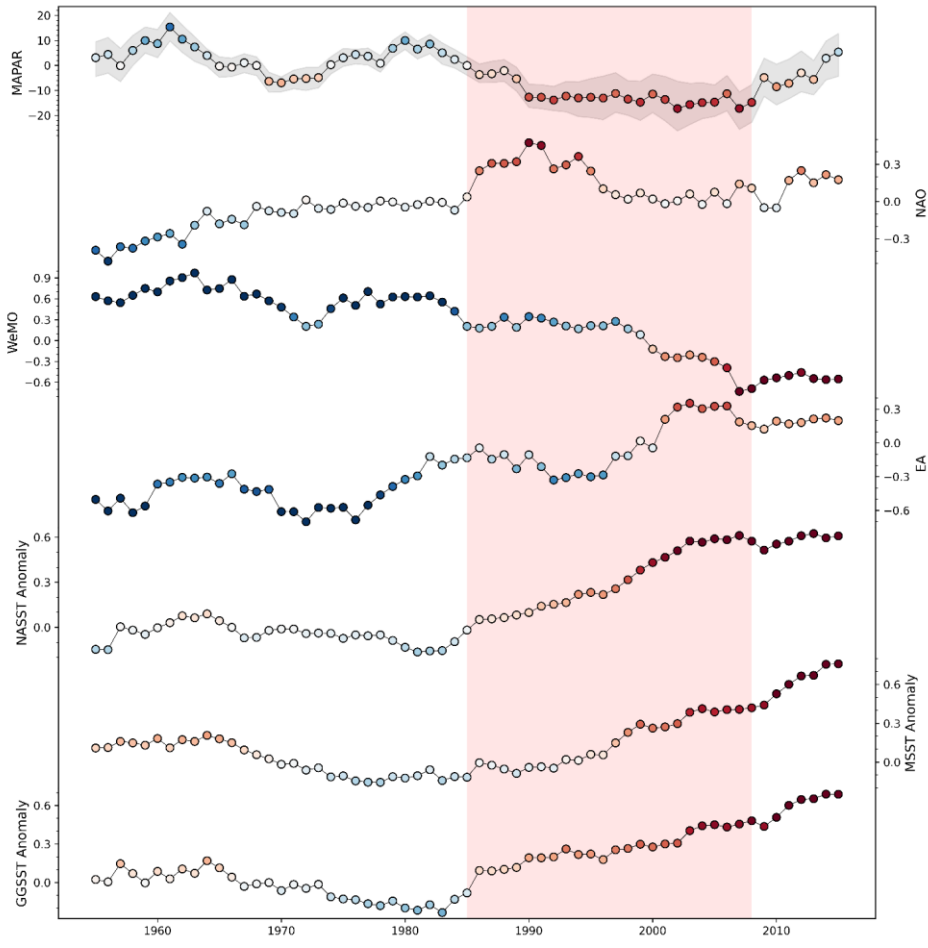
572



Commented [m1]: Cambiare fig MAPAR

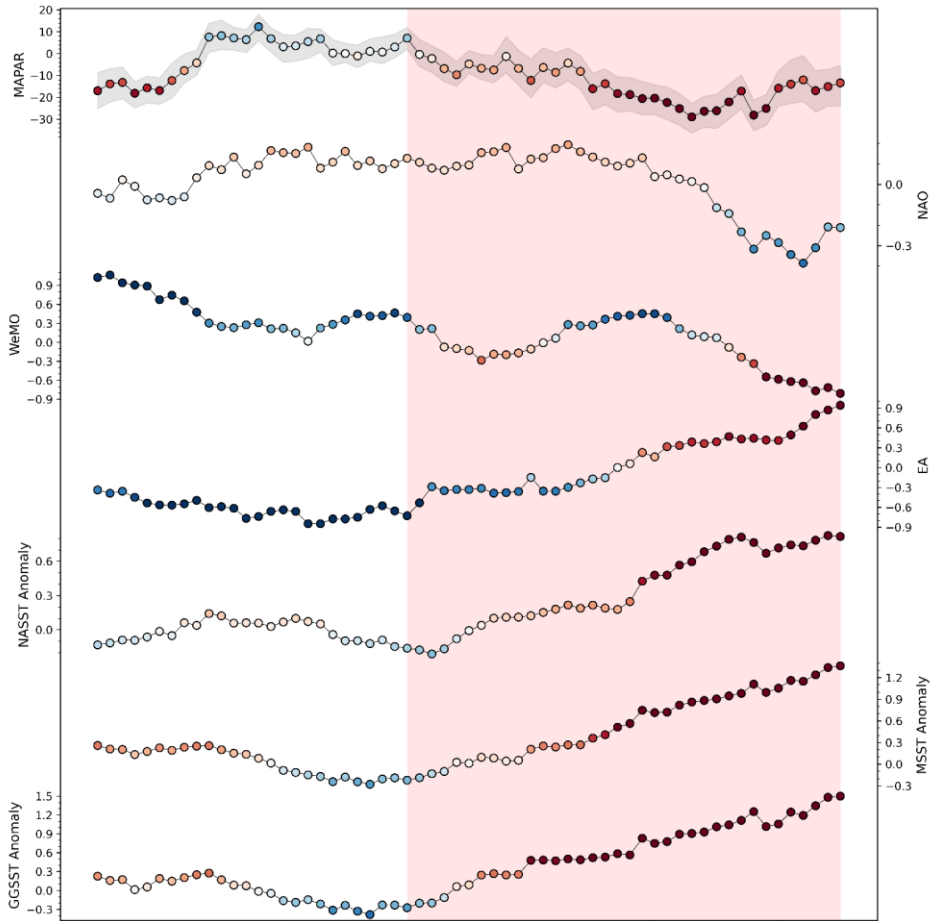
573

574 **Figure 3.** DJF season, trends of Mobile Average Percentage Anomaly Rainfall (MAPAR), NAO, WeMO, EA, North
 575 Atlantic Sea Surface Temperature (NASST), Mediterranean Sea Surface Temperature (MSST), and Genoa Gulf Sea
 576 Surface Temperature (GGSST). The trends are smoothed by a 10-year mobile window and the colour of the points varies
 577 between blue and red: blue is linked to wet periods, red to dry periods. The grey band on MAPAR represents the 25th and
 578 75th percentile, the dots represent the mean value. The pink band is referred to the main dry period of the time series.



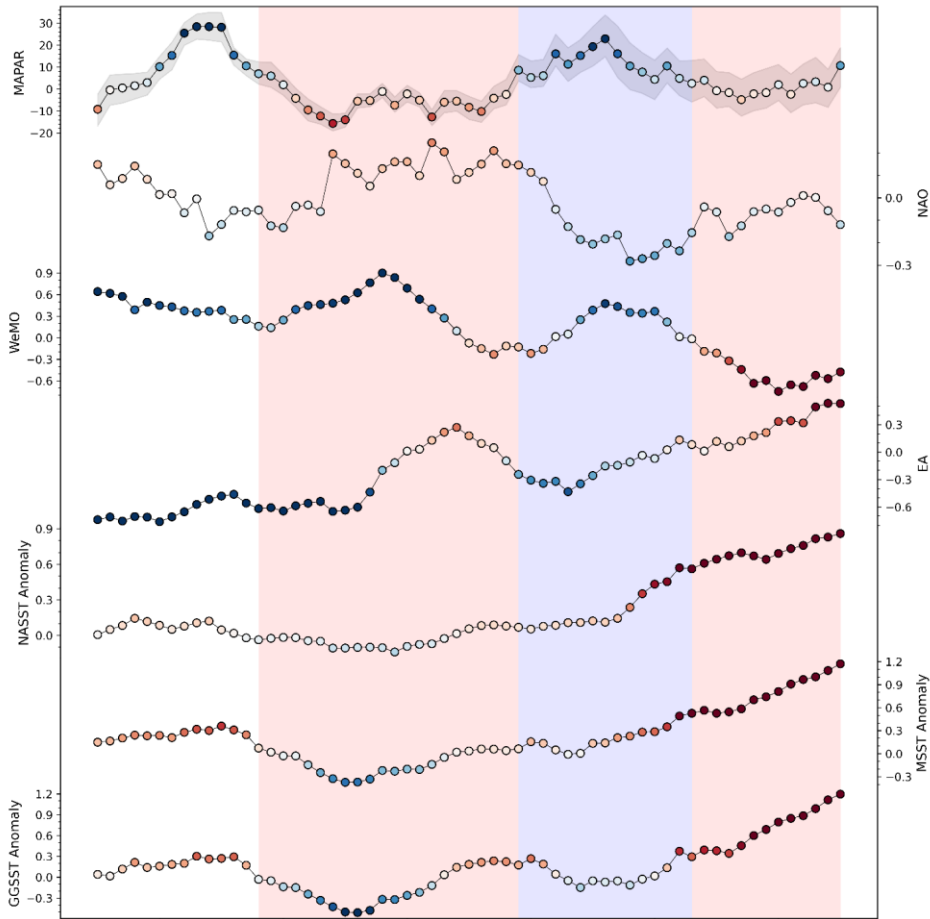
579

580 **Figure 4.** MAM season, trends of Mobile Average Percentage Anomaly Rainfall (MAPAR), NAO, WeMO, EA,
 581 North Atlantic Sea Surface Temperature (NASST), Mediterranean Sea Surface Temperature (MSST), and Genoa Gulf
 582 Sea Surface Temperature (GGSST) for the MAM season. The trends are smoothed by a 10-year mobile window and the
 583 colour of the points goes from blue to red: blue is linked to wet periods, red to dry periods. The grey band on MAPAR
 584 represents the 25th and 75th percentiles, the dots represent the mean value. The pink band refers to the main dry period
 585 of the time series.



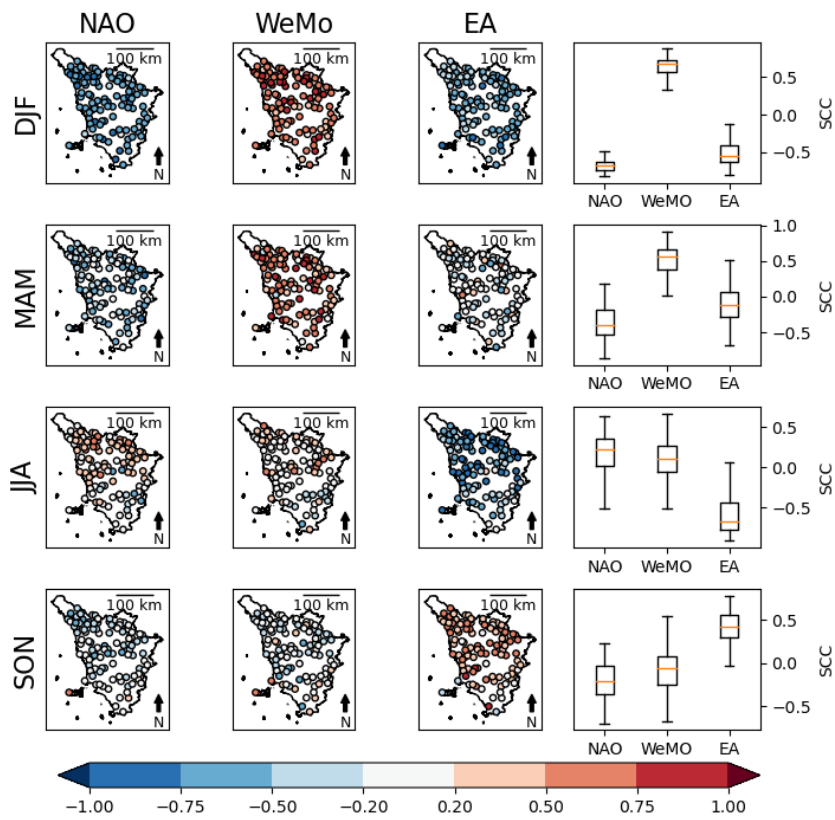
586

587 **Figure 5.** JJA, trends of Mobile Average Percentage Anomaly Rainfall (MAPAR), NAO, WeMO, EA, North Atlantic
 588 Sea Surface Temperature (NASST), Mediterranean Sea Surface Temperature (MSST), and Genoa Gulf Sea Surface
 589 Temperature (GGSST). The trends are smoothed with a 10-year mobile window and the colour of the points varies
 590 between blue to red: blue is linked to wet periods, while red is linked to dry periods. The grey band on MAPAR represents
 591 the 25th and 75th percentile, the dots represent the mean value. The pink band refers to the main dry period of the time
 592 series.



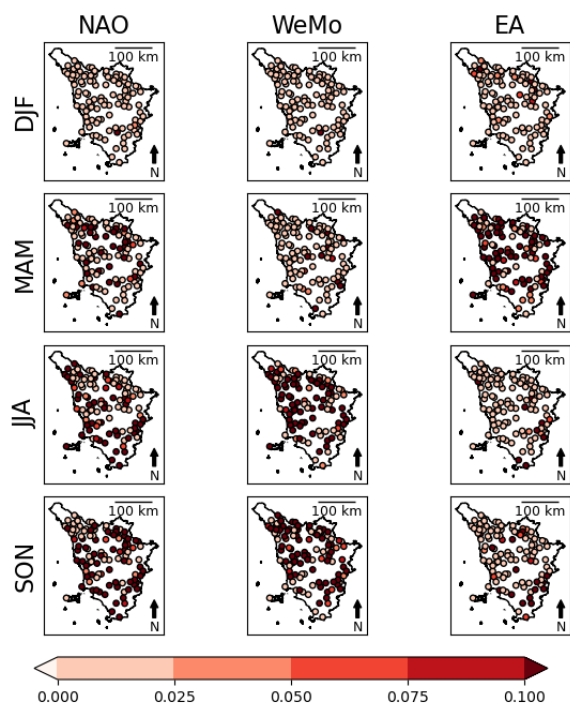
593

594 **Figure 6** SON season, trends of Mobile Average Percentage Anomaly Rainfall (MAPAR), NAO, WeMO, EA, North
 595 Atlantic Sea Surface Temperature (NASST), Mediterranean Sea Surface Temperature (MSST), and Genoa Gulf Sea
 596 Surface Temperature (GGSST). The trends are smoothed with a 10-year mobile window and the colour of the points
 597 varies between blue to red: blue indicates wet periods, red indicates dry periods. The grey band on MAPAR represents
 598 the 25th and 75th percentile, the dots represent the mean value. The pink band is referred to the main dry period of the
 599 time series, while the blue band is referred to the main wet period of the time series.



600

601 **Figure 7.** Spearman's correlation coefficients (SCC) between season rainfall and climatic patterns. For each season,
 602 we report the correlation with NAO, EA and WeMo and the relative boxplots. The boxes represent the interval between
 603 the 25th and 75th percentiles (Q1 and Q3). IQR is the interquartile range Q3-Q1. The upper whisker will extend to the last
 604 datum lower than $Q3 + 1.5 \times IQR$. Similarly, the lower whisker will reach the first datum higher than $Q1 - 1.5 \times IQR$. The
 605 orange lines represent the medians.

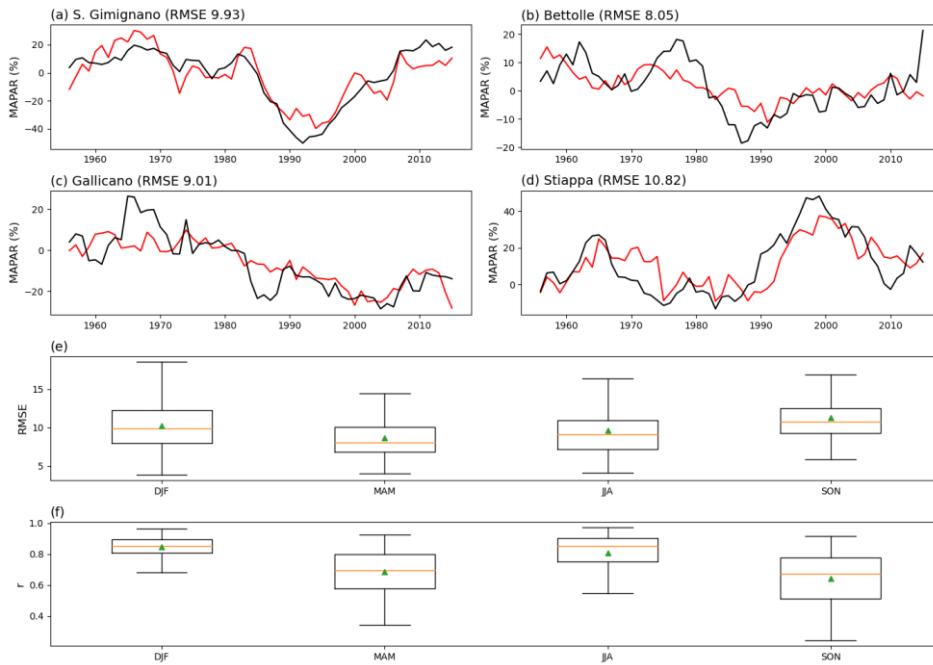


606

607

Figure 8. P-values of Spearman's correlation coefficients (SCC).

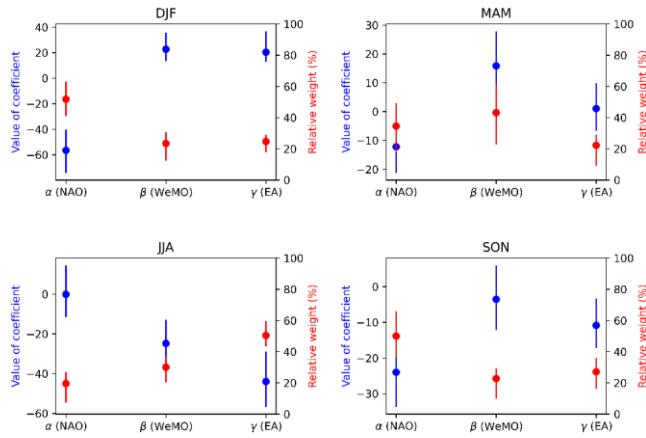
608



609

610 **Figure 9.** a-d) Four examples of observed MAPAR (black line) and predicted MAPAR (red line) respectively for the
 611 seasons DJF, MAM, JJA and SON. e) the boxplots represent the Root Mean Square Error (RMSE) of the linear models
 612 for the four seasons. f) the boxplots represent the Correlation Coefficient (r) of the linear models for the four seasons. The
 613 boxes represent the interval between the 25th and 75th percentiles (Q1 and Q3). IQR is the interquartile range Q3-Q1.
 614 The upper whisker will extend to the last datum lower than $Q3 + 1.5 \times IQR$. Similarly, the lower whisker will reach the
 615 first datum higher than $Q1 - 1.5 \times IQR$. The orange lines represent the medians, while the green triangles represent the
 616 means.

Commented [ml2]: In tutte le figure semplificare questa scritta che al primo editor non piace è troppo lunga



617

618 **Figure 10.** Setting of the linear model coefficients used to understand the relationship between climate patterns and
 619 rainfall. The blue circle is the mean absolute value of the coefficient, whereas the red circle represents the mean relative
 620 weight of the coefficient on the prediction. The results are reported for each season. The blue and red lines represent the
 621 interval between the 25th and 75th percentiles of the coefficient distributions (DJF: December-January-February; MAM:
 622 March-April-May; JJA: June-July-August; SON: September-October-November).

Reviewer #1: This manuscript presents a simple and straightforward method for correlating precipitation patterns with large-scale atmospheric and water temperature variables in the region of Tuscany, Italy. The methods in general are interesting and potentially useful for a wide audience, and I believe it represents a useful contribution to the field; but there are some flaws in the logic and, I believe, some over-interpretation (which I describe below); and the manuscript needs extensive editing and revision to be suitable for publication in a scientific journal like the Journal of Hydrology.

As I describe in detail below, my main concerns are:

1. Most of the introduction is a list of atmospheric and water temperature indices, with general statements of how they vary and are related to other weather-related conditions. These metrics need to be presented and synthesized in a more systematic way. In its current state, these indices feel arbitrarily placed in the introduction, without connection beyond interrelationships. I think this needs to be revised to be clearer and better-related (or perhaps better-balanced; see below).
2. There are two issues related to logic that I think the authors need to explain and address: First, the authors need to explain the PAR term more clearly and why they define the PAR term relative to a mean of only a fraction of the total data (1960-1990, rather than the entire period 1950-2020); and if this is the reason why the PAR values in the JJA graph in Figure 2 are virtually all below zero. The authors also need to explain the methods relative to Figures 2 and 3 more clearly. I have guessed from context, and my interpretation may be mistaken because the methods are not sufficiently described. Second, I am skeptical of whether the PAR patterns shown in Figures 3 through 6 (possibly the 10 year averaged PAR values) match the PAR in Figure 2 (especially DJF) and most importantly, whether this represents a declining trend (as described in the results) or increased variability (so that the PAR is driven by a few low values).
3. The manuscript also needs extensive editing, with many suggestions provided below.

Detailed comments:

Lines 21-23: missing some words; and it feels a little too uncertain. ("show a possible decrease"? Either they do or they don't, right?)

We removed the word "possible". In this way the phrase is more affirmative.

Line 30: Check with instructions for authors about naming headings. I think just "Introduction" is sufficient; the idea of identifying goals is implied. (similar for Methods—just Methods). Also, note that J Hydrology requires headings and subheadings to be numbered.

We added the headings and subheadings and modify "Introduction" and "Methods"

Line 39: not sure this is certain. What shows increasing water demand? Is population increasing? Demand has increased since year zero, but is it increasing recently?

In according to reduce the introduction as suggested, we removed this phrase which was not necessary for the introduction of the work

Lines 53-90: Overall, I think this part of the introduction would benefit from improved organization. I've read this introduction several times, and it may be sufficient to end the first paragraph at the Trigo et al reference, and then begin the next paragraph with a sentence "Several atmospheric patterns affect weather in the Mediterranean region. During the winter months..." (picking up with the rest of paragraph 1). Also in the introduction, some of the indices get much more explanation than others. NAO and EA are digestible for a wide range of hydrologists; WeMO has much more detail and feels unnecessarily extensive. I recommend revising to match description of NAO and

EA. Additionally, the connection between NAO, EAP and SST seems disjointed because it appears after WeMO. Overall, I recommend editing this part of the introduction to focus on the indices and how they are related, with sufficient but not overabundant detail.

This part of the introduction was modified in several parts in according with the suggestions of all reviewers

Lines 91-103: Some of this part of the introduction dives into methods. Describing rainfall data sets and how they have been used is suitable for the introduction; describing how they are used in this study (e.g., lines 94-96) is better suited for methods. Also, edit to remove phrases such as "allowed us to" and "helped us to" (not appropriate for a technical manuscript).

I also think there is value in additional explanation about water resource limitations in the Mediterranean: why be concerned about water resources? Seasonality? Is it useful to predict the magnitude of summer drought? Of winter torrents?

We removed the sentence, and improve the introduction adding lines 93-97

Line 106 (study area) - this should be under Methods (double-check with Authors guide)

We moved the "Study area" paragraph into Methods

Line 111 and Figure 1: note that the text in Figure 1 gives an upper range of MAP at 3000 mm but the figure implies the upper limit is 2000 mm. this needs to be edited.

We modified the figure

Line 120: data download description should include the date when data were obtained.

We added when the data was obtained

The grouping of data and their use (line 124-134) is not as clear as it could (or should) be.

- Consider omitting the sentence beginning in line 126, "In many cases,..." because it is redundant.
- The phrase "with a difference in quote of the measurement" is not a phrase that has meaning. Revise with a different phrase.
- Remove "see section linear models"; edit sentence line 133-134 (maybe in to two sentences, removing the word "instead").
- Line 133: "absolute values" - is this rainfall values?

We changed the term "quote" with "altimetry, remove the words indicated and divided the sentence of line 125-126 in two sentences

Lines 134-135: There appears to be a breakdown in logic: the period of record for the 117 time series is 1950-2020 (70 years), but PAR only considers mean rainfall between 1961 and 1990 (30 years). Why omit most of the rainfall data set for calculating such an important part of this metric? Was this intentional? If so, what is the rationale?

The anomaly of a variable is the variation relative to the climatological normal. The normal is the long-term average of the same variable and is used as a baseline value. The normal is typically computed by calculating a climatology over a period of at least 30 years (the climate normal period).

Line 134-136: The PAR is not clear. The variable x_i is labeled as the rainfall amount. Can you be more specific? Is it the annual rainfall for year i ? or is it the average for the previous 5 years and the following five years (i.e., a 10-year mobile window)? If the 10 year mobile window is an added calculation, a way to graphically represent the PAR, it should be described as such. Also, is PAR a seasonal calculation? Is x_i a seasonal x_i and mean x_i a seasonal average? This is not clearly described.

We modified the line 128-138, distinguishing the calculation of the anomalies (PAR) with the mobile average (MAPAR). We have also modified the text in Results and Discussion change the term PAR with the term MAPAR where it's necessary. In this way, we hope that the methodology is clearer.

Lines 151-152: these are some broad areas. Can you describe whether you just use the water portion of these areas?

We think that all information is provided. The dataset used is Sea Surface Temperatures, for this is only the temperature on the seas.

Line 161: vice versa is two words.

Thanks, we modified it

167-168: a little too colloquial. Remove first sentence, revise the second to read "We created linear models to predict..."

We removed the first sentence

Lines 171-172: revise sentence

We modified the sentence

Figure 2: Figure 2 is important to show the date range on the x-axis for each graph. This is critical for making the PAR characterization for Figures 3-6 (as described in the Results section) understandable and believable. Consider making these full width of the page, stacked four high, rather than side-by-side in a 2-by 2-grid. I have other concerns about the results and their interpretation below.

We have modified the text in methods and results to try to clarify figures 2 and figures 3-6 regarding the PAR quantity. Figure 2 shows the PAR values obtained with equation 2 for each station on the x axis. We modified the Figure 2, and we hope that now it is clearer.

Also, for Figure 2: I am trying to figure out why the PAR values (red dots) for the JJA graph are almost all below zero. I have been experimenting with example datasets trying to re-create this pattern and cannot. I believe there is a problem with this figure the authors need to fix; and if I am incorrect, the authors need to explain in the results why a metric that should mostly be centered around zero (like the other three plots in Figure 2) is almost entirely below zero. (is this because the PAR is only based on the mean of values from 1960 to 1990?)

After the distinction between PAR and MAPAR, the modification of the text and of the figures 2, 3-6, we hope that now it is clearer the difference between the figure 2 and the figures 3-6.

Also for Figure 2, the caption (begin line 519): move the season description (lines 523-524) to

earlier, following the word "seasons" (line 520). The description of ICR and whiskers can be abbreviated to one sentence (it is currently 3, which is too wordy).

We move the season description to the start of the figure

I've read the methods section and the results section a few times, and I cannot identify the difference between the PAR values in Figure 2 and the PAR values shown in Figures 3 through 6. Despite that both are labeled PAR and appear to be on the same axis, they are clearly different data sets. For example, the decline in PAR shown in the top part of Figure 3 (PAR, DJF) is not shown in the DJF graph for Figure 2. If the differences between the PAR data shown in Figure 2 and Figure 3 is that Figure 2 is the PAR for each year and Figure 3 is the 10-year averaged value for each year, this distinction should be articulated in the Methods section (reflecting that both were calculated) and in the results section. For example, consider line 184. (continued below)

I also recommend the authors be careful about wording. In particular, line 184 states that Figures 3 through 6 express the trend in PAR and other variables. Do they in fact express the trend, or would it be more accurate to say they show the variation in these variables expressed over the 10-year window, and that these data exhibit a trend?

As explained in the previous answers, we hope that with the modification done it is clearer the difference between the figures. We have modified the phrase of line 184.

Line 186-188: Based on the data shown in Figures 2 and 3-6, I am not certain that I agree with the authors' interpretation of the results related to variation in PAR. The authors state that PAR is reduced in the first years of the 1990s, by a magnitude of 30-40%. If I have interpreted the methods and results clearly (see notes above), Figures 3 through 6 are showing PAR averaged over a 10-year moving window. While Figure 3 shows DJF 10-year averaged PAR declining for each year, Figure 2 for DJF suggests this is driven by a handful (maybe five?) of anomalously low values; other than these anomalous values, PAR appears to be within the same range as it had been over the previous decades.

Also, much of this Rainfall Trends paragraph is not suitably written for a scientific journal article. Terms like "we can observe", "we observe", "very different", "between ca -10 and 20%", "a weakly increase", "presented a certain variability", and the typing error FiguresFigure are stylistic problems with this section and need to be changed. A larger problem is that the authors are interpreting the results of data analyses in a way that, I believe, is not consistent with the data. The changes shown in Figures 3 through 6 are changes in 10-year averaged PAR, not annual PAR and not annual rainfall. I recommend the authors re-write this section to improve the overall technical quality of the writing and to more clearly interpret the results presented.

The Figure 2 and the Figure 3-6 cannot be compared among them. This figures represent the same data but in different way. As above indicated, we hope that now is clearer the distinction. We have modified this paragraph with the reviewer's suggestions.

Lines 195-208 (Results, Atmospheric teleconnection trends): I suggest the authors structure this by season rather than by index. Presentation of these variables may be sufficient in their current condition, but organizing by season has two benefits: the authors can describe similarities and differences by season, which is significant to the regression analysis; and the graphs are already created by season. Also, stylistically, revise to remove phrases such as "we observe". Also, while it is suitable to generalize about trends or patterns, phrases indicating exceptions like "except for some years" and "except for some cases" are too vague and insufficient for a technical manuscript. These need to be more clearly described and phrased another way relative to the overall pattern, or removed.

We rewritten the paragraph with a reorganization as suggesting by the reviewer

Lines 210-212 (Sea surface temperature trends) is clear and succinct; I suggest the authors revise for stylistic purposes to avoid phrases like "Figures 3-6 show...". Also, line 212: consider replacing the word "higher" with "greater".

We modified the word higher with greater and change the begin of the paragraph.

Lines 224-225: revise to remove phrase "on the other hand." These sentences can probably be combined to improve clarity.

We modified it merging the two sentences

Lines 227-228: are the authors certain that a positive EA phase determines increased precipitation? Couldn't other factors determine the precipitation pattern? I think you would need to test this with a circulation model to say for certain that the positive EA determines increased precipitation.

In results, we only present the results obtained by the elaborations. We discuss in line 292-295: "In autumn, the statistical correlations do not allow to make a link between large-scale circulation and rainfall. Indeed, we can observe a weak anticorrelation with NAO, a weak correlation with EA, and no correlation with WeMO. This method seems unsuitable to represent the autumn season with its atmospheric dynamics."

In the results, we would not want to change the phrase. In this paragraph, we have to describe only the results, in discussion we compare the two elaboration applied, that in this case the statistical correlation does not describe well the behaviour in the autumn. This is written in lines 298-304: "In autumn, the analysis of the linear models identifies an important role of NAO, and therefore a link between the northern Atlantic atmospheric circulation and the rainfall in the study area. In autumn, the coefficients of NAO (are set negative and this means that an increase in the index is linked to a decrease in rainfall in the study area. This mathematical result is more plausible than that obtained from the analysis of correlations based on the notions of atmospheric physics that we introduced previously. The linear model-based method allowed us to refine our investigations and to improve our knowledge of the dynamics in the Mediterranean over the seasons. "

Figure 7 caption should be revised as suggested for Figure 2 caption.

We changed it

Line 232 (Figures 8a-d): the results are quite striking. Which terms are used for these relationships? All? What are the coefficients used? I think these should be reported (possibly in the table recommended below to replace Figure 9?).

We explicated the coefficients α , β and γ for the four cases reported in figure 8.

Figure 8: the caption only needs to include the first sentence (through "...and SON") and then "e) the boxplots...four seasons." Everything else is stated in methods. It could also include the sentence "The orange lines represent the medians, while the green triangles represent the means.", but the seasonal explanation (lines 566-567) can be omitted.

We modified the caption as suggest by the reviewer

Lines 236-249: some of this may be more suitable in the Discussion. review this paragraph to

include only those topics that are reflected in the results; additional description of the meaning of relationships are better suited in the Discussion.

We modified these lines; we removed or modified the discussion sentences. We left the general considerations which allow to understand and read the Figure 9

Consider replacing Figure 9 with a table.

We apologize with the reviewer, but we think that the Figure 9 is very important for the paper and their information is better represented in this way than the use of a table. A graphical representation allows to understand immediately the relationship among the different coefficients.

Line 255, and elsewhere in the discussion: no need to refer to figures here unless something specific is being discussed.

We removed the refers to figures where they are not necessary.

Also, line 255: is this the first paper that links climate patterns on local rainfall? Or just for Tuscany? (this is not the first research to link climate patterns to local or regional rainfall.)

No, we didn't affirm it in the manuscript. In introduction we talk about of several works which study the relationship between synoptic conditions and rainfalls at different scales. The study doesn't want only quantify the relationship between rainfall and indices, but understanding the trends of the first ones basing on the second ones. Lines 87-88: "The purpose of this study is to understand the rainfall seasonal trends of the last 70 years in Tuscany (central Italy), in relation to mesoscale circulation and to the indices defined above."

Lines 284-289 (and this section of the Discussion in general): if the value of this method is not to develop the best prediction, what is its value? Could it be to illustrate the general utility of simple tools for these predictions, which could be applied more broadly elsewhere? Or by data analysts who may lack the technical know-how of PhD-level climatologists? For example, managers in a region may be able to use these methods (albeit with different climate datasets, depending on the region) to predict conditions for planning purposes.

As written in Methods (lines: 183-184) and in Discussion (lines: 307-308), the aim of the use of linear models is not create an instrument for the forecasting, but use them for understand the influences of the inputs (the indices) on the outputs (rainfall as MAPAR)

Line 287: sentence beginning "If we wanted..." seems to undermine the utility of this research. consider re-writing this sentence something like "A more complex model may be better suited to reduce overall model error; however, it would have...". This way, it suggests the value of this research as comparable.

We rewritten it

Line 306: re-write to remove the phrase "As a matter of fact"

Done it

Lines 304-316: synthesize this into one single paragraph, rather than four separate ones.

Done it

Lines 331-337: the connections to global warming feel forced and not clearly connected to the results of the paper. I think these should be removed. Instead, I recommend ending with a statement about the potential utility of these methods applied elsewhere to help understand the relationships between atmospheric patterns and precipitation and to steer management priorities in the future, or something similar to highlight the utility of the method.

We modified these lines. We think that all considerations are based on the bibliography and/or the results of this study. We denote the greatest increase of SST in summer (bibliographic information), this influences the indices (bibliographic information) which are correlated with the rainfall (our results). We changed the term “can” with “could” for a more precautionary sentence.

Reviewer #2: This paper investigates the relationship between several climate patterns and seasonal rainfall over a key Mediterranean area. However, I consider that there are some unclear points needing a major revision. I list my concerns as follows:

1. The title emphasizes the influence of the atmospheric circulation on regional rainfall, but from the manuscript I can not see the related mechanisms being confirmed. Results are only based on correlations or a simple comparison. Exactly how the NAO, EA and WeMO jointly influence the seasonal rainfall over the study region needs to be further analyzed.

We changed the title removed the word “Influence” and indicating better using the term relationship”

2. In the abstract (Lines 24-27), the authors outlined that the changes of SSTs lead to the variation of atmospheric pressure, but the visual information (e.g., the pressure fields related to SSTs and/or seasonal rainfall over the study region) is not provided in the manuscript, which needs to be added if possible.

SST influences the climate patterns as introduced mainly in lines 60 – 70. It’s not the aim of the study to demonstrated it or to quantify the influences. For this discussion, we are based on other studies and on the international knowledge of this phenomena.

3. The analysis in the introduction is relatively weak, and the narration is only a simple list, which needs to be strengthened. Specifically, how seasonal rainfall in the Mediterranean region is affected by the atmospheric circulation, which can be concluded from the previous studies, needs to be further outlined in this part.

We have modified the introduction also as suggesting by the other reviewers

4. It would be better if the quality of the rainfall datasets in this paper can be evaluated if it has not been evaluated by previous studies. Also, the approach of merging stations (Lines 126-130) is originally defined by the authors or some previous studies? The authors should state this point more clearly if possible.

We modified the paragraph by adding information on the dataset used. The procedure is all explained because we use this elaboration of the dataset for the first time. If some previous work had used the same procedure, we would have mentioned it. The quality of the dataset is guaranteed by the provider, future works will study if this database with more than 6 million of data is well validated. This dataset is used by high-resolution works in this study area. We added this in text lines 115-118

5. The trends are calculated based on a 10-year mobile window (Line 150). However, I consider that the window length is too short since 10-year trends are likely to be dominated by the climate internal variability. In that case, the influence of the current global warming is likely to be wrongly estimated.

We motivated the choose of range time: lines 137 - 138.

6. To confirm the contributions of atmospheric circulation on rainfall, I consider that correlation needs to be based on detrended series. And if the contributions are confirmed, the trend correlation can be further investigated by the SCC used in this paper to describe the effect of global warming, as well as the different contributions of trends of climate patterns on those of seasonal rainfalls in the study region.

We thank the reviewer for the observation, there are several works, in this field, which use this method in not appropriate way (lines 161 -166). We have demonstrated that the SCC, in the study area, is little influenced by the trends of the time series. For this we have added the lines 174 – 179 and added more details in supplementary material. Furthermore, this work proposed the use of a different method for the investigation of this relationship (lines 182-194). We think that the second method use is more efficient but we have to compare it with the most used method in this thematic area (lines 305 – 310).

7. The statistical significance of all the results of correlation analysis needs to be evaluated in the manuscript.

We added it, it is the new Figure 8.

8. Besides RMSE, other metrics (e.g., anomaly correlation coefficient) needs to be added for more comprehensive evaluation of the linear model.

We added the metric of Correlation Coefficient (r) adding text in methods (lines 193 -194) and in results lines 256-257

Reviewer #3: This study aims to analyze the influence of large-scale atmospheric circulation on the rainfall of a key Mediterranean area. The subject of the study fits to the major themes of the journal. The quality of the graphic material of the manuscript are good. However, I have two major concern regarding this study.

(1) The authors made a deep review about the global climate events (NAO, EA and WeMO) and their possible teleconnection with regional climate. However, the authors did not pointed out the innovation or possible new findings of this study. The motivation of this study should be further clarified.

We modified the introduction of the paper in according also with the other reviewer suggestions

(2) The Mediterranean is located between the European humid domain and the North African arid belt, and annual mean precipitation is quite different from the northern and southern parts (Figure 1a). This study mainly focuses on the entire study area without considering the spatial heterogeneity, which may cause bias in results, especially in Figures 2, 3, 4, 5, and 6. It may be better to analyze in different sub-regions separately, such as the northern and southern parts.

We have tested and analyzed the spatial variability of the results but there isn't significant evidences of this. This can be noted by the variability of PAR (Figure 2) as commented in lines 198 – 199. The area is quite homogenous.

Comments and suggestions:

1) The significance of Spearman's correlation analysis should be given in Figure 7.

We added it, it is the new Figure 8.

2) The linear model may not be an innovative approach to predict rainfall based on large-scale atmospheric circulation indexes in Lines 100-101.

We removed the sentence

3) The datasets are described repeatedly in Lines 94-99 and dataset section.

We modified it, in according also with the other reviewers

Marco Luppichini: Conceptualization, Methodology, Software, Investigation, Data curation, Formal analysis, Writing-Original draft preparation

Monica Bini: Conceptualization, Supervision, Writing-Reviewing and Editing

Michele Barsanti: Writing- Reviewing and Editing.

Roberto Giannecchini: Writing- Reviewing and Editing.

Giovanni Zanchetta: Conceptualization, Supervision, Writing-Reviewing and Editing.

Abstract

Current global warming causes a change in atmospheric dynamics, with consequent variations in the rainfall regimes. Understanding the relationship between global climate patterns, global warming, and rainfall regimes is crucial for the creation of future scenarios and for the relative modification of water management. The aim of this study is to improve knowledge of the relationship between North Atlantic Oscillation (NAO), East Atlantic (EA), and Western Mediterranean Oscillation (WeMO) with the seasonal rainfalls in Tuscany, Italy. The study area occupies a strategic position since it lies in a transition zone between the wet area of northern Europe and the dry area of the northern coast of Africa. This research, based on a statistical correlation method and on linear models, is designed to understand the relationship between seasonal rainfalls and climate patterns. The results of this study demonstrate that the use of linear models can yield more information than traditional statistical correlations. The results show a decrease in rainfall in the warm period of the year, namely in the summer, when its expression is most visible. This phenomenon is ascribable to current global warming, which causes an increase in sea-surface temperatures. An increase in the Northern Atlantic Sea Surface Temperature and in the Mediterranean Sea Surface Temperature causes a reduction of the Iceland Low, with an extension of the Azores High. Moreover, an increase in the Genoa Gulf SST induces a weakening of the Genoa Gulf Low, one of the main cyclogenetic systems of the Mediterranean.

Highlights

1. Seasonal Rainfall trend in Tuscany (Italy) during the last 70 years
2. Statistical and mathematical correlation between atmospheric teleconnections and rainfall amount
3. Influence of the atmospheric teleconnection variations on the rainfall regime
4. Influence of current global climate change on the rainfall regime in an area of the Mediterranean